



HAL
open science

A lysine-based 2:1- $[\alpha/\text{aza}]$ -pseudopeptide series used as additives in polymeric membranes for CO₂ capture: synthesis, structural studies, and application

Mohamed I. A. Ibrahim, Xavier Solimando, Loïc Stefan, Guillaume Pickaert, Jérôme Babin, Carole Arnal-Herault, Denis Roizard, Anne Jonquières, Jacques Bodiguel, Marie-Christine Averlant-Petit

► To cite this version:

Mohamed I. A. Ibrahim, Xavier Solimando, Loïc Stefan, Guillaume Pickaert, Jérôme Babin, et al.. A lysine-based 2:1- $[\alpha/\text{aza}]$ -pseudopeptide series used as additives in polymeric membranes for CO₂ capture: synthesis, structural studies, and application. RSC Advances, 2023, 13 (15), pp.10051-10067. 10.1039/d3ra00409k . hal-04251129

HAL Id: hal-04251129

<https://hal.univ-lorraine.fr/hal-04251129v1>

Submitted on 20 Oct 2023

HAL is a multi-disciplinary open access archive for the deposit and dissemination of scientific research documents, whether they are published or not. The documents may come from teaching and research institutions in France or abroad, or from public or private research centers.

L'archive ouverte pluridisciplinaire **HAL**, est destinée au dépôt et à la diffusion de documents scientifiques de niveau recherche, publiés ou non, émanant des établissements d'enseignement et de recherche français ou étrangers, des laboratoires publics ou privés.



Lysine-based 2:1-[α /aza]- pseudopeptide series used as additives in polymeric membranes for CO₂ capture: synthesis, structural studies, and application

Journal:	<i>Journal of Materials Chemistry A</i>
Manuscript ID	Draft
Article Type:	Paper
Date Submitted by the Author:	n/a
Complete List of Authors:	<p>Ibrahim, Mohamed Ibrahim AbdelMoneim ; Université de Lorraine, Laboratoire de Chimie Physique Macromoléculaire UMR7375; National Institute of Oceanography and Fisheries (NIOF), , Marine Environment Division</p> <p>Solimando, Xavier; Université de Lorraine, Laboratoire de Chimie Physique Macromoléculaire</p> <p>Stefan, Loic; Laboratoire de Chimie physique Macromoleculaire, Pickaert, Guillaume; Université de Lorraine, Laboratoire de Chimie Physique Macromoléculaire</p> <p>Babin, Jerome; Université de Lorraine, Laboratoire de Chimie Physique Macromoléculaire</p> <p>Arnal-Herault, Carole; Université de Lorraine, Laboratoire de Chimie Physique Macromoléculaire</p> <p>Roizard, Denis; Université de Lorraine, laboratoire des Réactions et Génie de Procédés</p> <p>Jonquieres, Anne; Université de Lorraine, Laboratoire de Chimie Physique Macromoléculaire</p> <p>Bodiguel, Jacques; Université de Lorraine, Laboratoire de Chimie Physique Macromoléculaire</p> <p>Averlant-Petit, Marie-Christine; Université de Lorraine, Laboratoire de Chimie Physique Macromoléculaire; CNRS, Laboratoire de Chimie Physique Macromoléculaire</p>

ARTICLE

Lysine-based 2:1-[α /aza]- pseudopeptide series used as additives in polymeric membranes for CO₂ capture: synthesis, structural studies, and application

Received 00th January 20xx,
Accepted 00th January 20xx

DOI: 10.1039/x0xx00000x

Mohamed I. A. Ibrahim*^{a, b}, Xavier Solimando^a, Loïc Stefan^a, Guillaume Pickaert^a, Jérôme Babin^a, Carole Arnal-Herault^a, Denis Roizard^c, Anne Jonquière^a, Jacques Bodiguel^a, and Marie-Christine Averlant-Petit*^a

Abstract The current study presents for the first time the synthesis of a new 2:1-[α /aza]-pseudopeptide series possessing charged amino acid (*i.e.*, lysine) and aims at studying the influences of chirality, backbone length, and nature of the lysine side chains on the conformation of the 2:1-[α /aza]-oligomers in solution using NMR, FTIR spectroscopy and molecular dynamic calculations. The spectroscopic results emphasized the conservation of the β -turn conformation adopted by the trimers regardless of the chirality which demonstrated a noticeable effect on the conformation of homochiral hexamer compared with the hetero-analogue. The molecular dynamic calculations predicted that the chirality and the side chain of the lysine residues caused a little distortion from the classical β -turn conformation in case of short trimer sequences, while the chirality and the backbone length exerted more distortion on the β -turn adopted by the longer hexamer sequences. The large disturbance in hexamers from classical β -turn was attributed to increasing the flexibility and the possibility of molecules to adopt more energetically favorable conformation stabilized by non-classical β -turn intramolecular hydrogen bonds. Thus, alternating *D*- and *L*-lysine amino acids in the 2:1-[α /aza]-hexamer decreases the high steric hindrance between the lysine side chains, as in the homo analogue, and the distortion is less recognized. Finally, short sequences of aza-pseudopeptides containing lysine residues improve CO₂ separation when used as additives in Pebax[®] 1074 membranes. The best membrane performances were obtained with a pseudopeptidic dimer as additive, with an increase in both ideal selectivity $\alpha_{\text{CO}_2/\text{N}_2}$ (from 42.8 to 47.6) and CO₂ permeability (from 132 to 148 Barrer) compared to the virgin Pebax[®] 1074 membrane.

Introduction

Pseudopeptides are modified peptides containing non-proteinogenic or modified amino acid building blocks or modified peptide bonds.¹ Chemists used the approach of introducing chemical changes in the peptide backbone or side chains in order to improve the physical and chemical properties of the parent peptides, predicting their promising potentials as candidates for medicinal, environmental and industrial applications.²⁻⁶ Among the modifications in the peptide backbone are those occurring on the amide bond leaving the side

chains without any changes.⁷ Peptide backbones can be modified in various ways either by extending the peptide chain by one more atom (s) or by changing at least one peptide bond with an isosteric or isoelectronic surrogate, depsipeptide, ketomethylene isoester,⁸ azapeptide,^{8,9} retro-inverso,^{10,11} aminoxy acid,^{12,13} hydrazino acid,^{14,15} and β -amino acid¹⁶. Interestingly, Gellmann investigated the ability of some pseudopeptides to self-organize in solution to give stable, reproducible secondary structures that mimic protein secondary structures such as helices, sheets or turns, also known as "Foldamers". The term "Foldamer", as proposed by Gellmann, refers to unnatural polymers or oligomers that have strong tendency to self-organize into a predictable well defined compact structure in solution.¹⁷

For several decades, our laboratory has demonstrated the design, synthesis, and conformational study of pseudopeptide oligomers¹⁸⁻²⁰. Specifically, we have been focused on pseudopeptidic bis-nitrogen compounds such as hydrazinopeptides²¹⁻²³ and *N*-aminopeptides²⁴⁻²⁶. More recently, we have extended the interests on the synthesis

^a Université de Lorraine, CNRS, LCPM, F-54000 Nancy, France

^b National Institute of Oceanography and Fisheries, NIOF, Egypt.

^c Université de Lorraine, CNRS, LRGP, F-54000 Nancy, France.

† Footnotes relating to the title and/or authors should appear here.

Electronic Supplementary Information (ESI) available: [details of any supplementary information available should be included here]. See DOI: 10.1039/x0xx00000x

and conformational study of azapeptides^{20, 27-31} in which the α -carbon(s) of one or more of the amino acid residues is/are replaced with one nitrogen atom^{9, 32-35}. Azapeptides have been studied since the early sixties and actively developed by Gante⁹ and by Dutta and Morley³⁶. Synthesis of azapeptides has been particularly investigated by Gante^{9, 33, 34} and our group^{20, 27, 29-31, 37} in liquid-phase peptide synthesis, and by Gray *et al.*³⁸ in solid-phase. Interestingly, several studies demonstrate that the insertion of an aza-residue into a peptide backbone has intense effects not only on the geometrical structure, but also on its physical and chemical properties. Among the impact of such chemical modification on the conformation, we can mention that: (i) the CO-N amide bonds are elongated by 0.03 Å³⁹ while the N-N α and N α -CO bonds are shortened by 0.06 Å compared to N-C α and C α -CO in the natural peptide; (ii) the N-N α -CO angle is larger by about 4 - 5° than the N-C α -CO bond angle; (iii) the substituted nitrogen atom N α adopts chiral property with a pyramidal nature of sp³ type;^{18, 39} (iv) the flexibility is reduced in the formed azapeptides compared with the parent one due to the replacement of the rotatable C α -C(O) bond by a more rigid urea N α -C(O) structure; and (v) an electronic repulsion of the lone pairs of the two adjacent nitrogens restricts motion of the dihedral angle (ϕ)^{40, 41}. Thus, based on these data, the conformational restrictions in the azapeptides which bend the peptide backbone at the aza-amino acid residue away from a linear geometry, could be predicted.⁴² Several spectroscopic,^{21, 43-46} crystallographic,^{18, 21, 37, 47, 48} and computational^{41, 43, 49-52} studies demonstrate the ability of azapeptides to induce β -turn conformations of type I, type II, and type VI when aza-residue occupying the position (i + 1) or (i + 2) in the peptide sequence, stabilized by intramolecular hydrogen bonds.^{18, 19, 21, 43, 46, 49, 52}

Previous studies^{30, 31} have proved, using FTIR, NMR spectroscopy techniques as well as molecular dynamic calculations, the propensity of the azapeptides (**7a**, **7b**, **8a**, and **8b**, **Scheme 1**) to adopt β -turn conformations stabilized by intramolecular hydrogen bonds in both solution and solid states. However, not much studies are reported concerning the effect of introducing charged amino acid in azapeptides sequences on their conformations. Consequently, we decided to focus our attention to the synthesis and studies of new 2:1-[α /aza]-oligomers containing charged amino acid moieties such as lysine. Indeed, we suggested that the incorporation of basic amino acid(s) (lysine) with a nitrogen atom N ϵ H in its/their side chain(s) may: i) produce oligomers with good selectivity in gases separation, especially (N₂/CO₂) by membrane technology, and ii) increase the hydrophilicity of the final oligomers which may support the formation of hydrogels with promising potential applications.

In this context, the current work focus on the synthesis of new series of 2:1-[α /aza]-oligomers possessing lysine residues in solution state. Then, the conformational studies of some synthesized oligomers (**7c**, **7d**, **8c** and **8d**, **Scheme 1**) were elucidated in solution state using spectroscopic techniques (NMR and FTIR) and molecular dynamic calculations (Amber 12). In addition, the work extended to test a selection of these azapeptide oligomers as new

pseudopeptide-based additives for gas separation membranes for CO₂ capture. The study focused on the influence of the azapeptide oligomer length and of the nature of the side group of the amino acids (with or without protected or non-protected lysine residues) on the gas permeation properties of Pebax® 1074 membranes containing the new bio-inspired additives.

EXPERIMENTAL SECTION

General: Unless otherwise stated, all chemicals and reagents were purchased from commercial suppliers (Sigma-Aldrich, Fluka, Merck or Alfa-Aesar). Dry CH₂Cl₂ was obtained by distillation over P₂O₅ under an argon atmosphere, MeOH was purchased in anhydrous form, and other reagent-grade solvents were used without further purification as received. Reactions were monitored by thin-layer chromatography (TLC) using aluminum-backed silica gel plates. TLC spots were viewed under UV light or/and by heating the plate after treatment with a staining solution of phosphomolybdic acid. Flash chromatography was carried out on silica gel 60 (0.04 – 0.063 μ m Mesh ASTM). All yields were calculated from pure isolated products. Electron spray ionization mass spectra (ESI-MS) were recorded with a Bruker MicroTof-Q HR spectrometer in the "Service commun de Spectrométrie de Masse", Faculté des Sciences et Technologies, Vandoeuvre-lès-Nancy, France. All melting points (mp) were uncorrected.

NMR spectroscopy: 1D (¹H and ¹³C) and 2D (ROESY) NMR spectra were recorded using a Bruker NMR spectrometer (300 MHz) in CDCl₃, CD₃CN and DMSO-*d*₆ as solvents at room temperature with chemical shifts of 7.26, 1.94 and 2.50 ppm, respectively. The chemical shifts were reported in ppm (δ) relative to tetramethylsilane (TMS) served as an internal standard (δ = 0 ppm) for ¹H NMR, while CDCl₃ (δ = 77.16 ppm), CD₃CN (δ = 1.32 & 118.26 ppm) and DMSO-*d*₆ (δ = 39.5 ppm), were used as internal standards for ¹³C NMR. Multiplicities are reported as follows: s = singlet, d = doublet, q = quartet, m = multiplet, br = broad, arom = aromatic.

Fourier Transform Infrared Spectroscopy: FTIR spectra for all products in CDCl₃ were recorded with Bruker Tensor 27 over 128 scans and referenced to the residual solvent resonances. In addition, attenuated total reflectance (ATR-FTIR) measurements have been performed on solids for some products. All the spectra were recorded on Bruker Tensor 27 spectrometer equipped with a trough plate comprising of a germanium single crystal where the samples were loaded over it. Spectra were acquired in the 4000 - 400 cm⁻¹ range with a resolution of 4.0 cm⁻¹ over 128 scans, taken into consideration the background subtraction from each spectrum to correct for atmospheric interference.

Molecular Dynamic Calculations (AMBER 12): Calculations on molecules (**7c**, **7d**, **8c**, and **8d**) were carried out according to the protocol: 0.5 μ s with 2fs steps molecular dynamics simulations were calculated in explicit solvent (chloroform; CHCl₃ box) without any ROE constraints under constant pressure periodic boundary conditions, pressure relaxation time of 0.5 μ s, and constant

temperature 300 K, using the package of molecular dynamics simulation programs AMBER 12. The starting molecules were constructed using MarvinSketch (ChemAxon), Antechamber and Xleap modules from AMBER programs suite. Molecular simulation was done with Sander program with general AMBER force field (GAFF) and included amino acid parameters (ff99SB). Ptraj module of AMBER 12 programs suite was employed for the analysis of the 2ns trajectory sampled with 25,000 calculated structures.^{53, 54}

Synthesis of *N*-tert-butylloxycarbonylaminophthalimide (2): Phthalic anhydride (1.0 equiv) and tertbutylcarbazate (1.0 equiv) were dissolved in toluene in a monocol with a Dean-Stark. The suspension is refluxed for 12 h. The mixture was cooled and the *N*-tert-butylloxycarbonylaminophthalimide **2** precipitated. The solid was filtered off and recrystallized with EtOAc.

Characterization data: *N*-tert-butylloxycarbonylaminophthalimide (**2**) was obtained as a white crystal (yield 86%) after recrystallization from ethyl acetate; m.p. 214 - 216 °C; ¹H NMR (300 MHz, CDCl₃, 8.0 mmol L⁻¹) δ_H 1.49 (2 s, 9H, C(CH₃)₃), 6.61 (br s, 1H, NH), 7.76-7.79 (m, 2H, H arom Phth), 7.89-7.92 (m, 2H, H arom Phth). ¹³C NMR (75 MHz, CDCl₃, 8.0 mmol L⁻¹) δ_C 28.4 (C(CH₃)₃), 83.81 (C(CH₃)₃), 124.65 (CH arom Phth), 130.68 (C arom Phth), 135.37 (CH arom Phth), 154.07 (N-COOt-Bu), 166.13 (O=C-Pht). IR (KBr) $\tilde{\nu}_{\max}$ = 3395 cm⁻¹ (NH); 1706 cm⁻¹, 1740 cm⁻¹, 1783 cm⁻¹ (C=O). HRMS (ESI) for [C₁₃H₁₄N₂O₄]: calculated [M+H]⁺ (m/z) 263.0954; found, 263.1034.

Synthesis of *N*-benzyl-*N*-tert-butylloxycarbonylaminophthalimide (3): To a solution of *N*-tert-butylloxycarbonylaminophthalimide **2** (1.0 equiv), PPh₃ (1.5 equiv) and benzyl alcohol (3.0 equiv) in dry THF, DEAD (1.5 equiv) was added in one portion under N₂ and stirring at 0-5 °C. The resulting solution was stirred overnight (monitored by TLC until completion) and concentrated under vacuum. The residue was triturated in EtOAc, placed in a refrigerator and most of the triphenylphosphine oxide was precipitated which then removed by filtration. The filtrate was evaporated, and the residue was purified by column chromatography on silica gel.

Characterization data: *N*-benzyl-*N*-tert-butylloxycarbonylaminophthalimide (**3**) was obtained as white solid (yield 90%) after flash chromatography (0.04 - 0.063 μm) using (15% ethyl acetate : 85% petroleum ether) as eluent; m.p. 107 - 109 °C; ¹H NMR (300 MHz, CDCl₃, 8.0 mmol L⁻¹) δ_H 1.37 and 1.52 (2 s, 9H, C(CH₃)₃), 4.85 and 4.89 (2 s, 2H, NCH₂), 7.27 - 7.44 (2 m, 5H, H arom Ph), 7.73-7.84 (m, 4H, H arom Phth). ¹³C NMR (75 MHz, CDCl₃, 8.0 mmol L⁻¹) δ_C 28.59 and 28.86 (C(CH₃)₃), 53.35 and 55.32 (NCH₂), 83.17 and 83.95 (C(CH₃)₃), 124.41 (CH arom Phth), 128.58 (CH arom Ph), 129.02 (CH arom Ph), 129.20 (CH arom Ph), 129.73 (CH arom Ph), 130.44 (C arom), 130.64 (C arom), 135.20 (CH arom Phth), 154.18 (N-COOt-Bu), 165.71 (O=C-Pht). IR (NaCl) $\tilde{\nu}_{\max}$ = 1737 cm⁻¹, 1796 cm⁻¹ (C=O). HRMS (ESI) for [C₂₀H₂₀N₂O₄]: calculated [M+Na]⁺ (m/z) 375.1321; found, 375.1314.

Synthesis of *N*-alkylaminophthalimide (4): To a solution of *N*-alkyl-*N*-tert-butylloxycarbonylaminophthalimide **3** (1.0 equiv) in CH₂Cl₂, trifluoroacetic acid (10.0 equiv, 8.0% in CH₂Cl₂) was added at 0 °C. The mixture was stirred overnight (monitored by TLC). The solution

was concentrated under vacuum, and then the residue was dissolved in CH₂Cl₂, neutralized with a saturated solution of NaHCO₃ (pH = 7) and extracted three times with CH₂Cl₂. The combined organic layers were dried over MgSO₄ and evaporated under vacuum giving a yellow solid which was immediately used without further purification.

Characterization data: *N*-alkylaminophthalimide (**4**) was obtained as a pure yellow solid (quantitative 100%) without purification; m.p. 109 - 110 °C; ¹H NMR (300 MHz, CDCl₃, 8.0 mmol L⁻¹) δ_H 4.22 (s, 2H, NCH₂), 4.56 (br, 1H, NH), 7.27-7.47 (m, 5H, H arom Ph), 7.71-7.83 (m, 4H, H arom Phth). ¹³C NMR (75 MHz, CDCl₃, 10.0 mmol L⁻¹) δ_C 55.97 (NCH₂), 124.07 (CH arom Phth), 128.73 (CH arom Ph), 129.22 (CH arom Ph), 129.89 (CH arom Ph), 130.92 (C arom Phth), 134.87 (CH arom Phth), 136.69 (C arom Ph), 167.06 (O=C-Pht). IR (NaCl) $\tilde{\nu}_{\max}$ = 3290 cm⁻¹ (NH); 1774 cm⁻¹, 1719 cm⁻¹ (C=O). HRMS (ESI) for [C₁₅H₁₂N₂O₂]: calculated [M+H]⁺ (m/z) 253.0977; found, 253.0963.

Synthesis of *Pht*-azaPhe-Ala-OMe (5a): To a mixture of *N*-alkylaminophthalimide (**4**) (1.0 equiv) and DIPEA (2.2 equiv) in dry CH₂Cl₂, phosgene 20% in toluene (1.5 equiv) was added. After 15 min stirring, the toluene solvent and excess of phosgene gas were removed by rotary evaporator under ventilated hood. The white acid chloride residue was re-dissolved in dry CH₂Cl₂, then solution of alanine methyl ester hydrochloride (1.0 equiv) and DIPEA (1.5 equiv) in dry CH₂Cl₂ was added in one portion. The reaction mixture was stirred for 1 h at RT. The solvent was evaporated to dryness, diluted with CH₂Cl₂, washed with aqueous HCl (1N), aqueous NaHCO₃ (1N) and brine, dried over MgSO₄ and evaporated. Compound **5a** was obtained in pure form after precipitation in cold diethyl ether.

Characterization data: *Pht*-azaPhe-Ala-OMe (**5a**) was obtained as a pure white solid (yield 92%) after trituration with cold diethyl ether; m.p. 158 - 161 °C; ¹H NMR (300 MHz, CDCl₃, 8.0 mmol L⁻¹) δ_H 1.38 and 1.40 (d, 3H, CH₃), 3.72 (s, 3H, COOCH₃), 4.53 (m, 1H, C^αH), 4.86-4.97 (m, 2H, CH₂), 5.31 and 5.37 (d, 1H, NH), 7.23-7.42 (m, 5H, H arom Ph), 7.75-7.85 (m, 4H, H arom Phth). ¹³C NMR (75 MHz, CDCl₃, 10.0 mmol L⁻¹) δ_C 19.60 (CH₃), 50.19 (C^αH), 53.14 (COOCH₃), 53.62 (NCH₂), 124.62 (CH arom Phth), 128.89 (CH arom Ph), 129.20 (CH arom Ph), 129.80 (C arom Phth), 135.33 (C arom Ph), 135.51 (CH arom Phth), 156.15 (O=C-NH), 165.84 (O=C-Pht), 174.32 (COOCH₃). IR (ATR) $\tilde{\nu}_{\max}$ = 3353 cm⁻¹ (NH); 1647 cm⁻¹, 1677 cm⁻¹, 1736 cm⁻¹, 1751 cm⁻¹ (C=O). HRMS (ESI) for [C₂₀H₁₉N₃O₅]: calculated [M+Na+MeOH]⁺ (m/z) 436.1479; found, 436.1457.

Synthesis of *Pht*-azaPhe-Lys(z)-OMe (5b): To a mixture of *N*-alkylaminophthalimide (**4**) (1.0 equiv) and DIPEA (2.2 equiv) in dry CH₂Cl₂, phosgene 20% in toluene (1.5 equiv) was added. After 15 min stirring, the toluene solvent and excess of phosgene gas were removed by rotary evaporator under ventilated hood. The white acid chloride residue was further re-dissolved in dry CH₂Cl₂, then solution of lysine(z) methyl ester hydrochloride (1.0 equiv) and DIPEA (1.5 equiv) in dry CH₂Cl₂ was added in one portion. The reaction mixture was stirred for 1 h at RT. The solvent was evaporated to dryness, diluted with CH₂Cl₂, washed with aqueous HCl (1N), aqueous NaHCO₃ (1N)

and brine, dried over MgSO_4 and evaporated. Compound **5b** was obtained in pure form after precipitation in cold EtOAc.

Characterization data: Pht-azaPhe-Lys(z)-OMe (**5b**) was obtained as a pure white solid (yield 88%) after precipitation with cold ethyl acetate; m.p. 134 - 135 °C; $^1\text{H NMR}$ (300 MHz, CDCl_3 , 8.0 mmol L^{-1}) δ_{H} 1.23-1.86 (m, 6H, ($\text{C}^{\beta}\text{H}_2$, $\text{C}^{\delta}\text{H}_2$, $\text{C}^{\delta}\text{H}_2$)), 3.13-3.15 (m, 2H, $\text{C}^{\epsilon}\text{H}_2$), 3.66 (s, 3H, COOCH_3), 4.47-4.54 (m, 1H, $\text{C}^{\alpha}\text{H}$), 4.87 (s, 2H, NCH_2), 5.01 (br s, 1H, $\text{NH}(\text{Z})$), 5.06 (s, 2H, $\text{CH}_2(\text{Z})$), 5.42 and 5.44 (d, 1H, NH), 7.20-7.38 (m, 10H, H arom Ph), 7.68-7.81 (m, 4H, H arom Phth). $^{13}\text{C NMR}$ (75 MHz, CDCl_3 , 10.0 mmol L^{-1}) δ_{C} 22.68 ($\text{C}^{\gamma}\text{H}_2$), 29.82 ($\text{C}^{\delta}\text{H}_2$), 33.01 ($\text{C}^{\beta}\text{H}_2$), 41.39 ($\text{C}^{\epsilon}\text{H}_2$), 53.14 (OCH_3), 53.82 (NCH_2), 53.97 ($\text{C}^{\alpha}\text{H}$), 67.23 (OCH_2), 124.71 (CH arom Phth), 128.70 (CH arom Ph), 128.94 (CH arom Ph), 129.18 (CH arom Ph), 129.24 (CH arom Ph), 129.80 (CH arom Ph), 130.15 (C arom Phth), 130.22 (C arom Phth), 135.37 (C arom Ph), 135.54 (CH arom Phth), 137.42 (C arom Ph), 156.35 (O=C-NH), 157.16 (COOCH_2Ph), 165.82 (O=C-Phth), 165.99 (O=C-Phth), 173.67 (COOCH_3). **IR (ATR)** $\tilde{\nu}_{\text{max}}$ = 3336 cm^{-1} , 3405 cm^{-1} (NH); 1698 cm^{-1} , 1672 cm^{-1} , 1735 cm^{-1} , 1752 cm^{-1} (C=O). **HRMS (ESI)** for $[\text{C}_{31}\text{H}_{32}\text{N}_4\text{O}_7]$: calculated $[\text{M}+\text{Na}]^+$ (m/z) 595.2169; found, 595.2170; calculated $[\text{M}+\text{K}]^+$ (m/z) 611.3254; found, 611.1909.

Synthesis of Boc-azaPhe-Ala-OMe (6a): To a solution of Phth-azaPhe-Ala- OCH_3 (**5a**) (1.0 equiv) in THF, pyrrolidine (3.0 equiv) was added at RT. The mixture was stirred at RT until completion (4 h, monitored by TLC). The solvent and the excess of amine were removed under vacuum giving foam residue. The obtained residue was dissolved in THF, then Boc_2O (1.5 equiv) and a catalytic amount of DMAP (0.15 equiv) were added. The mixture was stirred at RT until completion (12 h, monitored by TLC). The solvent was removed under vacuum, the residue was dissolved in THF and a freshly prepared solution of methylamine (1.5 equiv, 2M in MeOH) was added at RT. The mixture was stirred at RT until completion (12 h, monitored by TLC), the solvent and the excess of amine were removed under vacuum and the residue was purified by column chromatography on silica gel.

Characterization data: Boc-azaPhe-Ala-OMe (**6a**) was obtained as a pure white solid (yield 89%) after flash chromatography (0.04 - 0.063 μm) using (30% ethyl acetate : 70% petroleum ether) as eluent; m.p. 90 - 91 °C; $^1\text{H NMR}$ (300 MHz, CDCl_3 , 8.0 mmol L^{-1}) δ_{H} 1.42-1.47 (m, 12H, CH_3 and $\text{C}(\text{CH}_3)_3$), 3.76 (s, 3H, COOCH_3), 4.50-4.60 (m, 1H, $\text{C}^{\alpha}\text{H}$), 4.85 (br s, 2H, NCH_2), 5.91 and 5.94 (d, 1H, NH), 5.97 (br s, 1H, $\text{NH}(\text{Boc})$), 7.26-7.37 (m, 5H, H arom Ph). $^{13}\text{C NMR}$ (75 MHz, CDCl_3 , 10.0 mmol L^{-1}) δ_{C} 19.70 (CH_3), 28.75 ($\text{C}(\text{CH}_3)_3$), 49.84 ($\text{C}^{\alpha}\text{H}$), 51.25 (NCH_2), 52.99 (COOCH_3), 83.04 ($\text{C}(\text{CH}_3)_3$), 128.53 (CH arom Ph), 129.45 (CH arom Ph), 129.59 (CH arom Ph), 136.73 (C arom Ph), 154.90 ($\text{COO}t\text{-Bu}$), 157.61 (O=C-NH), 174.75 (COOCH_3). **IR (ATR)** $\tilde{\nu}_{\text{max}}$ = 3207 cm^{-1} , 3415 cm^{-1} (NH); 1647 cm^{-1} , 1723 cm^{-1} , 1732 cm^{-1} (C=O). **HRMS (ESI)** for $[\text{C}_{17}\text{H}_{25}\text{N}_3\text{O}_5]$: calculated $[\text{M}+\text{H}]^+$ (m/z) 352.1872; found, 352.1878.

Synthesis of Boc-azaPhe-Lys(z)-OMe (6b): To a solution of Phth-azaPhe-Lys(z)- OCH_3 (**5b**) (1.0 equiv) in THF, pyrrolidine (3.0 equiv) was added at RT. The mixture was stirred at RT until completion (5 h, monitored by TLC). The solvent and the excess of amine were removed under vacuum giving foam residue. The obtained residue

was dissolved in THF, then Boc_2O (1.5 equiv) and a catalytic amount of DMAP (0.15 equiv) were added. The mixture was stirred at RT until completion (12 h, monitored by TLC). The solvent was removed under vacuum, the residue was re-dissolved in THF and a freshly prepared solution of methylamine (1.5 equiv, 2M in MeOH) was added at RT. After a night and by TLC monitoring, the solvent and the excess of amine were removed under vacuum and the residue was purified by column chromatography on silica gel. The volume of the THF during the second step (addition of Boc_2O) is twice the volume used for the first and third steps (pyrrolidine or methyl amine) to inhibit the reactivity of the $\text{N}^{\epsilon}\text{H}$ of lysine in concentrated condition.

Characterization data: Boc-azaPhe-Lys(z)-OMe (**6b**) was obtained as an oily sticky product (yield 85%) after flash chromatography (0.04 - 0.063 μm) using (45% ethyl acetate : 55% petroleum ether) as eluent; $^1\text{H NMR}$ (300 MHz, CDCl_3 , 8.0 mmol L^{-1}) δ_{H} 1.40-1.90 (m, 15H, ($\text{C}^{\beta}\text{H}_2$, $\text{C}^{\delta}\text{H}_2$, $\text{C}^{\delta}\text{H}_2$) and $\text{C}(\text{CH}_3)_3$), 3.15-3.21 (m, 2H, $\text{C}^{\epsilon}\text{H}_2$), 3.73 (s, 3H, COOCH_3), 4.51-4.58 (m, 1H, $\text{C}^{\alpha}\text{H}$), 4.99 (br s, 2H, NCH_2), 5.07 (s, 2H, $\text{CH}_2(\text{Z})$), 5.89 and 5.92 (d, 1H, NH), 6.02 (br s, 1H, $\text{NH}(\text{Boc})$), 7.22-7.33 (m, 10H, H arom Ph). $^{13}\text{C NMR}$ (75 MHz, CDCl_3 , 10.0 mmol L^{-1}) δ_{C} .70 (CH_3), δ_{C} 22.89 ($\text{C}^{\gamma}\text{H}_2$), 28.73 ($\text{C}(\text{CH}_3)_3$), 29.82 ($\text{C}^{\delta}\text{H}_2$), 33.33 ($\text{C}^{\beta}\text{H}_2$), 41.39 ($\text{C}^{\epsilon}\text{H}_2$), 51.39 (NCH_2), 53.00 (OCH_3), 53.61 ($\text{C}^{\alpha}\text{H}$), 67.23 (OCH_2), 83.10 ($\text{C}(\text{CH}_3)_3$), 128.56 (CH arom Ph), 128.70 (CH arom Ph), 128.76 (CH arom Ph), 129.15 (CH arom Ph), 129.46 (CH arom Ph), 129.59 (CH arom Ph), 136.72 (C arom Ph), 137.38 (C arom Ph), 154.87 ($\text{COO}t\text{-Bu}$), 156.17 (O=C-NH), 157.86 (COOCH_2Ph), 174.13 (COOCH_3). **IR (ATR)** $\tilde{\nu}_{\text{max}}$ = 3331 cm^{-1} , 3439 cm^{-1} (NH); 1656 cm^{-1} , 1701 cm^{-1} , 1718 cm^{-1} , 1735 cm^{-1} (C=O). **HRMS (ESI)** for $[\text{C}_{28}\text{H}_{38}\text{N}_4\text{O}_7]$: calculated $[\text{M}+\text{Na}]^+$ (m/z) 565.2638; found, 565.2643; calculated $[\text{M}+\text{K}]^+$ (m/z) 581.3723; found, 581.2377.

General protocol for the synthesis of 2:1-[α /aza]-trimers:

Boc deprotection: To a stirred solution of Boc protected compound (**6**) (1.0 equiv) in CH_2Cl_2 , ethyl acetate (3.0 M HCl) was added at 0 °C. The resulting solution was stirred until completion (1-2 h, monitored by TLC) and concentrated under vacuum. The excess hydrochloride acid was co-evaporated with CH_2Cl_2 (4 times). The residue was used in coupling reaction without further purification.

Acid fluoride preparation: To a stirred solution of Boc-*D*- or *L*-AA-OH (1.5 equiv, AA = Phe, Lys(z), *D*-Phe, or *D*-Lys(z)) in dry CH_2Cl_2 and pyridine (1.5 equiv) kept under a N_2 atmosphere, cyanuric fluoride (3.0 equiv) was added dropwise at -20 °C. The solution was stirred at -10 °C during 4 h and a precipitate or emulsion formed, and its amount gradually increased. Then, crushed ice was added along with an additional cold CH_2Cl_2 . The organic layer was separated, and the aqueous layer extracted with cold CH_2Cl_2 . The combined organic layers were washed with ice-cold water and dried over MgSO_4 , and the solvent was removed with a rotary evaporator at room temperature to yield the acyl fluoride product which was directly used in the coupling reaction.

Coupling reaction: Boc-*D*- or *L*-AA-F (1.5 equiv, AA = Phe, or Lys(z)) in CH_2Cl_2 was added dropwise to a stirred solution of HCl, H-azaPhe-AA-

OMe (1.0 equiv, AA = Ala, or Lys(z)) in CH₂Cl₂ and NaHCO₃ (2.0 equiv), pH = 7 - 8. The mixture was stirred at RT overnight monitoring by TLC. Then, the organic layer (CH₂Cl₂) was washed twice with HCl (1N), NaHCO₃ (1N) and saturated NaCl, and then was dried over MgSO₄ and the solvent was removed under vacuum and the residue was purified by column chromatography on silica gel.

Characterization data for 2:1-[α/aza]-trimers:

Boc-Phe-azaPhe-Ala-OMe (7a) was obtained as a white solid (yield 74%) after flash chromatography (0.04 – 0.063 μm) using (50% ethyl acetate : 50% petroleum ether) as eluent; m.p. 149 - 150 °C; ¹H NMR (300 MHz, CDCl₃, 10.0 mmol L⁻¹) δ_H 1.37-1.43 (m, 12H, CH₃ and C(CH₃)₃), 2.88-2.95 and 3.01-3.08 (m, 2H, CH₂), 3.71 (s, 3H, COOCH₃), 4.03 (m, 1H, CH), 4.28 (br s, 1H, NHBoc), 4.43-4.51 (m, 1H, CH), 4.90-4.95 (br m, 2H, NCH₂), 6.2 (br s, 1H, NH), 7.06-7.30 (m, 10H, H arom Ph), 7.73 (br s, 1H, NH). ¹³C NMR (75 MHz, CDCl₃) δ_C 18.71 (CH₃), 28.88 (C(CH₃)₃), 37.83 (CH₂), 50.11 (C^αH), 52.01 (NCH₂), 52.86 (COOCH₃), 56.0 (C^αH), 81.55 (C(CH₃)₃), 128.05 (CH arom Ph), 128.25 (CH arom Ph), 129.15 (CH arom Ph), 129.42 (CH arom Ph), 129.63 (CH arom Ph), 129.85 (CH arom Ph), 136.45 (C arom Ph), 137.10 (C arom Ph), 156.43 (COOt-Bu), 157.57 (O=C-NH), 171.08 (O=C-NH), 174.88 (COOCH₃). IR (CDCl₃) $\tilde{\nu}_{\max}$ = 3370 cm⁻¹, 3440 cm⁻¹ (NH); 1656 cm⁻¹, 1673 cm⁻¹, 1705 cm⁻¹, 1723 cm⁻¹, 1743 cm⁻¹ (C=O). HRMS (ESI) for [C₂₆H₃₄N₄O₆]: calculated [M+Na]⁺ (m/z) 521.2376; found, 521.2344.

Boc-D-Phe-azaPhe-Ala-OMe (7b) was obtained as a white solid (yield 70%) after flash chromatography (0.04 – 0.063 μm) using (50% ethyl acetate : 50% petroleum ether) as eluent; m.p. 72 - 73 °C; ¹H NMR (300 MHz, CDCl₃, 8.0 mmol L⁻¹) δ_H 1.39-1.41 (m, 12H, CH₃ and C(CH₃)₃), 2.82-2.89 and 3.09-3.16 (m, 2H, CH₂), 3.71 (s, 3H, COOCH₃), 4.09-4.16 (m, 1H, C^αH), 4.42-4.49 (br m, 1H, C^αH), 4.67 (br s, 2H, NCH₂), 4.79 (br d, 1H, NHBoc), 6.04 (br s, 1H, NH), 7.12-7.35 (m, 10H, H arom Ph), 7.52 (br s, 1H, NH). ¹³C NMR (75 MHz, CDCl₃, 10.0 mmol L⁻¹) δ_C 18.57 (CH₃), 28.88 (C(CH₃)₃), 37.90 (CH₂), 50.03 (C^αH), 51.86 (NCH₂), 52.85 (COOCH₃), 56.27 (C^αH), 81.96 (C(CH₃)₃), 128.16 (CH arom Ph), 128.35 (CH arom Ph), 129.23 (CH arom Ph), 129.56 (CH arom Ph), 129.75 (CH arom Ph), 129.82 (CH arom Ph), 136.30 (C arom Ph), 137.18 (C arom Ph), 156.69 (COOt-Bu), 157.54 (O=C-NH), 170.90 (O=C-NH), 174.67 (COOCH₃). IR (CDCl₃) $\tilde{\nu}_{\max}$ = 3372 cm⁻¹, 3439 cm⁻¹ (NH), 1657 cm⁻¹, 1674 cm⁻¹, 1705 cm⁻¹, 1721 cm⁻¹, 1741 cm⁻¹ (C=O). HRMS (ESI) for [C₂₆H₃₄N₄O₆]: calculated [M+Na]⁺ (m/z) 521.2376; found, 521.2389.

Boc-Lys(z)-azaPhe-Lys(z)-OMe (7c) was obtained as a white foam (yield 72%) after flash chromatography (0.04 – 0.063 μm) using (60% dichloromethane : 38.5% ethyl acetate : 1.5% methanol) as eluent; ¹H NMR (300 MHz, CDCl₃, 8.0 mmol L⁻¹) δ_H 1.31 (s, 9H, C(CH₃)₃), 1.32-1.78 (m, 12H, 2*(C^βH₂, C^εH₂, C^δH₂)), 2.98-3.04 (m, 2H, C^εH₂), 3.07-3.14 (m, 2H, C^εH₂), 3.62 (s, 3H, COOCH₃), 3.73 (br m, 1H, C^αH), 4.45-4.47 (m, 1H, C^αH), 4.78 (br s, 1H, NHZ), 4.36 and 4.86 (m, 2H, NCH₂), 4.99 (s, 2H, CH₂(Z)), 5.00 (s, 2H, CH₂(Z)), 5.06 (br, 1H, NHBoc), 5.24 (br s, 1H, NHZ), 5.91 (br s, 1H, NH), 7.17-7.26 (m, 15H, H arom Ph), 7.75 (br s, 1H, NH). ¹³C NMR (75 MHz, CDCl₃, 10.0 mmol L⁻¹) δ 22.79 (C^γH₂), 22.93 (C^γH₂), 29.01 (C(CH₃)₃), 29.51 (C^δH₂), 29.98 (C^δH₂), 31.23

(C^βH₂), 32.41 (C^βH₂), 40.70 (C^εH₂), 41.32 (C^εH₂), 51.91 (NCH₂), 52.92 (OCH₃), 53.76 (C^αH), 54.02 (C^αH), 67.33 (OCH₂), 67.43 (OCH₂), 81.27 (C(CH₃)₃), 128.40 (CH arom Ph), 128.75 (CH arom Ph), 128.85 (CH arom Ph), 129.19 (CH arom Ph), 129.30 (CH arom Ph), 129.35 (CH arom Ph), 137.20 (C arom Ph), 156.69 (COOt-Bu), 157.29 (O=C-CH₂Ph), 157.68 (O=C-NH), 172.20 (O=C-NH), 174.06 (COOCH₃). IR (CDCl₃) $\tilde{\nu}_{\max}$ = 3378 cm⁻¹, 3449 cm⁻¹ (NH), 1652 cm⁻¹, 1677 cm⁻¹, 1701 cm⁻¹, 1717 cm⁻¹, 1735 cm⁻¹, 1748 cm⁻¹ (C=O). HRMS (ESI) for [C₄₂H₅₆N₆O₁₀]: calculated [M+Na]⁺ (m/z) 827.3956 found, 827.3978; calculated [M+K]⁺ (m/z) 843.3695 found, 843.3715.

Boc-D-Lys(z)-azaPhe-Lys(z)-OMe (7d) was obtained as a white foam (yield 69%) after flash chromatography (0.04 – 0.063 μm) using (60% dichloromethane : 38.5% ethyl acetate : 1.5% methanol) as eluent; ¹H NMR (300 MHz, CDCl₃, 8.0 mmol L⁻¹) δ_H 1.41 (s, 9H, C(CH₃)₃), 1.42-1.87 (m, 12H, 2*(C^βH₂, C^εH₂, C^δH₂)), 3.06-3.11 (m, 2H, C^εH₂), 3.16-3.20 (m, 2H, C^εH₂), 3.68 (s, 3H, COOCH₃), 3.80 (m, 1H, C^αH), 4.41-4.44 (m, 1H, C^αH), 4.48 and 5.00 (m, 2H, NCH₂), 4.82 br s, 1H, NHZ), 5.05 (s, 2H, CH₂(Z)), 5.08 (s, 2H, CH₂(Z)), 5.24 (br, 1H, NHBoc), 5.43 (br s, 1H, NHZ), 6.15 and 6.16 (br d, 1H, NH), 7.26-7.34 (m, 15H, H arom Ph), 7.83 (br s, 1H, NH). ¹³C NMR (75 MHz, CDCl₃, 10.0 mmol L⁻¹) δ 22.51 (C^γH₂), 23.13 (C^γH₂), 28.99 (C(CH₃)₃), 29.43 (C^δH₂), 30.21 (C^δH₂), 30.92 (C^βH₂), 31.71 (C^βH₂), 40.27 (C^εH₂), 40.91 (C^εH₂), 51.96 (NCH₂), 52.82 (OCH₃), 54.18 (C^αH), 55.36 (C^αH), 67.09 (OCH₂), 67.48 (OCH₂), 81.81 (C(CH₃)₃), 128.35 (CH arom Ph), 128.65 (CH arom Ph), 128.83 (CH arom Ph), 128.91 (CH arom Ph), 129.15 (CH arom Ph), 129.23 (CH arom Ph), 129.59 (CH arom Ph), 137.10 (C arom Ph), 137.39 (C arom Ph), 137.55 (C arom Ph), 157.25 (COOt-Bu), 157.41 (O=C-CH₂Ph), 157.63 (O=C-CH₂Ph), 157.97 (O=C-NH), 171.82 (O=C-NH), 174.28 (COOCH₃). IR (CDCl₃) $\tilde{\nu}_{\max}$ = 3302 cm⁻¹, 3375 cm⁻¹, 3449 cm⁻¹ (NH), 1652 cm⁻¹, 1675 cm⁻¹, 1702 cm⁻¹, 1718 cm⁻¹, 1734 cm⁻¹, 1749 cm⁻¹ (C=O). HRMS (ESI) for [C₄₂H₅₆N₆O₁₀]: calculated [M+Na]⁺ (m/z) 827.3956 found, 827.3986; calculated [M+K]⁺ (m/z) 843.3695 found, 843.3714.

Boc-Phe-azaPhe-Lys(z)-OMe (7e) was obtained as a white foam (yield 65%) after flash chromatography (0.04 – 0.063 μm) using (70% dichloromethane : 29% ethyl acetate : 1.0% methanol) as eluent; ¹H NMR (300 MHz, CDCl₃, 10.0 mmol L⁻¹) δ_H 1.38 (s, 9H, C(CH₃)₃), 1.48-1.85 (m, 6H, (C^βH₂, C^εH₂, C^δH₂)), 2.74-2.80 and 2.94-3.01 (m, 2H, CH₂), 3.18-3.26 (m, 2H, C^εH₂), 3.69 (s, 3H, COOCH₃), 3.97 (m, 1H, C^αH), 4.02 (br s, 1H, NHBoc), 4.48-4.54 (m, 1H, C^αH), 5.02 and 5.03 (br d, 2H, NCH₂), 5.08 (s, 2H, CH₂(Z)), 5.40 (br s, 1H, NHZ), 5.97 and 5.99 (br d, 1H, NH), 6.97-7.34 (m, 15H, H arom Ph), 7.58 (br s, 1H, NH). ¹³C NMR (75 MHz, CDCl₃, 10.0 mmol L⁻¹) δ 22.89 (C^γH₂), 28.96 (C(CH₃)₃), 29.49 (C^δH₂), 32.33 (C^βH₂), 37.61 (CH₂Ph), 41.23 (C^εH₂), 52.12 (NCH₂), 52.80 (OCH₃), 53.75 (C^αH), 55.91 (C^αH), 67.28 (OCH₂), 81.61 (C(CH₃)₃), 128.01 (CH arom Ph), 128.28 (CH arom Ph), 128.74 (CH arom Ph), 128.90 (CH arom Ph), 129.18 (CH arom Ph), 129.36 (CH arom Ph), 129.57 (CH arom Ph), 129.93 (CH arom Ph), 136.55 (C arom Ph), 137.07 (C arom Ph), 137.35 (C arom Ph), 156.46 (COOt-Bu), 157.19 (O=C-CH₂Ph), 157.45 (O=C-NH), 171.20 (O=C-NH), 173.87 (COOCH₃). IR (CDCl₃) $\tilde{\nu}_{\max}$ = 3374 cm⁻¹, 3444 cm⁻¹ (NH), 1653 cm⁻¹, 1674 cm⁻¹, 1706 cm⁻¹, 1721 cm⁻¹, 1744 cm⁻¹ (C=O). HRMS (ESI) for [C₃₇H₄₇N₅O₈]:

calculated $[M+Na]^+$ (m/z) 712.3322 found, 712.3339; calculated $[M+K]^+$ (m/z) 728.3062 found, 728.3042.

Boc-D-Phe-azaPhe-Lys(z)-OMe (7f) was obtained as a white foam (yield 62%) after flash chromatography (0.04–0.063 μ m) using (70% dichloromethane : 29% ethyl acetate : 1.0% methanol) as eluent; 1H NMR (300 MHz, $CDCl_3$, 10.0 mmol L⁻¹) δ_H 1.37 (s, 9H, C(CH₃)), 1.23–1.87 (m, 6H, (C ^{β} H₂, C ^{ϵ} H₂, C ^{δ} H₂)), 2.71–2.79 and 2.93–3.00 (m, 2H, CH₂), 3.18–3.23 (m, 2H, C ^{ϵ} H₂), 3.68 (s, 3H, COOCH₃), 4.11–4.14 (m, 1H, C ^{α} H), 4.37–4.44 (m, 1H, C ^{α} H), 4.55 and 4.68 (br, 2H, NCH₂), 4.75 (br s, 1H, NHBoc), 5.02 (s, 2H, CH₂(Z)), 5.24–5.31 (br m, 1H, NHZ), 6.08 and 6.10 (br d, 1H, NH), 7.10–7.33 (m, 15H, H arom Ph), 7.78 (br s, 1H, NH). ^{13}C NMR (75 MHz, $CDCl_3$, 10.0 mmol L⁻¹) δ 23.37 (C ^{γ} H₂), 28.90 (C(CH₃)), 29.51 (C ^{δ} H₂), 31.70 (C ^{β} H₂), 37.81 (CH₂Ph), 41.01 (C ^{ϵ} H₂), 52.07 (NCH₂), 52.78 (OCH₃), 54.18 (C ^{α} H), 56.18 (C ^{α} H), 67.13 (OCH₂), 81.09 (C(CH₃)₃), 128.15 (CH arom Ph), 128.30 (CH arom Ph), 128.69 (CH arom Ph), 129.17 (CH arom Ph), 129.52 (CH arom Ph), 129.73 (CH arom Ph), 136.11 (C arom Ph), 137.36 (C arom Ph), 156.95 (COO^{*t*}-Bu), 157.22 (O=C-CH₂Ph), 157.85 (O=C-NH), 171.10 (O=C-NH), 174.04 (COOCH₃). IR ($CDCl_3$) $\tilde{\nu}_{max}$ = 3376 cm⁻¹, 3444 cm⁻¹ (NH), 1652 cm⁻¹, 1673 cm⁻¹, 1707 cm⁻¹, 1720 cm⁻¹, 1744 cm⁻¹ (C=O). HRMS (ESI) for [C₃₇H₄₇N₅O₈]: calculated $[M+Na]^+$ (m/z) 712.3322 found, 712.3327; calculated $[M+K]^+$ (m/z) 728.3062 found, 728.3028.

General protocol for the synthesis of 2:1-[α /aza]-oligomer:

Homo and heterochiral 2:1-[α /aza]-hexamers (**8**) were obtained by classical peptidic coupling based on the monomeric building blocks of 2:1-[α /aza]-trimers (**7**).

Boc deprotection: To a stirred solution of Boc protected compound (**7**, 1.0 equiv) in CH₂Cl₂, ethyl acetate (2M HCl) was added at 0 °C. The resulting solution was stirred until completion monitored by TLC (2–4 h) and concentrated under vacuum. The excess of hydrochloric acid was co-evaporated with CH₂Cl₂ (4 times). The residue was used in coupling reaction without further purification.

Methyl ester deprotection: To a stirred solution of methyl ester protected compound (**7**, 1.0 equiv) in CH₃CN, an aqueous solution of NaOH 1N (2.0 equiv) was added at 0 °C. The resulting solution was stirred until completion monitored by TLC (4–10 h), then aqueous HCl (2N) was added under vigorously stirring (pH = 2). The aqueous layer was extracted twice with CH₂Cl₂, then the combined organic layers were dried over MgSO₄ and evaporated. The residue was used in coupling reaction without further purification.

Coupling reaction: To a stirred solution of the Boc-deprotected trimer (amine partner, 1.0 equiv) in CH₂Cl₂ were successively added at RT; DIPEA (2.2 equiv), deprotected methyl ester trimer (acid partner, 1.1 equiv) and HOBT (1.2 equiv). After a night to 24 h, the mixture was diluted with aqueous HCl (1N) under vigorously stirring (pH = 2). The organic layer was washed with water, aqueous NaHCO₃ (0.5N), brine, dried over MgSO₄ and evaporated. The residue was purified by column chromatography on silica gel.

It should be mentioned that the better yields of hexamers containing lysine residues (**8c** and **8d**) were obtained upon carrying the coupling reaction in CH₃CN with HBTU/DIPEA.

Characterization data for 2:1-[α /aza]-hexamers:

Boc-(Phe-azaPhe-Ala)₂-OMe (8a) was obtained as a white solid (yield 87%) after flash chromatography (0.04 – 0.063 μ m) using (60% ethyl acetate : 40% petroleum ether) as eluent; m.p. 132 – 133 °C; 1H NMR (300 MHz, CD_3CN , 8.0 mmol L⁻¹) δ_H 1.18 and 1.21 (d, 3H, CH₃), 1.34–1.38 (m, 12H, CH₃ and C(CH₃)₃), 2.77–2.84 (m, 1H, CH₂), 2.96–3.04 (m, 2H, CH₂), 3.18–3.24 (m, 1H, CH₂), 3.62 (s, 3H, COOCH₃), 3.89–3.98 (m, 1H, C ^{α} H), 4.02–4.09 (m, 1H, C ^{α} H), 4.20–4.29 (m, 2H, 2* ^{α} H), 4.48–4.84 (br m, 4H, 2*NCH₂), 5.62 (br s, 1H, NH), 6.37 (br s, 1H, NH), 6.53 (br s, 1H, NH), 7.17–7.32 (m, 21H: 20H, arom Ph, and 1H, NH), 9.01 (br s, 2H, 2*NH). ^{13}C NMR (75 MHz, CD_3CN , 10.0 mmol L⁻¹) δ_C 17.33 (CH₃), 18.02 (CH₃), 28.62 (C(CH₃)₃), 37.46 (CH₂), 37.59 (CH₂), 50.52 (C ^{α} H), 50.66 (C ^{α} H), 52.75 (C ^{α} H and COOCH₃), 52.94 (NCH₂), 53.32 (NCH₂), 54.63 (C ^{α} H), 81.3 (C(CH₃)₃), 127.81 (CH arom Ph), 128.30 (CH arom Ph), 128.78 (CH arom Ph), 129.19 (CH arom Ph), 129.34 (CH arom Ph), 129.53 (CH arom Ph), 129.70 (CH arom Ph), 129.83 (CH arom Ph), 130.20 (CH arom Ph), 130.28 (CH arom Ph), 130.37 (CH arom Ph), 130.68 (CH arom Ph), 137.61 (C arom Ph), 138.01 (C arom Ph), 138.52 (C arom Ph), 139.91 (C arom Ph), 158.03 (O=C-NH), 159.41 (O=C-NH), 171.4 (O=C-NH), 175.33 (COOCH₃). IR ($CDCl_3$) $\tilde{\nu}_{max}$ = 3259 cm⁻¹, 3351 cm⁻¹, 3401 cm⁻¹, 3438 cm⁻¹ (NH), 1665 cm⁻¹, 1700 cm⁻¹, 1741 cm⁻¹ (C=O). HRMS (ESI) for [C₄₆H₅₆N₈O₉]: calculated $[M+Na]^+$ (m/z) 887.4062 found, 887.4068.

Boc-(D-Phe-azaPhe-Ala)₂-OMe (8b) was obtained as a white solid (yield 85%) after flash chromatography (0.04 – 0.063 μ m) using (60% ethyl acetate : 40% petroleum ether) as eluent; m.p. 172 – 173 °C; 1H NMR (300 MHz, CD_3CN , 8.0 mmol L⁻¹) δ_H 1.28 and 1.30 (d, 3H, CH₃), 1.34 (s, 9H, C(CH₃)₃), 1.35 and 1.37 (d, 3H, CH₃), 2.73–2.81 (m, 1H, CH₂), 2.91–2.98 (m, 1H, CH₂), 3.06–3.10 (m, 1H, CH₂), 3.17–3.23 (m, 1H, CH₂), 3.62 (s, 3H, COOCH₃), 3.89–4.08 (m, 2H, 2* ^{α} H), 4.10–4.24 (m, 2H, 2* ^{α} H), 4.33–4.67 (br m, 4H, 2*NCH₂), 5.62 (br s, 1H, NH), 6.45–6.57 (br, 2H, 2NH), 7.12–7.31 (m, 21H: 20H, arom Ph, and 1H, NH), 8.73 (s, 1H, NH), 9.13 (br s, 1H, NH). ^{13}C NMR (75 MHz, CD_3CN , 10.0 mmol L⁻¹) δ_C 17.11 (CH₃), 18.11 (CH₃), 28.70 (C(CH₃)₃), 36.81 (CH₂), 37.36 (CH₂), 50.52 (C ^{α} H), 52.27 (NCH₂), 52.64 (C ^{α} H and COOCH₃), 52.86 (NCH₂), 55.63 (C ^{α} H), 56.43 (C ^{α} H), 81.18 (C(CH₃)₃), 127.83 (CH arom Ph), 127.96 (CH arom Ph), 128.13 (CH arom Ph), 128.43 (CH arom Ph), 129.20 (CH arom Ph), 129.28 (CH arom Ph), 129.61 (CH arom Ph), 129.77 (CH arom Ph), 130.35 (CH arom Ph), 137.95 (C arom Ph), 138.41 (C arom Ph), 138.96 (C arom Ph), 158.32 (O=C-NH), 159.12 (O=C-NH), 171.26 (O=C-NH), 176.38 (COOCH₃). IR ($CDCl_3$) $\tilde{\nu}_{max}$ = 3240 cm⁻¹, 3351 cm⁻¹, 3423 cm⁻¹ (NH), 1635 cm⁻¹, 1665 cm⁻¹, 1704 cm⁻¹, 1741 cm⁻¹ (C=O). HRMS (ESI) for [C₄₆H₅₆N₈O₉]: calculated $[M+Na]^+$ (m/z) 887.4062 found, 887.4066.

Boc-(Lys(z)-azaPhe-Lys(z))₂-OMe (8c) was obtained as a white foam (yield 64%) after flash chromatography (0.04 – 0.063 μ m) using (50% dichloromethane : 48% ethyl acetate : 2% methanol) as eluent; 1H NMR (300 MHz, CD_3CN , 8.0 mmol L⁻¹) δ_H 1.37 (s, 9H, C(CH₃)), 1.38–

1.78 (m, 24H, 4*(C^βH₂, C^δH₂, and C^εH₂)), 3.02-3.09 (m, 8H, 4*(C^εH₂)), 3.64 (s, 3H, COOCH₃), 3.66-3.69 (br m, 1H, C^αH), 3.93-3.99 (m, 2H, 2*C^αH), 4.13-4.20 (m, 1H, C^αH), 4.32-4.95 (br m, 4H, 2*NCH₂), 5.02 (s, 2H, CH₂(Z)), 5.04 (s, 2H, CH₂(Z)), 5.68 (br s, 2H, 2*NHZ), 5.76 (br s, 1H, NHZ), 5.83 (br s, 1H, NHZ), 5.93 (br, 1H, NHBoc), 6.29 and 6.31 (d, 1H, NH), 6.53 (br s, 1H, NH), 7.03 (d, 1H, NH), 7.16-7.34 (m, 30H, H arom Ph), 8.91 (br s, 1H, NH), 9.02 (br s, 1H, NH). ¹³C NMR (75 MHz, CD₃CN, 10.0 mmol L⁻¹) δ_C 23.21 (C^γH₂), 24.06 (C^γH₂), 28.77 (C(CH₃)), 30.29 (C^δH₂), 31.11 (C^δH₂), 31.49 (C^δH₂), 32.19 (C^δH₂), 40.88 (C^εH₂), 41.43 (C^εH₂), 41.49 (C^εH₂), 41.62 (C^εH₂), 52.09 (NCH₂), 52.56 (OCH₃), 53.02 (NCH₂), 54.91 (C^αH), 66.74 (OCH₂), 66.79 (OCH₂), 66.88 (OCH₂), 66.94 (OCH₂), 81.15(C(CH₃)₃), 128.22 (CH arom Ph), 128.60 (CH arom Ph), 128.73 (CH arom Ph), 128.83 (CH arom Ph), 128.89 (CH arom Ph), 128.95 (CH arom Ph), 129.33 (CH arom Ph), 129.52 (CH arom Ph), 130.22 (CH arom Ph), 138.50 (C arom Ph), 138.59 (C arom Ph), 138.67 (C arom Ph), 138.81 (C arom Ph), 157.50 (COO^t-Bu), 157.81 (O=C-CH₂Ph), 158.56 (O=C-CH₂Ph), 159.80 (O=C-NH), 159.98 (O=C-NH), 172.07 (O=C-NH), 174.69 (COOCH₃). IR (CDCl₃) $\tilde{\nu}_{\max}$ = 3256 cm⁻¹, 3349 cm⁻¹, 3450 cm⁻¹ (NH), 1651 cm⁻¹, 1667 cm⁻¹, 1699 cm⁻¹, 1712 cm⁻¹, 1724 cm⁻¹, 1740 cm⁻¹ (C=O). HRMS (ESI) for [C₇₈H₁₀₀N₁₂O₁₇]: calculated [M+Na]⁺ (m/z) 1499.7227, found, 1499.7181; calculated [M²⁺+Na] (m/z) 761.3615, found 761.3664.

Boc-(D-Lys(z)-azaPhe-Lys(z))₂-OMe (**8d**) was obtained as a white foam (yield 62%) after flash chromatography (0.04 – 0.063 μm) using (50% dichloromethane : 48% ethyl acetate : 2% methanol) as eluent; ¹H NMR (300 MHz, CDCl₃, 8.0 mmol L⁻¹) δ_H 1.36 (s, 9H, C(CH₃)), 1.37-1.77 (m, 24H, 4*(C^βH₂, C^δH₂, and C^εH₂)), 3.03-3.14 (m, 8H, 4*(C^εH₂)), 3.46 (s, 3H, COOCH₃), 3.70-3.75 (br m, 1H, C^αH), 3.87-3.93 (m, H, C^αH), 4.04-4.08 (m, 1H, C^αH), 4.56-4.60 (m, 1H, C^αH), 4.21 (d) and 5.23 (br s) (2H, NCH₂), 4.40 (d) and 4.64 (br s) (2H, NCH₂), 4.82-4.87 (br s, 2H, 2*NHZ), 5.05 (s, 2H, CH₂(Z)), 5.07 (s, 2H, CH₂(Z)), 5.10 (s, 2H, CH₂(Z)), 5.11 (s, 2H, CH₂(Z)), 5.3 (br s, 1H, NHZ), 5.46 (br, 1H, NHBoc), 5.88 (br s, 1H, NHZ), 6.21 and 6.23 (d, 1H, NH), 6.54 (br s, 1H, NH), 7.16-7.34 (m, 31H; 30H arom Ph and 1H, NH), 8.85 (br s, 1H, NH), 9.46 (br s, 1H, NH). ¹³C NMR (75 MHz, CDCl₃, 10.0 mmol L⁻¹) δ_C 21.66 (C^γH₂), 22.42 (C^γH₂), 23.24 (C^γH₂), 23.56 (C^γH₂), 29.27 (C(CH₃)), 29.58 (C^δH₂), 30.23 (C^δH₂), 30.39 (C^δH₂), 31.77 (C^δH₂), 32.18 (C^δH₂), 40.75 (C^εH₂), 40.83 (C^εH₂), 40.85 (C^εH₂), 40.99 (C^εH₂), 51.67 (NCH₂), 52.29 (NCH₂), 52.59 (OCH₃), 53.45 (C^αH), 55.32 (C^αH), 56.59 (C^αH), 56.93 (C^αH), 66.93 (OCH₂), 67.12 (OCH₂), 67.44 (OCH₂), 67.74 (OCH₂), 81.65(C(CH₃)₃), 127.81 (CH arom Ph), 128.20 (CH arom Ph), 128.66 (CH arom Ph), 128.82 (CH arom Ph), 129.00 (CH arom Ph), 129.09 (CH arom Ph), 129.15 (CH arom Ph), 129.30 (CH arom Ph), 130.16 (CH arom Ph), 136.36 (C arom Ph), 136.91 (C arom Ph), 137.15 (C arom Ph), 137.52 (C arom Ph), 137.81 (C arom Ph), 157.17 (COO^t-Bu), 157.44 (O=C-CH₂Ph), 157.79 (O=C-CH₂Ph), 157.96 (O=C-CH₂Ph), 158.21(O=C-NH), 159.41 (O=C-NH), 171.13 (O=C-NH), 171.62 (O=C-NH), 175.8 (COOCH₃). IR (CDCl₃) $\tilde{\nu}_{\max}$ = 3212 cm⁻¹, 3342 cm⁻¹, 3450 cm⁻¹ (NH), 1637 cm⁻¹, 1652 cm⁻¹, 1667 cm⁻¹, 1690 cm⁻¹, 1705 cm⁻¹, 1718 cm⁻¹, 1738 cm⁻¹ (C=O). HRMS (ESI) for [C₇₈H₁₀₀N₁₂O₁₇]: calculated [M+Na]⁺ (m/z) 1499.7227, found, 1499.7153; calculated [M²⁺+Na] (m/z) 761.3615, found 761.3592.

Synthesis of 6b', 7c' and 8c' molecules by deprotection of Z-group from the corresponding protected analogues:

To a stirred solution of an appropriate protected side chain(s) azapeptide (200 mg) in methanol (5.0 mL), 10% Pd/C (20 mg / each Z-group) was added. The resulting reaction mixture was stirred under stream of H₂ gas at room temperature. After completion of the hydrogenolysis (4 – 12 h), the mixture was filtered through a celite bed and washed with methanol. The combined filtrates were evaporated and then the residue was dried well under vacuum before verification by ¹H NMR in DMSO-*d*₆. The deprotection was considered to be successfully achieved if the signals belong to the CH₂ and the aromatic protons of Z-group have been disappeared in the ¹H NMR spectrum.

Membrane preparation: For membrane casting, the Pebax[®]1074 polymer and pseudopeptide additives were dissolved in *n*-butanol during 2 h at 80 °C to obtain a total concentration of 2.5 w/v%. Different series of membranes were prepared using the same weight percentage (4.0 wt%) for each pseudopeptide in the different membranes. After filtering on glass fibers, the solutions were cast on a PTFE mold. After butanol evaporation in a thermal oven at 40 °C, the membranes were easily taken off the mold and were then dried under vacuum at 60 °C for 12 h. Their thicknesses were measured with an Elcometer[™] micrometer after calibration in the thickness range of interest (measurement error: ± 1 μm). The average thickness for the different membranes was ca. 80 μm with a maximum thickness difference between two membrane points of 5 μm.

Gas permeation experiments: The gas permeation properties were determined by the "time-lag" method using an experimental procedure described in our former work on other bio-based pseudopeptide for CO₂ capture membranes.⁵⁵ The gas permeation properties were determined for CO₂ and N₂ pure gases (high purity gases purchased from Messer company) at 35°C and 2 bar. The gas permeation experiments were repeated five times for each membrane and each tested gas to assess the reproducibility from the corresponding experimental errors.

The gas permeability was calculated from the steady-state membrane flux J_{st} estimated from the steady-state slope of the gas permeation curve (describing the pressure increase with time at the membrane downstream side) and the membrane thickness l according to equation (1). In this equation, the downstream side pressure was neglected as usual for "time-lag" experiments because it was much lower than the upstream side pressure of 2 bar:

$$P = \frac{J_{st} \times l}{\Delta p} = \frac{J_{st} \times l}{P_{upstream}} \quad (1)$$

The membrane ideal selectivity was estimated as the ratio of the permeability for pure CO₂ and N₂ according to equation (2):

$$\alpha_{CO_2/N_2} = \frac{P_{CO_2}}{P_{N_2}} \quad (2)$$

ARTICLE

The gas diffusion coefficient D was calculated from the “time-lag” q given by the intercept of the steady-state asymptote of the gas permeation curve on the time axis by equation (3).

$$D = \frac{l^2}{6\theta} \quad (3)$$

Gas permeability is the product of gas diffusion and sorption coefficients according to the solution-diffusion model expressed by equation (4), describing gas permeation in the dense (non-porous) membranes used in this work⁵⁶:

$$P = D \times S \quad (4)$$

Consequently, the gas sorption coefficient (S) was then calculated as the ratio of the permeability (P) to the diffusion coefficient (D).

Results and discussion

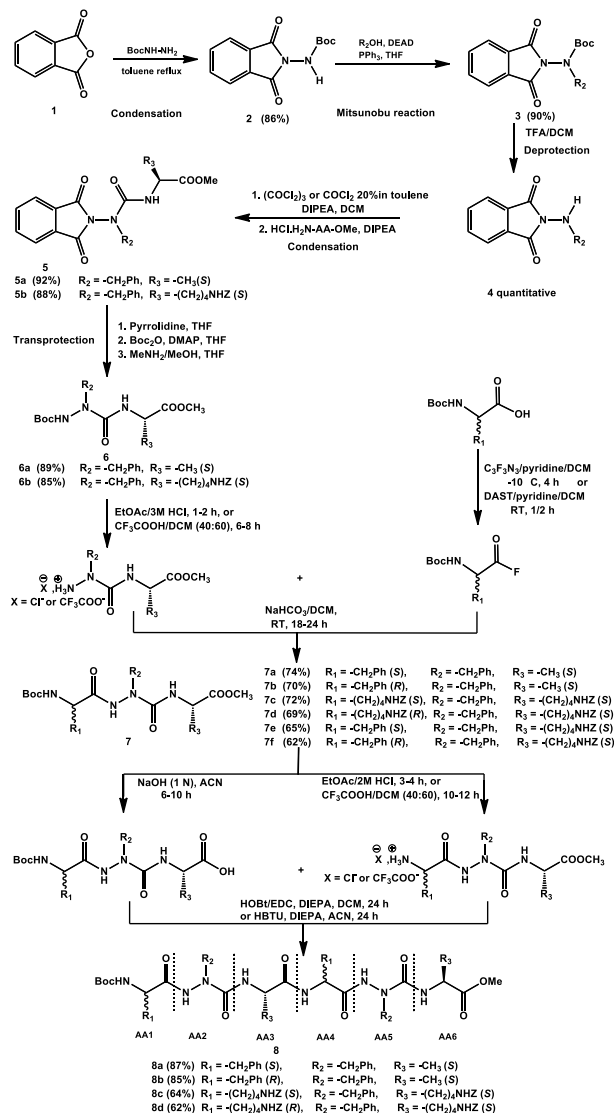
Various homo and hetero 2:1-[α /aza]-oligomers i.e., six trimers (7a – 7f) and four hexamers (8a – 8d) were synthesized in good yields after purification by silica column chromatography. The general stepwise strategy used to design a new series of 2:1-[α /aza]-oligomers is mainly based on the protocol discussed and reported in previous studies, depicted Scheme 1.^{30, 31}

NMR and FTIR spectroscopic studies of 2:1-[α /aza]-trimers:

¹H NMR studies of compounds (7c) and (7d) were carried out at dilute concentration in CDCl₃ (3.0 mmol L⁻¹, 300 K) to avoid intermolecular interactions. The spectra showed well resolved signals and the CH₂ protons of the azaPhe moiety are non-equivalent magnetically, (Supporting Information, Figures S1 and S2). In addition, 2D NMR (ROESY) experiments for compound (7c) revealed the presence of a moderate correlation between the protons of C ^{α} H (Lys1) and the NH (azaPhe), as well as a weak correlation between the protons of NH (azaPhe) and NH (Lys2), (Supporting Information, Figure S3)

The same ROE correlations were observed for compound (7d) (Supporting Information, Figure S4) with also moderate and weak correlations between C ^{α} H (*D*-Lys1) and the NH (azaPhe) protons, and between the NH (azaPhe) and NH (Lys2) protons, respectively. These results indicate that the molecules (7c) and (7d) may induce β II- and β II'-turn conformations in solution, respectively, Figure 1.^{30, 49, 57}

To strengthen the presence of secondary structures, intramolecular hydrogen bonds were investigated by studying the effect of solvent composition by NMR technique.



Scheme 1. General stepwise strategy for the synthesis of new series of 2:1-[α /aza]-oligomers based lysine amino acid residue.^{30, 31}

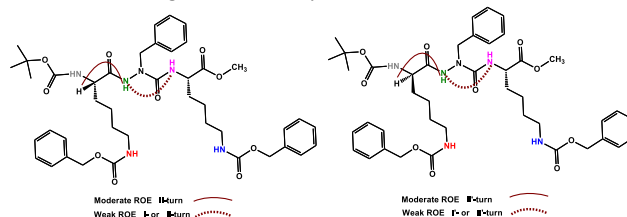


Figure 1. ROE correlations of β II- and β II'-turn conformations in 7c (left) and 7d (right), respectively; (300 MHz, 3.0 mmol L⁻¹, CDCl₃, 300 K).

The method measures the sensitivity of the NH protons through their chemical shift variations as a function of the [CDCl₃/DMSO-*d*₆] ratio.⁴⁴ The results (Figures 2a, b) demonstrated that most of the NH protons of (7c) and (7d) were sensitive to solvent variation, while the NH (Lys2) are weakly perturbed. These results suggest that the NH (Lys2) might be involved in intramolecular hydrogen bonds, in contrast to

all the other free NH protons (*i.e.*, NH (Lys1 or *D*-Lys1), NH (azaPhe2), and N^εH of lysine side chains) (**Supporting Information, Figures S5**).

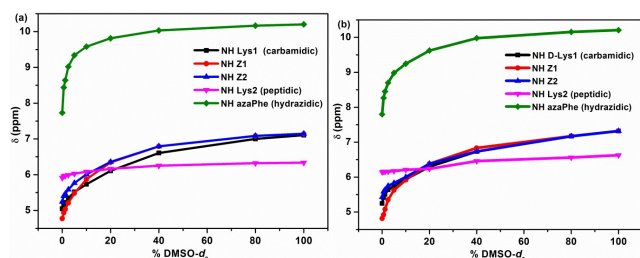


Figure 2. Chemical shift-variations (δ) of HN protons for: (a) **7c**, and (b) **7d** as a function of % [CDCl₃/DMSO-*d*₆] mixtures.

The existence of certain conformation and intramolecular hydrogen bonds within the compounds (**7c**) and (**7d**) were further identified using infrared spectroscopy (FT-IR) in dilute condition (3.0 mmol L⁻¹, CDCl₃), focusing on the two characteristic NH and CO stretching regions. For compound (**7c**), the NH region reveals the presence of free NH band around 3449 cm⁻¹ that was assigned to the free amide proton (Lys1), N^εH (Lys1 + Lys2) and hydrazino NH (azaPhe), in addition to a very broad band with a maximum at 3378 cm⁻¹ assigned to the bound Lys2 amide NH proton, (**Figure 3a**). The NH stretching region of compound (**7d**) shows the presence of two characteristic bands centered at 3449 cm⁻¹ corresponding to the free NH (Lys1), N^εH (*D*-Lys1 + Lys2) and NH (azaPhe), and at 3375 cm⁻¹ (very broad), assigned to the bound NH (Lys2). Moreover, in **Figure 3b**, there is an additional band at 3302 cm⁻¹ which might be assigned to N^εH proton of the lysine involved in a weak intramolecular hydrogen bond. These results for both compounds are agreed with the NMR solvent composition study.

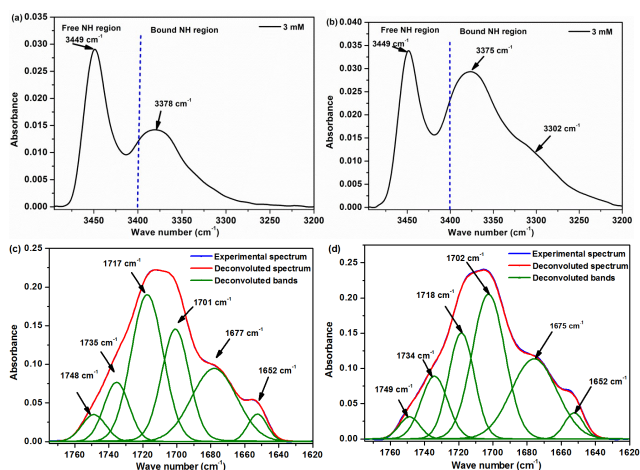


Figure 3. FTIR spectra belong to the NH stretching region (up spectra), and CO stretching region (bottom spectra) for: (a, c) **7c**, and (b, d) **7d** (3.0 mmol L⁻¹, CDCl₃).

Regarding the CO vibration region, the two spectra are very similar with broadening and overlapping of the CO groups which was solved by the help of the 2nd derivative deconvolution method,

(**Figures 3c, d**). The assignment of the CO groups of (**7c**) and (**7d**) were based on their small precursors and previously studied oligomers belong to the same series.^{30, 31} Subsequently, seven bands could be assigned (**Supporting Information, Table S1**), particularly the band at 1652 cm⁻¹ which was assigned to the CO of the Boc group involved in a hydrogen bond.

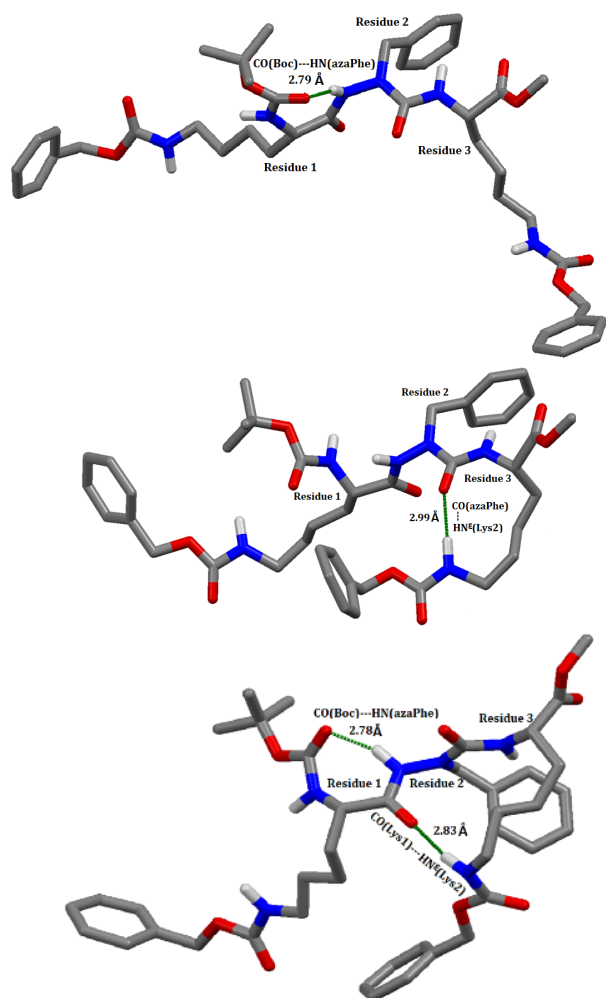
Accordingly, the NH (Lys4) in both compounds (**7c**) and (**7d**) was assumed to be involved in intramolecular hydrogen bonds with the CO (Boc) which stabilizes a pseudocycle of 10 atoms, typical of a β -turn conformation (**Figure 1**), while the other CO groups are in free states in dilute solution, as noticed from their higher frequencies.^{30, 31}

Molecular dynamic calculations of 2:1-[α /aza]-trimers:

To investigate the major conformation(s), as well as the possible intramolecular hydrogen bonds in the 2:1-[α /aza]-oligomers (trimers and hexamers), molecular dynamic calculations for the four molecules (**7c**, **7d**, **8c** and **8d**) were carried out using AMBER software package, according to the protocol described in experimental section. For each molecule, a 2ns trajectory of 25000 structures was calculated using AMBER software package. Analysis of the trajectory assess the possible existence of hydrogen bond and values of the torsion angles. It has been reported that the secondary structure of azapeptides is based on the structural backbone elements which composed of the hydrazine and an urea constituent, in which the two parts are described by the torsion angles φ and ψ , respectively, (**Supporting Information, Figure S6**).⁴⁹

The statistical analysis of the dihedral angles for each trajectory suggests that Boc-Lys(Z)-azaPhe-Lys(Z)-OMe (**7c**) adopts distorted β IV-turn conformation between the three residues, however Boc-*D*-Lys(Z)-azaPhe-Lys(Z)-OMe (**7d**) deviated largely from the β I'-turn conformation as noticed specifically from the values $\varphi_1 = 128.4^\circ$ and $\psi_1 = -64.94^\circ$, (**Supporting Information, Table S2**). The deviation in the dihedral angles [(**7c**) < (**7d**)] may be explained, first by the flexibility of the compounds' structures which mainly associated with the presence of additional interactions, causing disturbance in the torsional angles. These results are consistent with the FT-IR spectra which showed only one broad band for (**7c**) and two bands for (**7d**).

In this context, the possible existence of intramolecular hydrogen bonds within the molecules (**7c**), (**7d**), (**8c**), and (**8d**) was predicted using molecular dynamics calculations by applying the most favorable parameters for hydrogen bond formation (bond angle < 120° and the hydrogen bond atoms distance > 3.2 Å).^{49, 58} In compound (**7c**), the calculations predicted the possible presence of two hydrogen bonds: (i) between CO (Boc) and the NH (azaPhe) of 2.86 Å closing a pseudocycle of 7 atoms,



large deviation from the classical β I'-turn conformation particularly in the torsion angles ($\phi_1, \psi_1 = 128.40^\circ, -64.24^\circ$) for (**7d**), related to the

Figure 4. Selected frames for (**7c**) obtained by molecular dynamic simulations, illustrating different intramolecular hydrogen bonds (green dots); type i (left), type ii (middle), and types i & ii together (right). The H atoms, except those of the NH groups, have been omitted for clarity.

and (ii) between CO (azaPhe) and the N^HH (Lys2) of 2.96 Å closing a pseudocycle of 10 atoms, with occurrences of 36% and 35%, respectively, **Table S3 (Supporting Information) and Figure 4**. Regarding compound (**7d**), the calculations indicated the possible existence of three hydrogen bonds: the first and second hydrogen bonds (i & ii) exist between the CO(Z) (Lys3) and both the NH (azaPhe2) of 2.89 Å, and the NH (Lys1) of 2.91 Å, forming pseudocycles of 13 and 16 atoms, with occurrences of 40% and 26%, respectively. The third hydrogen bond (iii) exists with less occurrence of 22% between CO (Boc) and the N^HH (Lys1) of 2.98 Å closing a pseudocycle of 10 atoms, **Table S3 (Supporting Information) and Figure 5**.

Based on molecular dynamic calculations, the disturbance from the classical β IV-turn in (**7c**) can be attributed to the involvement of the N^HH (Lys2) side chain residue in intramolecular hydrogen bonds with either CO (azaPhe), or CO (Lys1), **Figure 4**. Similarly, we observed a

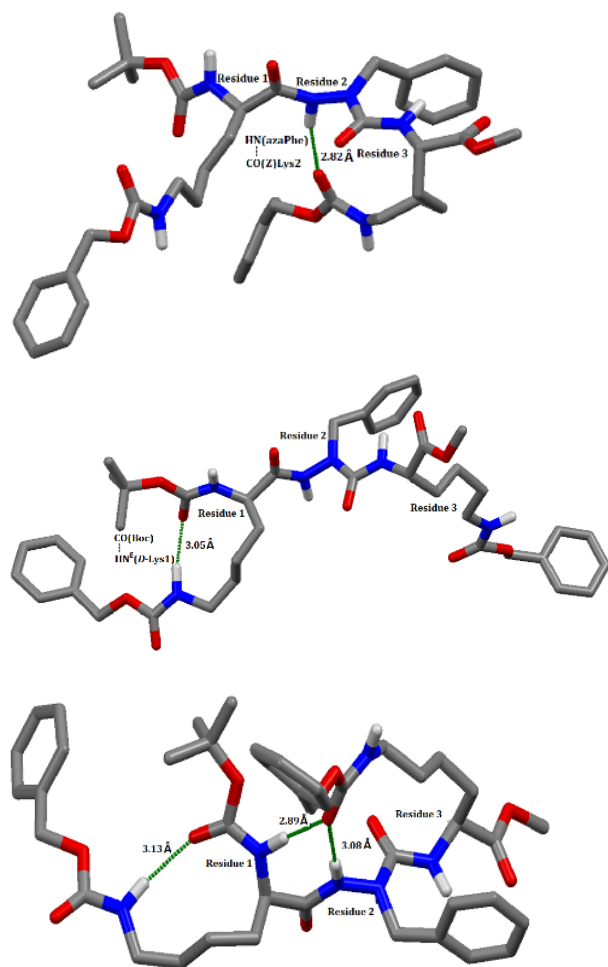


Figure 5. Selected frames for (**8c**) obtained by molecular dynamic simulations, illustrating different intramolecular hydrogen bonds (green dots); type i (left), type iii (middle), types i, ii & iii (right). The H atoms, except those of the NH groups, have been omitted for clarity.

Based on molecular dynamic calculations, the disturbance from the classical β IV-turn in (**7c**) can be attributed to the involvement of the $N^{\epsilon}H$ (Lys2) side chain residue in intramolecular hydrogen bonds with either CO (azaPhe), or CO (Lys1), **Figure 4**. Similarly, we observed the possible existence of three intramolecular hydrogen bonds: (a) CO(Z)(Lys2) with NH (azaPhe2), (b) CO(Z)(Lys3) with NH (*D*-Lys1), and (c) CO(Boc) with $N^{\epsilon}H$ (*D*-Lys1), **Figure 5**.

NMR and FTIR spectroscopic studies of 2:1-[α /aza]-hexamers:

1H NMR studies for compounds (**8c**) and (**8d**) were carried out in $CDCl_3$ (4.0 mmol L^{-1} , 300 K). The 1H spectrum of (**8d**) showed well resolved signals compared to the spectrum of (**8c**) (**Supporting Information, Figures S7 – S10**). The conformations favored by (**8c**) and (**8d**) in solution were investigated using 2D NMR (ROESY) experiments. Unfortunately, not too many ROE correlations for compound (**8c**) were observed (**Supporting Information, Figure S11**). Thus, it can be explained by the high steric hindrance between the

four lysine side chains with the same *S*-configuration in (**8c**), allowing the molecule to be more flexible and hence adopting more energetically stable conformations. Only the presence of weak correlation between NH (azaPhe5) and $C^{\alpha}H$ (Lys6), and a moderate correlation between the NH (azaPhe5) and NH (Lys6) protons suggested that the C-terminal amino acid residues of compound **8c** might be folded in β -turn conformation, **Figure 6a**.^{30, 49, 57}

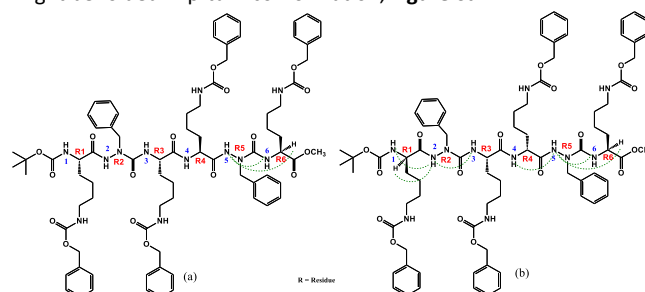


Figure 6. ROE correlations of β -turn conformations in: (a) **8c**, and (b) **8d** (300 MHz, 4.0 mmol L^{-1} , $CDCl_3$, 300 K).

Concerning the solvent composition experiment by NMR technique, increasing the [$DMSO-d_6/CDCl_3$] mixture ratio showed that the $NH1$ (Lys1; **8c**) or (*D*-Lys1, **8d**) and all the $N^{\epsilon}H$ protons of the lysine side chains ($NH7 - NH10$; except $NH10$ of **8d**) for both compounds were very sensitive to the solvent variations (**Supporting Information, Figure S13**). Accordingly, these protons are supposed to be free and not involved in intramolecular hydrogen.⁴⁴ In contrast, the NH protons of the $NH3$ (Lys3) and $NH6$ (Lys6) of both compounds (**8c**) and (**8d**) were not sensitive to the solvent variations (**Figure 7**). These findings suggested that these protons may be involved in strong intramolecular hydrogen bonds.⁴⁴

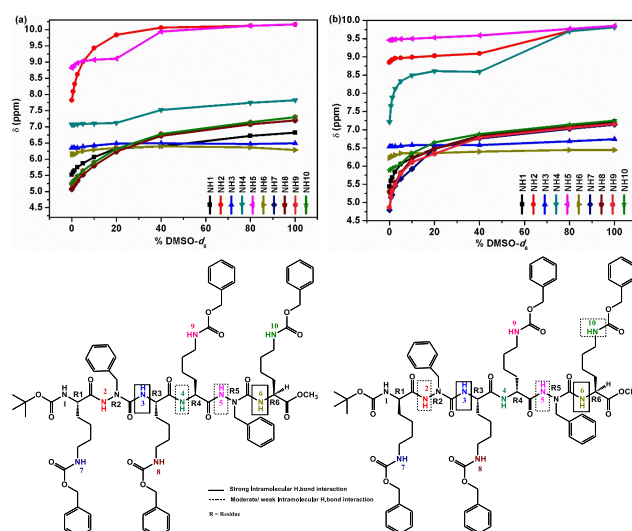


Figure 7. Chemical shift-variations (δ) of NH protons for: (a) **8c**, and (b) **8d** as a function of % [$CDCl_3/DMSO-d_6$] mixtures.

For compound (**8c**), the $NH2$ (azaPhe2) is strongly affected by increasing % $DMSO-d_6$, which reflects the free state of this proton in solution (**Supporting Information, S13**), while $NH4$ (Lys4), and $NH5$ (azaPhe5) proton chemical shifts are not significantly shifted up to

20% DMSO- d_6 , and more affected at higher DMSO- d_6 concentrations. These observations give indication that these NH protons are probably involved in weak intramolecular hydrogen bonds (**Figure 7a**).⁴⁴ Concerning compound (**8d**), we observe (**Figure 7b**) that the chemical shifts of the NH2 (azaPhe2) and NH5 (azaPhe5) protons are not affected small percentage of DMSO- d_6 , but are down-shielded by higher DMSO- d_6 proportion, which indicates that these protons may be engaged in weak intramolecular hydrogen bonds (**Figure 7b**). In contrast, the substantial change of the chemical shift of the NH4 (*D*-Lys4) upon gradual addition of DMSO- d_6 confirms that this proton is free and not involved in intramolecular hydrogen bonds (**Supporting Information, Figure S13**). Interestingly, NH10 (Lys6) proton revealed weak dependency on %DMSO- d_6 till 5%, then its chemical shift acquired high values with increasing %DMSO- d_6 , supposing the possibility of this proton to form a weak intramolecular hydrogen bond.

Similar to trimers, the IR spectra were recorded for hexamers (**8c**) and (**8d**) in dilute condition (3.0 mmol L⁻¹, CDCl₃). Both compounds (**8c** and **8d**) showed similar NH stretching regions as their trimers (**7c** and **7d**), respectively. The NH stretching region of both compounds demonstrates a band in the free NH region which assigned to the free NH protons. In addition, there was a very broad band in the bound NH region around 3345 cm⁻¹ for both molecules, attributed to the bound amide NH protons of Lys3 and Lys6 (**Figures 8a, b**). Interestingly, there is an additional broad band in the far NH stretching region (3235 – 3280 cm⁻¹) in (**8c**) and (3180 – 3230 cm⁻¹) in (**8d**) which were supposed to other intramolecular hydrogen bonds. Finally, one can notice that the bound NH bands in (**8d**) are more broadening with lower frequencies than those of the (**8c**), reflecting the presence of more number and stronger intramolecular hydrogen bonds in molecule (**8d**) than in (**8c**), (**Figure 8a, b**). These results are consistent with the solvent composition studies by NMR technique.

Regarding the CO stretching domain, the two spectra are very similar to the trimer analogs. But they showed broadening and overlapping of the CO bands that caused an obstacle to assign all the bands even with the help of the 2nd derivative deconvolution method. By comparing the CO spectra of the trimers and the corresponding hexamers (**Figures 8c, d**), both molecules exhibit new broad bands at (1635 - 1645 cm⁻¹) and (1630 - 1645 cm⁻¹) for (**8c**) and (**8d**) respectively, which are characteristic of the presence of β -turn. These observations are consistent with the NMR studies, particularly for compound (**8d**). Based on the spectroscopic results, the NH3 (Lys3) and NH6 (Lys6) in compound (**8d**) are suggested to be involved in intramolecular hydrogen bonds with the CO (Boc) and CO (Lys3), respectively, stabilizing the two β -turns observed by the 2D ROESY in its two terminals, forming two pseudocycles of 10 atoms.

Analyses of the results obtained from the molecular dynamic simulations for the two hexamers (**8c**) and (**8d**) were carried out.

ARTICLE

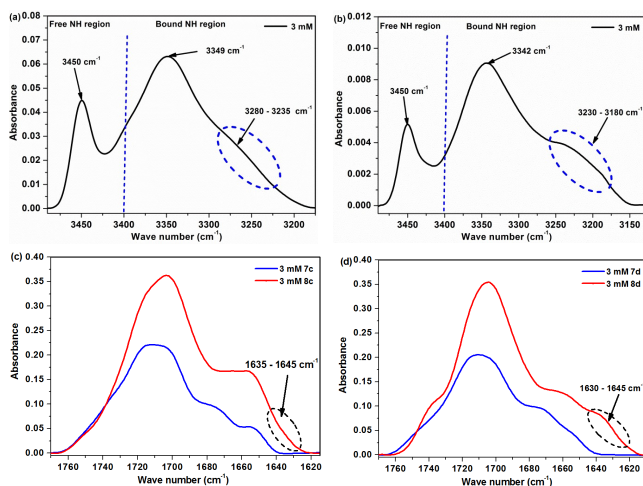


Figure 8. FTIR spectra belong to the NH (up spectra), and CO (bottom spectra) stretching regions for: (a & c) **8c**, and (b & d) **8d** (3.0 mmol L⁻¹, CDCl₃).

Based on the average values of the torsion angles on the calculated trajectories for the two oligomers (**8c**) and (**8d**) and comparing with the theoretical values (Supporting Information, Table S4), the results suggested that: (a) Boc-[Lys(Z)-azaPhe-Lys(Z)]₂-OMe (**8c**) exists in equilibrium between several distorted β -turn conformations. Residues [1 & 2] show non-classical β V-turn conformation. On the other hand, residues [3 & 4] and [4 & 5] deviate from the classical β IV-turn conformation. Unexpectedly, residues [2 / 3] demonstrate distorted β II'- or β V'-turn since the β '-turn types were only reported for molecules possessing *D*-amino acids.⁵⁹ (b) Boc-[*D*-Lys(Z)-azaPhe-Lys(Z)]₂-OMe (**8d**) adopts mainly two consecutive distorted turns: β II'-turn between residues [2 & 3], and β '-turn between residues [4 & 5]. (c) The deviation from the theoretical torsion angles values may be related to the involvement of the amide groups of the main backbone in non-classical β -turn intramolecular hydrogen bonds with either the amide groups of the main backbone and/or with the amide groups of the lysine side chains. These intramolecular hydrogen bonds affected the backbone dihedral angles leading to a deviation from the classical β -turn in natural peptides.

Accordingly, these results highlight that changing the chirality of the amino acid residues positioned at R1 and R4 from *L*-Lys in (**8c**) to *D*-Lys in (**8d**) promote the presence of more hydrogen bond interactions and then reduces the flexibility of the molecule (**8d**), which by consequence adopts a more defined conformation in solution compared to compound (**8c**). This behavior of lysine side chain was previously reported stating the ability of the lysine residues to be involved in hydrogen bonds with residues elsewhere in the structure or with solvent molecules.⁵⁹ These results are

consistent with the 2D NMR studies in solution as molecule (**8c**) shows weak correlations between the nuclei. Indeed, the molecule is highly flexible and exists in various conformations. In contrast, the strong correlation in the 2D spectrum of (**8d**) reflects that the *R* chirality of α carbons induces, for this molecule, defined β -turns, as confirmed by molecular dynamic calculations.

Additional analysis of the (**8c**) and (**8d**) trajectories assess how the non-classical β -turn hydrogen bonds disturb the conformations adopted by the two molecules. The calculations for both molecules predicted several intramolecular hydrogen bonds as summarized in Table S5 (Supporting Information).

Briefly, in compound (**8c**), the calculations indicated the possibility of 4 different hydrogen bonds between: (i) CO (azaPhe2) and NH (Lys4) closing a pseudocycle of 7 atoms occurring at 90% of the modelled frames; (ii) CO (Lys1) and N^εH (Lys4) closing a pseudocycle of 16 atoms with an occurrence of 64.9%; (iii) CO (Boc) and NH (azaPhe2) closing a pseudocycle of 7 atoms with an occurrence of 48.9%; and (iv) CO (azaPhe2) and NH (azaPhe5) closing a pseudocycle of 10 atoms with an occurrence of 32.9%. The calculations for compound (**8d**) predicted the possibility of 6 different hydrogen bonds. The hydrogen bonds are: (i) CO (*D*-Lys1) and NH (azaPhe5) closing a pseudocycle of 13 atoms occurring at 59.1% of the modelled frames, (ii) CO(Z) (Lys6) and NH (*D*-Lys1) closing a pseudoring of 25 atoms with occurrence of 58.7%; (iii) CO (azaPhe2) and NH (*D*-Lys4) closing a pseudocycle of 7 atoms with occurrence of 38.9%; (iv) (CO)_i Boc and NH_{i+2} (azaPhe2) closing a pseudocycle of 7 atoms with occurrence of 29.5%; (v) CO(Z) (*D*-Lys4) and N^εH (*D*-Lys1) closing a pseudocycle of 23 atoms with occurrence of 26.9%; and (vi) CO (azaPhe5) and N^εH (Lys3) closing a pseudocycle of 12 atoms with occurrence of 23.0%.

These results are consistent with NMR results which supposed that the NH protons of residues 4 and 5 are involved in weak hydrogen bonds in the case of (**8c**). Similarly, the NH protons of residues 2 and 5 in compound (**8d**) may be engaged in weak intramolecular hydrogen. In addition, the observed broad bands in the FTIR spectra for both molecules were assigned to NH involved in several hydrogen bonds as confirmed by molecular dynamic calculations.

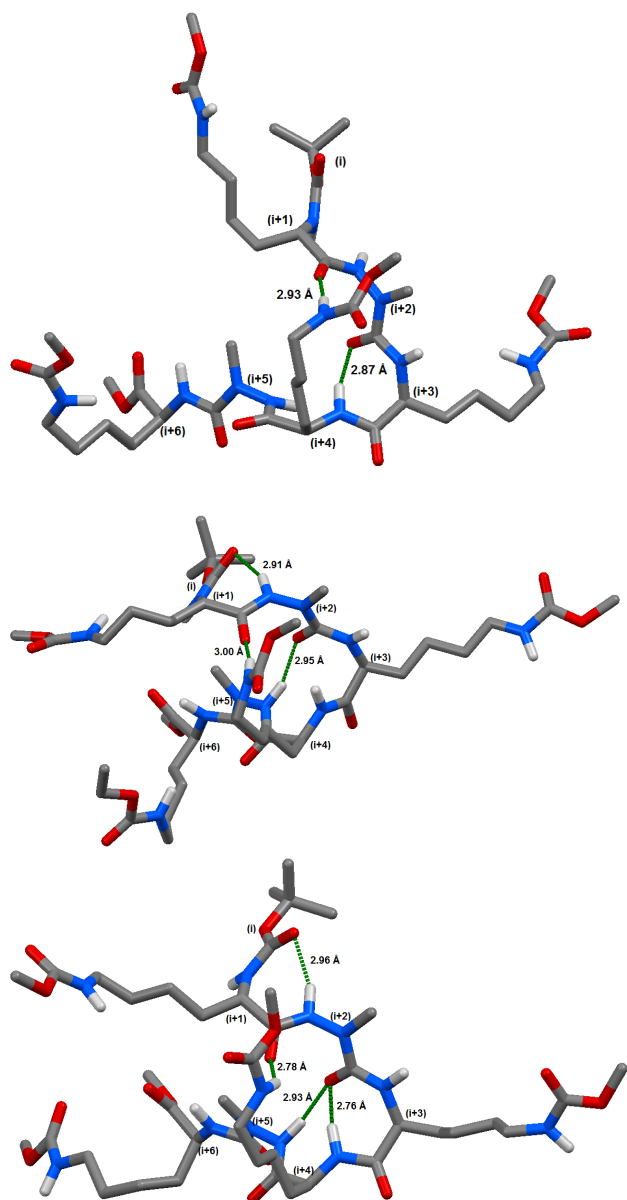


Figure 9. Selected frames for molecule (**8c**) obtained by molecular dynamic simulations, illustrating different intramolecular hydrogen bonds (green dots). The H atoms, except those of the NH groups, and the phenyl groups have been omitted for clarity.

Moreover, by applying the most favorable parameters for hydrogen bond formation,^{49, 58} the calculations gave an idea related to the average percentages for the predicted intramolecular hydrogen bonds in both molecules, (**Supporting Information, Tables S6 and S7**). Examples for a number of selected frames with more than one hydrogen bond representing molecules **8c** and **8d** are shown in **Figures 9 and 10**, respectively.

Application as additives in polymeric membranes for CO₂ capture

In this work, we have investigated the application of our sazeptides as bio-based additives in an original non-

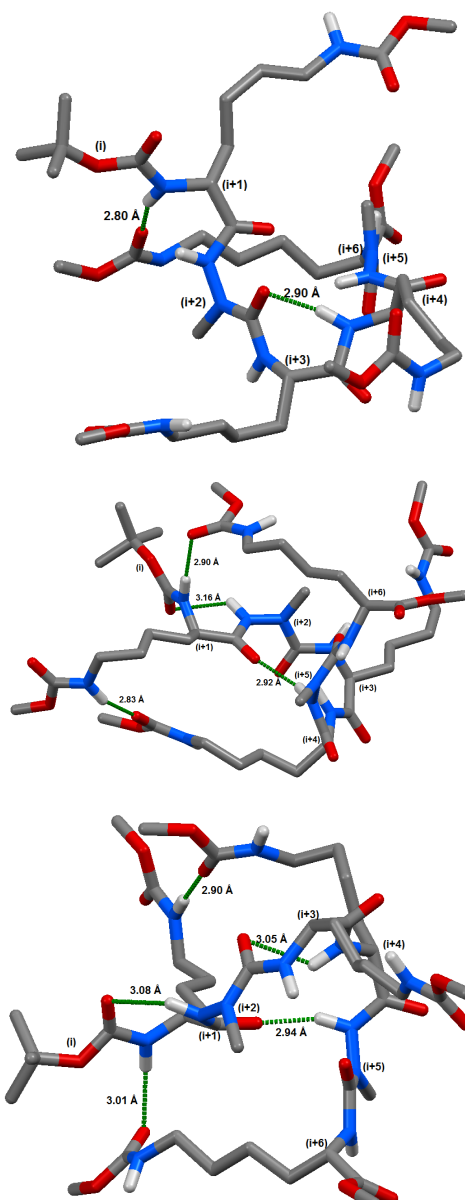


Figure 10. Selected frames for molecule (**8d**) obtained by molecular dynamic simulations, illustrating different intramolecular hydrogen bonds (green dots). The H atoms, except those of the NH groups, and the phenyl groups have been omitted for clarity.

medical application, the CO₂ membrane separation. If antibacterial peptides have been reported for a long time to limit biofouling for water treatment membranes, recent promising works have shown the high potential of peptides and polypeptides for increasing water permeability of dialysis, water purification and nanofiltration membranes.⁶⁰⁻⁶⁵ However, the use of peptides or pseudopeptides for CO₂ separation membranes has remained an almost unexplored field so far. In 2016, we have reported the first work on pseudopeptide additives and their corresponding bioconjugates with a CO₂-philic polymeric part for greatly improving CO₂ permeability through CO₂

separation membranes.⁵⁵ In 2019, Prasad *et al.* have used sericin polypeptide (*i.e.* a waste product of the silk industry) as additive in chitosan membranes for CO₂ separations.⁶⁶ At high temperatures (80 - 100 °C), one of these polypeptide-based membranes had CO₂/N₂ separation performances above the 2008 Robeson upper-bound. Furthermore, amino acids have also been used in bio-based ionic liquids (ILs) or poly(ionic liquid)s (PILs) for CO₂ absorption processes.⁶⁷⁻⁶⁹ These former works have shown that the ILs or PILs derived from amino acids containing an amine side group (*e.g.*, lysine or arginine) were performing better than the non-functional ILs or PILs. The strong interactions of CO₂ with the free amine groups were responsible for better CO₂ absorption performances. The presence of free amine groups is also responsible for the very high performance of several facilitated transport membranes for CO₂ separations.^{70, 71}

The seven aza-pseudopeptide oligomers (**6b**), (**6b'**), (**7a**), (**7c**), (**7c'**), (**8c**), and (**8c'**) (scheme 1 and Table 1) were tested as additives in Pebax® 1074 membrane, already known for its good performance for CO₂ capture^{55, 72, 73} (Supporting Information, Figure S14). These pseudopeptide oligomers differed in their length (from dimer to hexamer oligomers) and the type of their side group. In a first series of protected pseudopeptide oligomers, the side chain amine group of the lysine residue was protected with a carboxybenzyl (Z) group. In a second series of deprotected pseudopeptide oligomers, this amine side group was deprotected. For comparison, a pseudopeptide trimer without lysine residue was also tested to assess the influence of this charged amino acid on the gas permeation properties. The results of the membrane permeation properties for CO₂ and N₂ pure gases are reported in Table S8 (Supporting Information).

Table 1. Description of the aza-pseudopeptide oligomers tested as additives in Pebax® 1074 membrane for CO₂ capture.

ID	Pseudopeptide oligomer	No. of lysine residue(s)	Lysine residue(s)
6b	Dimer	1	Protected
6b' *		1	Free
7a	Trimer	0	----
7c		2	Protected
7c' *		2	Free
8c	Hexamer	4	Protected
8c' *		4	Free

*Deprotected azapeptides **6b'**, **7b'** and **8b'** were obtained from the corresponding protected analogues by catalytic hydrogenolysis (See Experimental Section).

Figure 11 shows the ideal selectivity $\alpha_{\text{CO}_2/\text{N}_2}$ as a function of CO₂ permeability (Robeson plot) for the different membranes at 2 bar and 35 °C, which are typical conditions for CO₂ capture. The protected pseudopeptide trimer with lysine residues and the deprotected pseudopeptide trimer had better CO₂ permeability compared to the corresponding trimer without lysine residue, showing the positive effect of the lysine for CO₂ permeation.

For both series of pseudopeptide oligomers, both the ideal selectivity and the CO₂ permeability decrease when the pseudopeptide oligomer length increases from dimer to hexamer, and this effect was reinforced for the deprotected pseudopeptide oligomers (Figure 11). The deprotection of the pseudopeptide oligomer leads to free amine side group for the lysine residue(s), resulting in a systematic improvement of the CO₂ permeability. It is well known that free amines have strong ability to interact with CO₂ and the incorporation of amine-based additives in polymer membranes usually improves CO₂ permeability.^{69, 74-78} In this work, the extent of this improvement increases when the pseudopeptide oligomer length decreases. Therefore, the best membrane properties were obtained for the deprotected pseudopeptide dimer, overcoming the usual selectivity/permeability trade-off⁷⁹⁻⁸¹ with an increase in both ideal selectivity $\alpha_{\text{CO}_2/\text{N}_2}$ (from 42.8 to 47.6) and CO₂ permeability (from 132 to 148 Barrer) compared to the virgin Pebax® 1074 membrane.

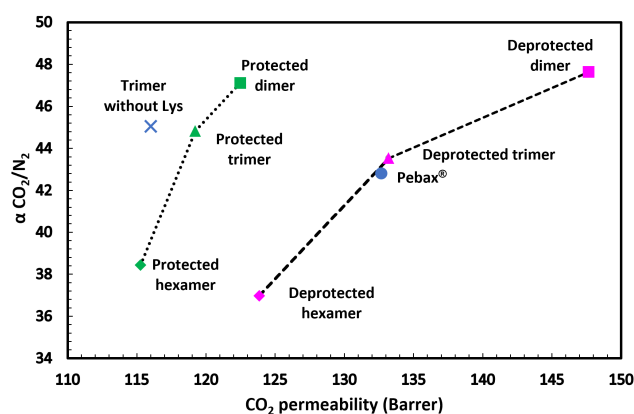


Figure 11. Ideal selectivity $\alpha_{\text{CO}_2/\text{N}_2}$ as function of CO₂ permeability (Robeson plot) for different Pebax® 1074 membranes with protected and deprotected pseudopeptide additives at 2 bar and 35 °C.

The CO₂ sorption coefficients obtained for the membranes with the different protected pseudopeptide additives were very close to each other and also to that of the virgin Pebax® 1074 membrane, meaning that the protected pseudopeptide additives did not have any significant effect on the sorption step during CO₂ permeation (Figure 12).

However, as expected, the deprotected pseudopeptide additives led to higher CO₂ sorption coefficients and the best sorption improvement was obtained for the deprotected hexamer, *i.e.* the longest pseudopeptide oligomer containing four deprotected lysine residues. The four corresponding free amine side groups strongly interacted with the CO₂ molecules and increased CO₂ sorption by 30%. This result is in good agreement with former works ILs and PILs based on amino acids, having shown the good interactions of CO₂ molecules with free amine side groups of lysine or arginine amino acids.⁶⁷⁻⁶⁹ The different protected pseudopeptide additives induce a very low reduction in the CO₂ diffusion coefficient partially due to the presence of the bulky carboxybenzyl (Z) protecting group slightly limiting the diffusion of CO₂ molecules (Figure 12).

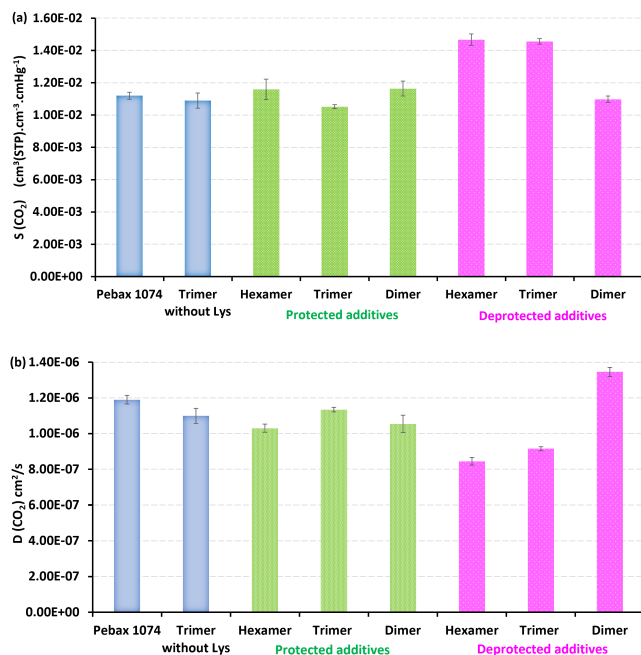


Figure 12. CO₂ sorption (a) and diffusion (b) coefficients for different Pebax® 1074 membranes with protected and deprotected pseudo-peptide additives at 2 bar and 35 °C.

However, the CO₂ diffusion coefficient was decreased by 23% and 30% for the deprotected trimer and hexamer additives, respectively, compared to that obtained with the virgin Pebax® 1074 membrane. On the other hand, the CO₂ diffusion coefficient slightly increased (+13%) for the deprotected dimer additive. Therefore, the deprotected pseudo-peptide length has a strong effect on the CO₂ diffusion coefficient, the longest additives hindering CO₂ diffusion. It has been shown in the first part of this work that increasing the length of the pseudo-peptide oligomers favors their structuration by involving more and more β -turn conformations when going from dimer to trimer and hexamer. It has also been shown that N^H might be involved in hydrogen bonds. For the series of deprotected pseudo-peptide additives, the best CO₂ diffusion coefficient was obtained for the less structured pseudo-peptide oligomer (dimer).

To conclude about the gas permeation results, the deprotected pseudo-peptide trimer and hexamer additives improve CO₂ sorption, the best improvement being obtained for the hexamer additive containing four lysine residues and four free amine side groups. The deprotected pseudo-peptide dimer additive did not have any significant effect on CO₂ sorption compared to that of the virgin Pebax® 1074 membrane. However, the strong structuration of the long deprotected additives induces a strong decrease of the CO₂ diffusion coefficient, finally resulting in a decrease in CO₂ permeability. Nevertheless, the low structuration of the deprotected dimer additive led to higher CO₂ diffusion coefficient (+13%), finally resulting in higher membrane CO₂ permeability (+12%) and better ideal selectivity $\alpha_{\text{CO}_2/\text{N}_2}$ (+11%).

Conclusions

The study overviewed the synthesis and conformational studies of a new series of 2:1-[α /aza]-oligomers (trimers and hexamers) incorporating lysine amino acid residue. The influence of the N^H on the conformation of these oligomers were established using NMR, FTIR and molecular dynamic calculations, at least in the protected oligomers. The spectroscopy techniques emphasized the adoption of the β -turn conformations regardless the chirality and side chain of lysine particularly in small sequence, while the chirality and chain length exerted their role in β -turn deviation. On the other hand, molecular dynamic simulations predicted the impact of the supplementary N^H of the lysine residue and of the chain length on the backbone torsion angles, highlighting the presence of intramolecular hydrogen bonds with the amide groups of the azapeptide backbone, causing distortion from the classical β -turn particularly in longer sequences (hexamers > trimers). In addition, increasing the chain length (hexamer) and the high steric hindrance caused by the four lysine residues (**8c** > **8d**) led to increasing the flexibility of the hexamers to fold into more energetically stable conformation stabilized by non-classical β -turn hydrogen bonds. Furthermore, the study investigated the synthesized short azapeptide based lysine moiety with free amine side chain (deprotected dimer) exerted a good improvement in CO₂ separation upon using them as additive in Pebax® matrix membrane.

Author Contributions

Mohamed I. A. Ibrahim: Methodology, Investigation, Data curation, Formal analysis & Writing the Manuscript. **Xavier Solimando:** Methodology & Data analysis for gases separation. **Loïc Stefan:** Validation and Writing, **Guillaume Pickaert:** Validation and Writing, **Jérôme Babin,** Validation **Carole Arnal-Herault** Methodology, Validation, Writing **Denis Roizard:** Anne Jonquères: Methodology, Validation, Writing, **Jacques Bodiguel**, Methodology, Data curation, and writing **Marie-Christine Averlant-Petit**: Conceptualization, Supervision, Formal Analysis, Validation and Writing

Conflicts of interest

There are no conflicts to declare.

Acknowledgements

M.C. Averlant-Petit acknowledge the Centre National de la Recherche Scientifique (CNRS) for funding.

M. I. A. Ibrahim acknowledge Erasmus and Université de Lorraine for funding, and NIOF for the scientific collaboration.

The authors acknowledge Mathilde Achard for supporting in HPLC and MS analyses of the synthesized peptides, and Olivier Fabre for NMR experiments.

Notes and references

1. I. Avan, C. D. Hall and A. R. Katritzky, Peptidomimetics via modifications of amino acids and peptide bonds *Chemical Society Reviews*, 2014, **43**, 3575-3594. <https://doi.org/10.1039/C3CS60384A>.
2. G. Cardillo, L. Gentilucci and A. Tolomelli, Aziridines and Oxazolines: Valuable Intermediates in the Synthesis of Unusual Amino Acids, Università di Bologna *Archive of Aldrichimica Acta*, 2003, **36**, 39-50. <https://www.sigmaaldrich.com/JP/en/collections/aldrichimica-acta>.
3. A. Perdih and M. Sollner Dolenc, Current Organic Chemistry: Recent Advances in the Synthesis of Unnatural α -Amino Acids *Bentham Science Publishers*, 2007, **11**, 801-832. <https://doi.org/10.2174/138527207780831701>.
4. A. Azam, S. Mallart, S. Illiano, O. Duclos, C. Prades and B. Maillère, Introduction of Non-natural Amino Acids Into T-Cell Epitopes to Mitigate Peptide-Specific T-Cell Responses, 2021, **12**. <https://doi.org/10.3389/fimmu.2021.637963>.
5. G. Cardillo, L. Gentilucci and A. Tolomelli, Unusual amino acids: synthesis and introduction into naturally occurring peptides and biologically active analogues *Mini reviews in medicinal chemistry*, 2006, **6**, 293-304. <https://doi.org/10.2174/138955706776073394>.
6. A. Dahal, J. J. Sonju, K. G. Kousoulas and S. D. Jois, Peptides and peptidomimetics as therapeutic agents for Covid-19 *Peptide Science*, 2022, **114**, e24245. <https://doi.org/10.1002/pep2.24245>.
7. N. Sewald and H.-D. Jakubke, *Journal*, 2002, 339-361.
8. J. V. N. Vara Prasad and D. H. Rich, Addition of Allylic Metals to α -Aminoaldehydes. Application to the Synthesis of Statine, Ketomethylene and Hydroxyethylene Dipeptide Isosteres *Tetrahedron Letters*, 1990, **31**, 1803-1806. [https://doi.org/10.1016/S0040-4039\(00\)98790-2](https://doi.org/10.1016/S0040-4039(00)98790-2).
9. J. Gante, Azapeptides *Synthesis*, 1989, **21**, 405-413. <https://doi.org/10.1055/s-1989-27269>.
10. J. Magrath and R. H. Abeles, Cysteine protease inhibition by azapeptide esters *Journal of Medicinal Chemistry*, 1992, **35**, 4279-4283. <https://doi.org/10.1021/jm00101a004>.
11. M. Chorev and M. Goodman, A dozen years of retro-inverso peptidomimetics *Accounts of Chemical Research*, 1993, **26**, 266-273. <https://doi.org/10.1021/ar00029a007>.
12. L. Thévenet, R. Vanderesse, M. Marraud, C. Didierjean and A. Aubry, Pseudopeptide fragments and local structures induced by an α -aminoxy acid in a dipeptide *Tetrahedron Letters*, 2000, **41**, 2361-2364. [https://doi.org/10.1016/S0040-4039\(00\)00200-8](https://doi.org/10.1016/S0040-4039(00)00200-8).
13. D. Yang, J. Qu, B. Li, F.-F. Ng, X.-C. Wang, K.-K. Cheung, D.-P. Wang and Y.-D. Wu, Novel Turns and Helices in Peptides of Chiral α -Aminoxy Acids *Journal of the American Chemical Society*, 1999, **121**, 589-590. <https://doi.org/10.1021/ja982528y>.
14. A. Aubry, J.-P. Mangeot, J. Vidal, A. Collet, S. Zerkout and M. Marraud, Crystal structure analysis of a β -turn mimic in hydrazino peptides *International Journal of Peptide and Protein Research*, 1994, **43**, 305-311. <https://doi.org/10.1111/j.1399-3011.1994.tb00395.x>.
15. A. Cheguillaume, F. Lehardy, K. Bouget, M. Baudy-Floc'h and P. Le Grel, Submonomer Solution Synthesis of Hydrazinoazapeptides, a New Class of Pseudopeptides *The Journal of Organic Chemistry*, 1999, **64**, 2924-2927. <https://doi.org/10.1021/jo981487l>.
16. A. Müller, C. Vogt and N. Sewald, Synthesis of Fmoc- β -Homoamino Acids by Ultrasound-Promoted Wolff Rearrangement *Synthesis*, 1998, **1998**, 837-841. <https://doi.org/10.1055/s-1998-2075>.
17. S. H. Gellman, Foldamers: A Manifesto *Accounts of Chemical Research*, 1998, **31**, 173-180. <https://doi.org/10.1021/ar960298r>.
18. F. André, G. Boussard, D. Bayeul, C. Didierjean, A. Aubry and M. Marraud, Aza-peptides. II. X-ray structures of aza-alanine and aza-asparagine-containing peptides *The Journal of Peptide Research : official journal of the American Peptide Society*, 1997, **49**, 556-562. <https://doi.org/10.1111/j.1399-3011.1997.tb01163.x>.
19. R. Vanderesse, V. Grand, D. Limal, A. Vicherat, M. Marraud, C. Didierjean and A. Aubry, Structural Comparison of Homologous Reduced Peptide, Reduced Azapeptide, Iminoazapeptide, and Methyleneoxy-peptide Analogues *Journal of the American Chemical Society*, 1998, **120**, 9444-9451. <https://doi.org/10.1021/ja980937o>.
20. M. I. A. Ibrahim, G. Pickaert, L. Stefan, B. Jamart-Grégoire, J. Bodiguel and M.-C. Averlant-Petit, Cyclohexamer [-(d-Phe-azaPhe-Ala)₂]-: good candidate to formulate supramolecular organogels *RSC Advances*, 2020, **10**, 43859-43869. [10.1039/D0RA07775E](https://doi.org/10.1039/D0RA07775E).
21. A. Lecoq, G. Boussard, M. Marraud and A. Aubry, The couple Pro/AzaPro : A means of β -turn formation control synthesis and conformation of two AzaPro-containing dipeptides *Tetrahedron Letters*, 1992, **33**, 5209-5212. [https://doi.org/10.1016/S0040-4039\(00\)79134-9](https://doi.org/10.1016/S0040-4039(00)79134-9).
22. I. Bouillon, N. Brosse, R. Vanderesse and B. Jamart-Grégoire, Synthesis of N α -Z, N β -Fmoc or Boc protected α -hydrazinoacids and study of the coupling reaction in solution of N α -Z- α -hydrazinoesters *Tetrahedron*, 2007, **63**, 2223-2234. <https://doi.org/10.1016/j.tet.2006.12.085>.
23. I. Bouillon, R. Vanderesse, N. Brosse, O. Fabre and B. Jamart-Grégoire, Solid-phase synthesis of hydrazinopeptides in Boc and Fmoc strategies monitored by HR-MAS NMR *Tetrahedron*, 2007, **63**, 9635-9641. <https://doi.org/10.1016/j.tet.2007.07.038>.
24. A.-S. Felten, S. Dautrey, J. Bodiguel, R. Vanderesse, C. Didierjean, A. Arrault and B. Jamart-Grégoire, Oligomerization of N-aminodipeptides: to the synthesis of heterogeneous backbone with 1:1 α : α -N-amino amino acid residue patterns *Tetrahedron*, 2008, **64**, 10741-10753. <https://doi.org/10.1016/j.tet.2008.08.087>.
25. R.-O. Moussodia, S. Acherar, A. Bordessa, R. Vanderesse and B. Jamart-Grégoire, An expedient and short synthesis of chiral α -hydrazinoesters: synthesis and conformational analysis of 1:1 [α : α -N α -hydrazino]mers *Tetrahedron*, 2012, **68**, 4682-4692. <https://doi.org/10.1016/j.tet.2012.04.018>.
26. A.-S. Felten, R. Vanderesse, N. Brosse, C. Didierjean and B. Jamart-Grégoire, Solid phase synthesis of N-aminodipeptides in high optical purity *Tetrahedron Letters*, 2008, **49**, 156-158. <https://doi.org/10.1016/j.tetlet.2007.10.152>.
27. M. I. A. Ibrahim, Z. Zhou, C. Deng, C. Didierjean, R. Vanderesse, J. Bodiguel, M.-C. Averlant-Petit and B. Jamart-Grégoire, Impact of Ca-Chirality on Supramolecular Self-Assembly in Cyclo-2:1-[α /aza]-Hexamers (d/l-Phe-azaPhe-Ala)₂ *European Journal of Organic Chemistry*, 2017, **2017**, 4703-4712. <https://doi.org/10.1002/ejoc.201700555>.
28. N. Brosse, A. Grandeur and B. Jamart-Grégoire, Original and efficient method for the preparation of N-aminoamide pseudodipeptides in high optical purity *Tetrahedron Letters*, 2002, **43**, 2009-2011. [https://doi.org/10.1016/S0040-4039\(02\)00119-3](https://doi.org/10.1016/S0040-4039(02)00119-3).
29. C. Abbas, B. Jamart Gregoire, R. Vanderesse and C. Didierjean, Boc-AzAla-Ala-OMe *Acta Crystallographica Section E*, 2009, **65**, o3079. <https://doi.org/10.1016/j.tetlet.2009.04.131>.
30. Z. Zhou, C. Deng, C. Abbas, C. Didierjean, M.-C. Averlant-Petit, J. Bodiguel, R. Vanderesse and B. Jamart-Grégoire, Synthesis and Structural Characterization of 2:1 [α /Aza]-oligomers *European*

- Journal of Organic Chemistry*, 2014, **2014**, 7643-7650. <https://doi.org/10.1002/ejoc.201402628>.
31. C. Abbas, G. Pickaert, C. Didierjean, B. J. Gregoire and R. Vanderesse, Original and efficient synthesis of 2:1-[a/aza]-oligomer precursors *Tetrahedron letters*, 2009, **50**, 4158-4160. <https://doi.org/10.1016/j.tetlet.2009.04.131>.
32. M. Marraud and A. Aubry, Crystal structures of peptides and modified peptides *Biopolymers*, 1996, **40**, 45-83. [https://doi.org/10.1002/\(sici\)1097-0282\(1996\)40:1<45::aid-bip3>3.0.co;2-3](https://doi.org/10.1002/(sici)1097-0282(1996)40:1<45::aid-bip3>3.0.co;2-3).
33. J. Gante, Peptidomimetics—Tailored Enzyme Inhibitors *Angewandte Chemie International Edition in English*, 1994, **33**, 1699-1720. <https://doi.org/10.1002/anie.199416991>.
34. J. Gante, M. Krug, G. Lauterbach, R. Weitzel and W. Hiller, Synthesis and properties of the first all-aza analogue of a biologically active peptide *Journal of peptide science : an official publication of the European Peptide Society*, 1995, **1**, 201-206. [10.1002/psc.310010307](https://doi.org/10.1002/psc.310010307).
35. K. Fan Cheng, S. VanPatten, M. He and Y. Al-Abed, Azapeptides - A History of Synthetic Milestones and Key Examples *Current medicinal chemistry*, 2022, DOI: <https://doi.org/10.2174/0929867329666220510214402>. <https://doi.org/10.2174/0929867329666220510214402>.
36. A. S. Dutta and J. S. Morley, Polypeptides. Part XIII. Preparation of α -aza-amino-acid (carbamic acid) derivatives and intermediates for the preparation of α -aza-peptides *J. Chem. Soc., Perkin. Tran. 1*, 1975, **1**, 1712-1720. <https://doi.org/10.1039/p19750001712>.
37. Z. Benatalah, A. Aubry, G. Boussard and M. Marraud, Evidence for a beta-turn in an azadipeptide sequence. Synthesis and crystal structure of ButCO-Pro-AzaAla-NHPri *International journal of peptide and protein research*, 1991, **38**, 603-605. <https://doi.org/10.1111/j.1399-3011.1991.tb01547.x>.
38. C. J. Gray, M. Quibell, N. Baggett and T. Hammerle, Incorporation of azaglutamine residues into peptides synthesised by the ultra-high load solid (gel)-phase technique *International Journal of Peptide and Protein Research*, 1992, **40**, 351-362. <https://doi.org/10.1111/j.1399-3011.1992.tb00311.x>.
39. E. Benedetti, *Journal*, 1977, 257-273.
40. C. H. Reynolds and R. E. Hormann, Theoretical Study of the Structure and Rotational Flexibility of Diacylhydrazines: Implications for the Structure of Nonsteroidal Ecdysone Agonists and Azapeptides *Journal of the American Chemical Society*, 1996, **118**, 9395-9401. <https://doi.org/10.1021/ja960214+>.
41. H.-J. Lee, M.-H. Lee, Y.-S. Choi, H.-M. Park and K.-B. Lee, NBO approach to evaluate origin of rotational barrier of diformylhydrazine *Journal of Molecular Structure: THEOCHEM*, 2003, **631**, 101-110. [https://doi.org/10.1016/S0166-1280\(03\)00191-X](https://doi.org/10.1016/S0166-1280(03)00191-X).
42. C. Proulx, D. Sabatino, R. Hopewell, J. Spiegel, Y. García Ramos and W. D. Lubell, Azapeptides and their therapeutic potential *Future medicinal chemistry*, 2011, **3**, 1139-1164. <https://doi.org/10.4155/fmc.11.74>.
43. H. J. Lee, I. A. Ahn, S. Ro, K. H. Choi, Y. S. Choi and K. B. Lee, Role of azaamino acid residue in beta-turn formation and stability in designed peptide *The journal of peptide research : official journal of the American Peptide Society*, 2000, **56**, 35-46. <https://doi.org/10.1034/j.1399-3011.2000.00717.x>.
44. F. André, A. Vicherat, G. Boussard, A. Aubry and M. Marraud, Azapeptides. III. Experimental structural analysis of aza-alanine and aza-asparagine-containing peptides *The journal of peptide research : official journal of the American Peptide Society*, 1997, **50**, 372-381. <https://doi.org/10.1111/j.1399-3011.1997.tb01197.x>.
45. M. Zouikri, A. Vicherat, A. Aubry, M. Marraud and G. Boussard, Azaproline as a beta-turn-inducer residue opposed to proline *The journal of peptide research : official journal of the American Peptide Society*, 1998, **52**, 19-26. <https://doi.org/10.1111/j.1399-3011.1998.tb00648.x>.
46. H. J. Lee, K. H. Choi, I. A. Ahn, S. Ro, H. G. Jang, Y. S. Choi and K. B. Lee, The β -turn preferential solution conformation of a tetrapeptide containing an azaamino acid residue *Journal of Molecular Structure*, 2001, **569**, 43-54. [https://doi.org/10.1016/S0022-2860\(00\)00861-9](https://doi.org/10.1016/S0022-2860(00)00861-9).
47. C. Didierjean, V. Del Duca, E. Benedetti, A. Aubry, M. Zouikri, M. Marraud and G. Boussard, X-ray structures of aza-proline-containing peptides *The journal of peptide research : official journal of the American Peptide Society*, 1997, **50**, 451-457. <https://doi.org/10.1111/j.1399-3011.1997.tb01208.x>.
48. A. Lecoq, G. Boussard, M. Marraud and A. Aubry, Crystal state conformation of three azapeptides containing the Azaproline residue, a β -turn regulator *Biopolymers*, 1993, **33**, 1051-1059. <https://doi.org/10.1002/bip.360330707>.
49. M. Thormann and H.-J. Hofmann, Conformational properties of azapeptides *Journal of Molecular Structure: THEOCHEM*, 1999, **469**, 63-76. [https://doi.org/10.1016/S0166-1280\(98\)00567-3](https://doi.org/10.1016/S0166-1280(98)00567-3).
50. H.-J. Lee, J.-W. Song, Y.-S. Choi, S. Ro and C.-J. Yoon, The energetically favorable cis peptide bond for the azaglycine-containing peptide: For-AzGly-NH2 model *Physical Chemistry Chemical Physics*, 2001, **3**, 1693-1698. <https://doi.org/10.1039/B009651M>.
51. W.-J. Zhang, A. Berglund, J. L. F. Kao, J.-P. Couty, M. C. Gershengorn and G. R. Marshall, Impact of Azaproline on Amide Cis-Trans Isomerism: Conformational Analyses and NMR Studies of Model Peptides Including TRH Analogues *Journal of the American Chemical Society*, 2003, **125**, 1221-1235. <https://doi.org/10.1021/ja020994o>.
52. H. J. Lee, J. W. Song, Y. S. Choi, H. M. Park and K. B. Lee, A theoretical study of conformational properties of N-methyl azapeptide derivatives *Journal of the American Chemical Society*, 2002, **124**, 11881-11893. <https://doi.org/10.1021/ja026496x>.
53. D. A. Case, T. E. Cheatham, 3rd, T. Darden, H. Gohlke, R. Luo, K. M. Merz, Jr., A. Onufriev, C. Simmerling, B. Wang and R. J. Woods, The Amber biomolecular simulation programs *Journal of computational chemistry*, 2005, **26**, 1668-1688. <https://doi.org/10.1002/jcc.20290>.
54. D. A. Pearlman, D. A. Case, J. W. Caldwell, W. S. Ross, T. E. Cheatham, S. DeBolt, D. Ferguson, G. Seibel and P. Kollman, AMBER, a package of computer programs for applying molecular mechanics, normal mode analysis, molecular dynamics and free energy calculations to simulate the structural and energetic properties of molecules *Computer Physics Communications*, 1995, **91**, 1-41. [https://doi.org/10.1016/0010-4655\(95\)00041-D](https://doi.org/10.1016/0010-4655(95)00041-D).
55. X. Solimando, C. Lherbier, J. Babin, C. Arnal-Herault, E. Romero, S. Acherar, B. Jamart-Gregoire, D. Barth, D. Roizard and A. Jonquieres, Pseudopeptide bioconjugate additives for CO2 separation membranes *Polymer International*, 2016, **65**, 1464-1473. <https://doi.org/10.1002/pi.5240>.
56. J. G. Wijmans and R. W. Baker, The solution-diffusion model: a review *Journal of Membrane Science*, 1995, **107**, 1-21. [https://doi.org/10.1016/0376-7388\(95\)00102-1](https://doi.org/10.1016/0376-7388(95)00102-1).
57. H.-J. Lee, H.-M. Park and K.-B. Lee, The β -turn scaffold of tripeptide containing an azaphenylalanine residue *Biophysical Chemistry*, 2007, **125**, 117-126. <https://doi.org/10.1016/j.bpc.2006.05.028>.

58. J. J. Dannenberg, An Introduction to Hydrogen Bonding By George A. Jeffrey (University of Pittsburgh). Oxford University Press: New York and Oxford. 1997. ix + 303 pp. \$60.00. ISBN 0-19-509549-9 *Journal of the American Chemical Society*, 1998, **120**, 5604-5604. <https://doi.org/10.1021/ja9756331>.
59. R. P. Cheng, P. Girinath and R. Ahmad, Effect of lysine side chain length on intra-helical glutamate-lysine ion pairing interactions *Biochemistry*, 2007, **46**, 10528-10537. [10.1021/bi700701z](https://doi.org/10.1021/bi700701z).
60. S. Bolisetty and R. Mezzenga, Amyloid-carbon hybrid membranes for universal water purification *Nature Nanotechnology*, 2016, **11**, 365-371. <https://doi.org/10.1038/nnano.2015.310>.
61. Y. He, H. Hoi, C. D. Montemagno and S. Abraham, Functionalized polymeric membrane with aquaporin using click chemistry for water purification application *Journal of Applied Polymer Science*, 2018, **135**, 46678. <https://doi.org/10.1002/app.46678>.
62. C. S. Lee, M.-k. Choi, Y. Y. Hwang, H. Kim, M. K. Kim and Y. J. Lee, Facilitated Water Transport through Graphene Oxide Membranes Functionalized with Aquaporin-Mimicking Peptides *Advanced Materials*, 2018, **30**, 1705944. <https://doi.org/10.1002/adma.201705944>.
63. B. Sutisna, P. Bilalis, V. Musteata, D.-M. Smilgies, K.-V. Peinemann, N. Hadjichristidis and S. P. Nunes, Self-Assembled Membranes with Featherlike and Lamellar Morphologies Containing α -Helical Polypeptides *Macromolecules*, 2018, **51**, 8174-8187. <https://doi.org/10.1021/acs.macromol.8b01446>.
64. S. Schöttner, M. Brodrecht, E. Uhlein, C. Dietz, H. Breitzke, A. A. Tietze, G. Buntkowsky and M. Gallei, Amine-Containing Block Copolymers for the Bottom-Up Preparation of Functional Porous Membranes *Macromolecules*, 2019, **52**, 2631-2641. <https://doi.org/10.1021/acs.macromol.8b02758>.
65. X. 88Niu, D. Li, Y. Chen and F. Ran, Modification of a polyethersulfone membrane with a block copolymer brush of poly(2-methacryloyloxyethyl phosphorylcholine-co-glycidyl methacrylate) and a branched polypeptide chain of Arg-Glu-Asp-Val *RSC Advances*, 2019, **9**, 25274-25284. <https://doi.org/10.1039/C9RA04234B>.
66. B. Prasad, R. M. Thakur, B. Mandal and B. Su, Enhanced CO₂ separation membrane prepared from waste by-product of silk fibroin *Journal of Membrane Science*, 2019, **587**, 117170. <https://doi.org/10.1016/j.memsci.2019.117170>.
67. H. Ohno and K. Fukumoto, Amino Acid Ionic Liquids *Accounts of Chemical Research*, 2007, **40**, 1122-1129. <https://doi.org/10.1021/ar700053z>.
68. Y. S. Sistla and A. Khanna, CO₂ absorption studies in amino acid-anion based ionic liquids *Chemical Engineering Journal*, 2015, **273**, 268-276. <https://doi.org/10.1016/j.cej.2014.09.043>.
69. M. S. Raja Shahrom, C. D. Wilfred, D. R. MacFarlane, R. Vijayraghavan and F. K. Chong, Amino acid based poly(ionic liquid) materials for CO₂ capture: Effect of anion *Journal of Molecular Liquids*, 2019, **276**, 644-652. <https://doi.org/10.1016/j.molliq.2018.12.044>.
70. Z. Tong and W. S. W. Ho, Facilitated transport membranes for CO₂ separation and capture *Separation Science and Technology*, 2017, **52**, 156-167. <https://doi.org/10.1080/01496395.2016.1217885>.
71. S. Rafiq, L. Deng and M.-B. Hägg, Role of Facilitated Transport Membranes and Composite Membranes for Efficient CO₂ Capture – A Review *ChemBioEng Reviews*, 2016, **3**, 68-85. <https://doi.org/10.1002/cben.201500013>.
72. V. I. Bondar, B. D. Freeman and I. Pinnau, Gas transport properties of poly(ether-b-amide) segmented block copolymers *Journal of Polymer Science Part B: Polymer Physics*, 2000, **38**, 2051-2062. [https://doi.org/10.1002/1099-0488\(20000801\)38:15<2051::AID-POLB100>3.0.CO;2-D](https://doi.org/10.1002/1099-0488(20000801)38:15<2051::AID-POLB100>3.0.CO;2-D).
73. V. Barbi, S. S. Funari, R. Gehrke, N. Scharnagl and N. Stribeck, SAXS and the Gas Transport in Polyether-block-polyamide Copolymer Membranes *Macromolecules*, 2003, **36**, 749-758. <https://doi.org/10.1021/ma0213403>.
74. L. M. Robeson, The upper bound revisited *Journal of Membrane Science*, 2008, **320**, 390-400. <https://doi.org/10.1016/j.memsci.2008.04.030>.
75. Y. Chen, L. Zhao, B. Wang, P. Dutta and W. S. Winston Ho, Amine-containing polymer/zeolite Y composite membranes for CO₂/N₂ separation *Journal of Membrane Science*, 2016, **497**, 21-28. <https://doi.org/10.1016/j.memsci.2015.09.036>.
76. R. Nasir, H. Mukhtar and Z. Man, Fabrication, Characterization and Performance Study of N-methyl-diethanolamine (MDEA)-Polyethersulfone (PES) Amine Polymeric Membrane for CO₂/CH₄ Separation *Journal of Applied Sciences*, 2014, **14**, 1186-1191. <https://doi.org/10.3923/jas.2014.1186.1191>.
77. G. Chen, T. Wang, G. Zhang, G. Liu and W. Jin, Membrane materials targeting carbon capture and utilization *Advanced Membranes*, 2022, **2**, 100025. <https://doi.org/10.1016/j.advmem.2022.100025>.
78. J. Shen, G. Liu, K. Huang, Q. Li, K. Guan, Y. Li and W. Jin, UiO-66-polyether block amide mixed matrix membranes for CO₂ separation *Journal of Membrane Science*, 2016, **513**, 155-165. <https://doi.org/10.1016/j.memsci.2016.04.045>.
79. J. Liu, X. Hou, H. B. Park and H. Lin, High-Performance Polymers for Membrane CO₂/N₂ Separation *Chemistry – A European Journal*, 2016, **22**, 15980-15990. <https://doi.org/10.1002/chem.201603002>.
80. S. L. Liu, L. Shao, M. L. Chua, C. H. Lau, H. Wang and S. Quan, Recent progress in the design of advanced PEO-containing membranes for CO₂ removal *Progress in Polymer Science*, 2013, **38**, 1089-1120. <https://doi.org/10.1016/j.progpolymsci.2013.02.002>.
81. H. A. Daynes and S. W. J. Smith, The process of diffusion through a rubber membrane, 1920, **97**, 286-307. <https://doi.org/10.1098/rspa.1920.0034>.

Supporting Information

Lysine-based 2:1-[α /aza]- pseudopeptide series used as additives in polymeric membranes for CO₂ capture: synthesis, structural studies, and application

Mohamed I. A. Ibrahim^{*a, b}, Xavier Solimando^a, Loïc Stefan^a, Guillaume Pickaert^a, Jérôme Babin^a, Carole Arnal-Herault^a, Denis Roizard^c, Anne Jonquière^a, Jacques Bodiguel^a, and Marie-Christine Averlant-Petit^{*a}

^aLaboratoire de Chimie-Physique Macromoléculaire (LCPM), UMR 7375, CNRS, Université de Lorraine, Nancy, France.

^bLaboratory of Marine Chemistry, National Institute of Oceanography and Fisheries, NIOF, Egypt.

^cLaboratoire Réactions et Génie des Procédés (LRGP), UMR 7274, CNRS, Université de Lorraine, Nancy, France.

*Corresponding authors :


Dr. Marie-Christine Averlant-Petit


marie.averlant@univ-lorraine.fr

 <https://orcid.org/0000-0001-89956-1231>

[IdHal](#) : marie-christine-averlant-petit

Dr. Mohamed Ibrahim Abdelmoneim Ibrahim

 <https://orcid.org/0000-0001-6190-5899>

 Scopus ID: 57195522700

m.ibrahim@niof.sci.eg / ibrahimmohamed2030@gmail.com

TABLE OF CONTENTS

Table S1. Assignment of the CO groups in 7c and 7d , (3.0 mmol L ⁻¹ , CDCl ₃).....	3
Table S2: Mean dihedral angles of molecules (7c) and (7d) calculated from 25.000 structures obtained by the molecular dynamic simulations versus the classical torsion angles in peptides and proteins.....	3
Table S3. The possible intramolecular hydrogen bonds predicted from 25.000 structures in (7c) and (7d) obtained by the molecular dynamic simulations	3
Table S4. Mean dihedral angles of molecules (8c) and (8d) calculated from 25.000 structures obtained by the molecular dynamic simulations versus the classical torsion angles in peptides and proteins.....	3
Table S5. Mean values of the bond distances and bond angles for the predicted intramolecular hydrogen bonds calculated from 25.000 structures in (8c) and (8d) obtained by the molecular dynamic simulations.....	5
Table S6. Average percentages of the expected intramolecular hydrogen bonds in (8c) obtained by the molecular dynamic simulations.....	5
Table S7. Average percentages of the expected intramolecular hydrogen bonds in (8d) obtained by the molecular dynamic simulations.....	6
Table S8. Membrane permeation properties for CO ₂ and N ₂ pure gases at 35 °C and 2 bar.....	7
Figure S1a. The ¹ H spectrum of (7c); (3.0 mmol L ⁻¹ , CDCl ₃ , 300 K).....	8
Figure S1b. The ¹³ C spectrum of (7c); (5.0 mmol L ⁻¹ , CDCl ₃ , 300 K).....	8
Figure S2a. The ¹ H spectrum of (7d); (3.0 mmol L ⁻¹ , CDCl ₃ , 300 K).....	9
Figure S2b. The ¹³ C spectrum of (7d); (5.0 mmol L ⁻¹ , CDCl ₃ , 300 K).....	9
Figure S3. The 2D ROESY spectrum illustrating the correlations of βII-turn conformation in (7c); (300 MHz, 3.0 mmol L ⁻¹ , CDCl ₃ , 300 K).....	10
Figure S4. The 2D ROESY spectrum illustrating the correlations of βII'-turn conformation in (7d); (300 MHz, 3.0 mmol L ⁻¹ , CDCl ₃ , 300 K).....	10
Figure S5. Chemical shift-variations (δ) ppm of NH protons for (7c) and (7d) as a function of % [CDCl ₃ /DMSO- <i>d</i> ₆] mixtures; (300 MHz, 3.0 mmol L ⁻¹).....	11
Figure S6. Nomenclature used for the backbone dihedral angles of four oligomers (7c , 7d , 8c and 8d).....	11
Figure S7. The ¹ H spectrum of (8c); (4.0 mmol L ⁻¹ , CDCl ₃ , 300 K).....	12
Figure S8a. The ¹ H spectrum of (8c); (4.0 mmol L ⁻¹ , CD ₃ CN, 300 K).....	13
Figure S8b. The ¹³ C spectrum of (8c); (4.0 mmol L ⁻¹ , CD ₃ CN, 300 K).....	13
Figure S9a. The ¹ H spectrum of (8d); (4.0 mmol L ⁻¹ , CDCl ₃ , 300 K).....	14
Figure S9b. The ¹³ C spectrum of (8d); (5.0 mmol L ⁻¹ , CDCl ₃ , 300 K).....	15
Figure S10. The ¹ H spectrum of (8d); (4.0 mmol L ⁻¹ , CD ₃ CN, 300 K).....	15
Figure S11. The 2D ROESY spectrum illustrating the β-turn conformation in (8c); (300 MHz, 4.0 mmol L ⁻¹ , CDCl ₃ , 300 K).....	16
Figure S12. The 2D ROESY spectrum illustrating the correlations of β-turn conformation in (8d); (300 MHz, 4.0 mmol L ⁻¹ , CDCl ₃ , 300 K).....	16
Figure S13. Chemical shift-variations (δ) of NH protons for: (8c ; up), and (8d ; bottom) as a function of % [CDCl ₃ /DMSO- <i>d</i> ₆] mixtures.....	17
Figure S14. (a) Evaporation of butanol during membrane casting on a PTFE mold, and (b) example of a prepared membrane containing 4.0 wt% of the deprotected trimer (7c') pseudopeptide as additive in Pebax@1074 polymer before gases separation test.....	18

Table S1. Assignment of the CO groups in **7c** and **7d**, (3.0 mmol L⁻¹, CDCl₃)

CO Molecule 7c	Free methyl ester	Free Lys1	Free CO(Z) (Lys1+Lys2)	Free Boc	Free azaPhe	Bound Boc
Wavenumber (cm ⁻¹)	1748	1735	1717	1701	1677	1652
CO Molecule 7d	Free methyl ester	Free Lys1	Free CO(Z) D-Lys1	Free CO(z) Lys2 + Boc	Free azaPhe	Bound Boc
Wavenumber (cm ⁻¹)	1749	1734	1718	1702	1675	1652

Table S2. Mean values of the dihedral angles of molecules (**7c**) and (**7d**) calculated from 25.000 structures issued of the molecular dynamic simulations *versus* the classical values of β -turns in natural peptides

	$\Phi 1$	$\Psi 1$	$\Phi 2$	$\Psi 2$	$\Phi 3$	$\Psi 3$
Molecule 7c	-29.70°	26.37°	-89.07°	47.89°	-138.60°	125.56°
Molecule 7d	128.40°	-64.94°	91.81°	38.83°	-146.91°	125.82°
β IV-turn	-61°	10°	-53°	17°	--	--
β I'-turn	60°	30°	90°	0°	--	--

Table S3. The possible intramolecular hydrogen bonds predicted from 25.000 structures in (**7c**) and (**7d**) issued of the molecular dynamic simulations

Molecule	Bond Ref.	Residue	Residue	Distance (Å) N-----O	Angle (°)	H-bond (%)
7c	i	CO (i)	HN (i + 2)	2.86	139.5	36
	ii	CO (i + 2)	HN ^ε (i + 3)	2.96	159.04	35
7d	i	CO(Z) (i + 3)	HN (i + 2)	2.89	162.01	40
	ii	CO(Z) (i + 3)	HN (i + 1)	2.91	158.44	26
	iii	CO (i)	HN ^ε (i + 1)	2.98	159.42	22

Table S4. Mean dihedral angles of molecules (**8c**) and (**8d**) calculated from 25.000 structures obtained by the molecular dynamic simulations versus the classical torsion angles in peptides and proteins

Torsion angles in (8c) and (8d)										
Compound	Φ_1	Ψ_1	Φ_2	Ψ_2	Φ_3	Ψ_3	Φ_4	Ψ_4	Φ_5	Ψ_5
8c	-85.81°	23.79°	86.23°	-68.93°	-66.15°	26.77°	-129.05°	13.11°	-88.26°	21.62°
8d	83.43°	-27.38°	79.51°	-112.39°	-68.92°	5.67°	131.28°	30.66°	97.04°	-9.78°

Classical torsion angles in peptides and proteins

Turn	Φ_i	Ψ_i	Φ_{i+1}	Ψ_{i+1}
$\beta I'$	60°	30°	90°	0°
$\beta II'$	60°	-120°	-80°	0°
βIV	-61°	10°	-53	17°
βV	-80°	80°	80°	-80°
$\beta V'$	80°	-80°	-80°	80°

Table S5. Mean values of the bond distances and bond angles for the predicted intramolecular hydrogen bonds calculated from 25.000 structures in **(8c)** and **(8d)** obtained by the molecular dynamic simulations

Intramolecular H-bonds in compounds (8c) and (8d)						
Molecule	Bond Ref.	Residue	Residue	Distance (Å) N-----O	Angle (°)	H-bond (%)
8c	i	CO (i+2)	NH (i + 4)	2.78	146.35	90.8
	ii	CO (i + 1)	N ^ε H (i + 4)	2.91	157.18	64.9
	iii	CO (i)	NH (i + 2)	2.89	140.85	48.9
	iv	CO (i+2)	NH (i + 5)	3.02	147.36	32.9
8d	i	CO (i + 1)	NH (i + 5)	2.97	149.60	59.1
	ii	CO(z) (i + 6)	NH (i + 1)	2.90	156.03	58.7
	iii	CO (i + 2)	NH (i + 4)	2.94	137.64	38.8
	iv	CO (i)	NH (i + 2)	2.84	143.62	29.5
	v	CO(z) (i + 4)	N ^ε H (i + 1)	2.95	159.04	26.9
	vi	CO (i + 5)	N ^ε H (i + 3)	2.94	155.21	23.0

Table S6. Average percentages of the expected intramolecular hydrogen bonds in **(8c)** obtained by the molecular dynamic simulations

Molecule	Bond Ref.	No. of frames	Frames (%)	Bond Ref.	No. of frames	Frames (%)
8c	(i + ii)	15115	60.5	(i + ii + iii)	7368	29.5
	(i + iii)	11154	44.6	(i + iii + iv)	3607	14.4
	(i + iv)	6952	27.8	(i + ii + iv)	4282	17.3
	(ii + iii)	7892	31.8	(ii + iii + iv)	2560	10.2
	(ii + iv)	4921	19.7	(i + ii + iii + iv)	2259	9.0
	(iii + iv)	4215	16.9			

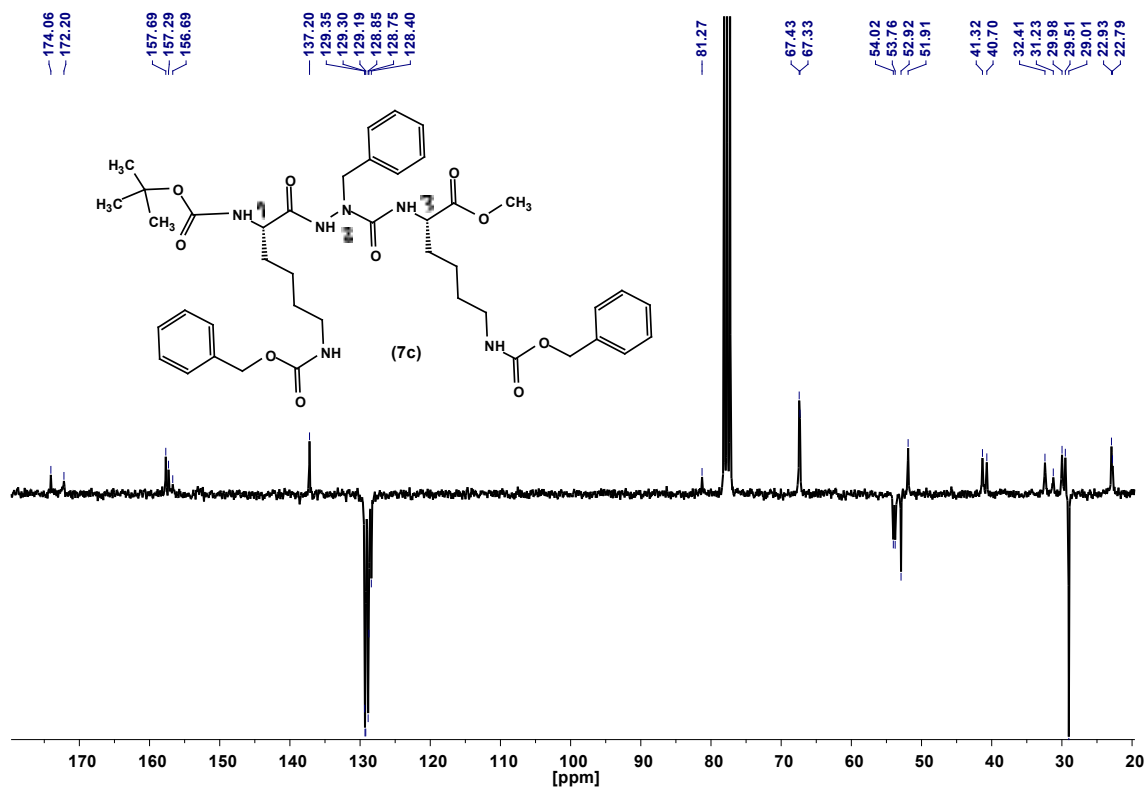
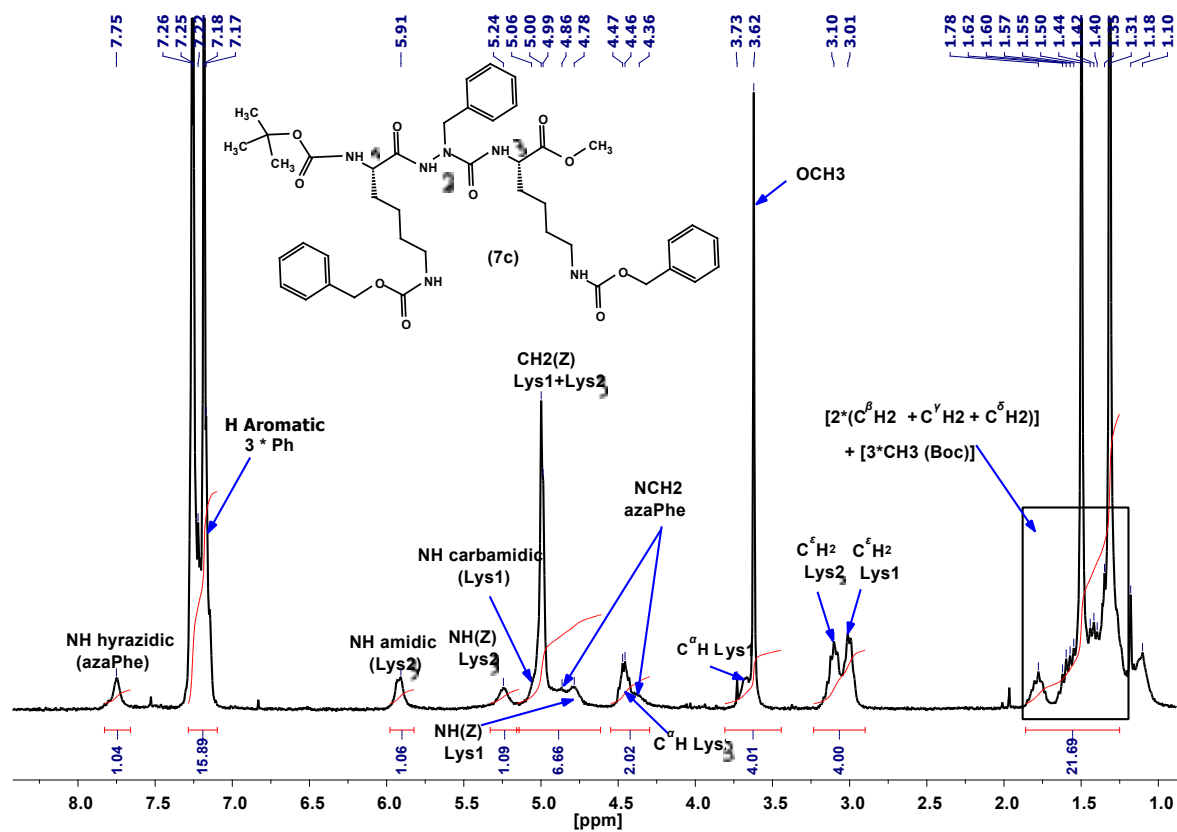
Table S7. Average percentages of the expected intramolecular hydrogen bonds in **(8d)** obtained by the molecular dynamic simulations

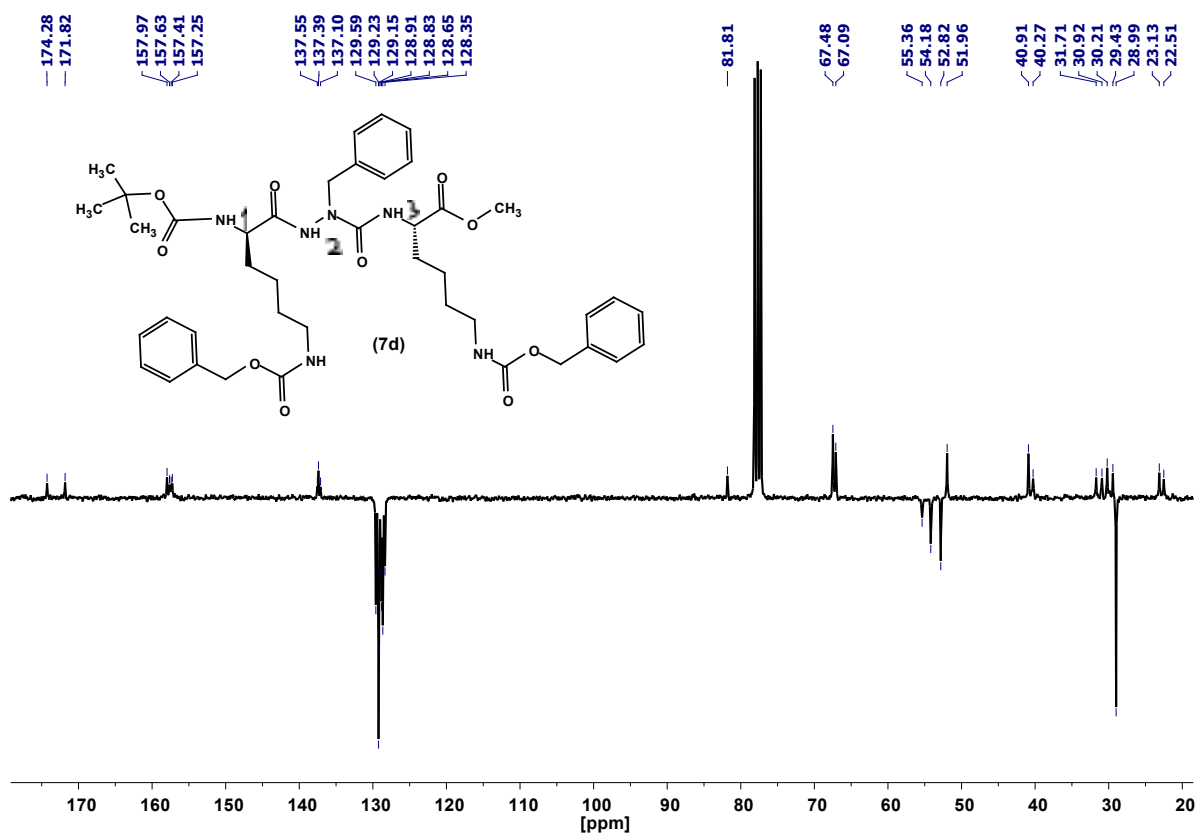
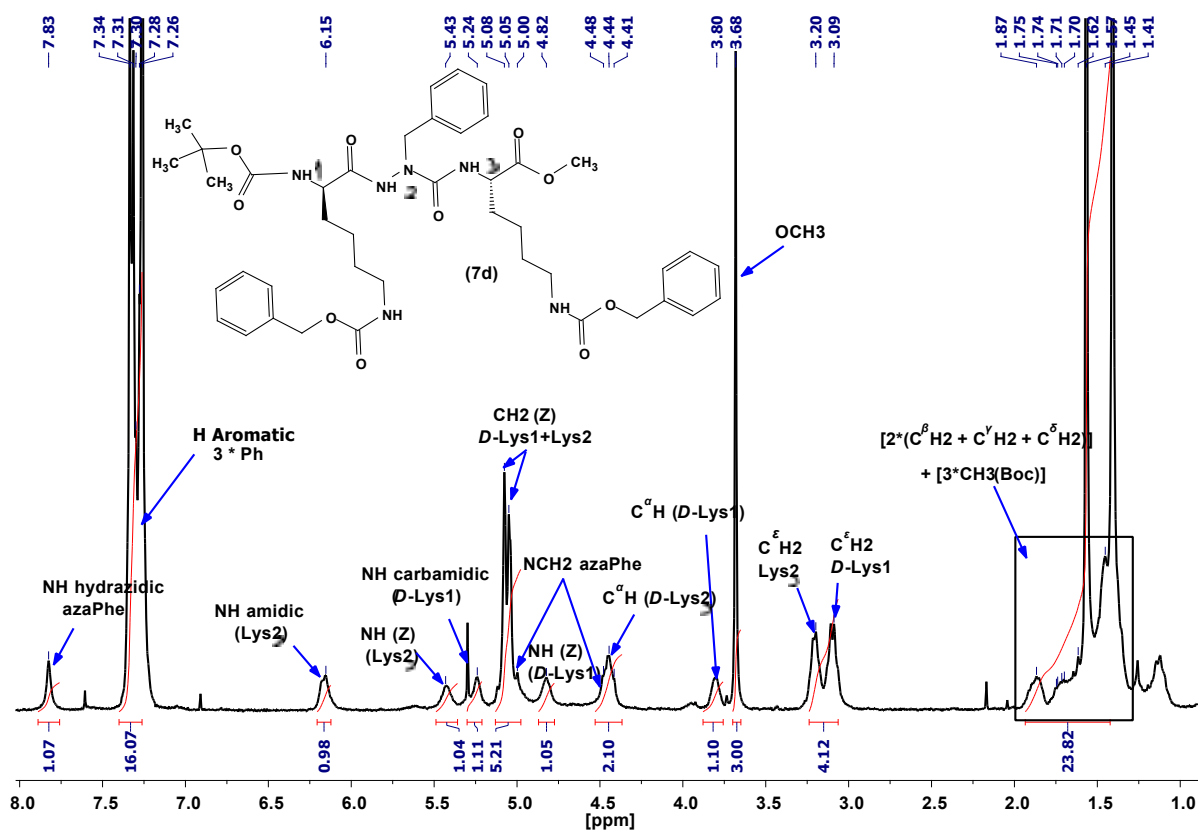
Molecule	Bond Ref.	No. of frames	Frames (%)	Bond Ref.	No. of frames	Frames (%)
8d	(i + ii)	8941	35.8	(iv + v)	2614	10.5
	(i + iii)	3069	12.3	(iv + vi)	1775	7.1
	(i + iv)	5439	21.8	(v + vi)	1997	8.0
	(i + v)	4378	17.5	(i + ii + iii)	1862	7.5
	(i + vi)	2306	9.2	(i + iii + iv)	1142	4.5
	(ii + iii)	4257	17.0	(i + ii + iv)	2972	11.9
	(ii + iv)	4753	19.0	(ii + iii + iv)	1405	5.6
	(ii + v)	4363	17.4	(iv + v + vi)	766	3.0
	(ii + vi)	4219	16.9	(i + ii + iii + iv)	650	2.6
	(iii + iv)	2871	11.5	(ii + iii + iv + v)	582	2.3
	(iii + v)	2314	9.2	(i + iv + v + vi)	473	1.9
	(iii + vi)	2277	9.1	(i + ii + iii + vi + v)	402	1.6

Table S8. Membrane permeation properties for CO₂ and N₂ pure gases at 35 °C and 2 bar

	Pseudopeptide oligomer	P (CO ₂) (Barrer)	P (N ₂) (Barrer)	D (CO ₂) x 10 ⁶ (cm ² /s)	D (N ₂) x 10 ⁷ (cm ² /s)	S (CO ₂) x 10 ² (cm ³ (STP).cm ⁻³ .cmHg ⁻¹)	S (N ₂) x 10 ⁴ (cm ³ (STP).cm ⁻³ .cmHg ⁻¹)
Pebax 1074		132.67 ± 0.52	3.10 ± 0.17	1.19 ± 0.02	3.76 ± 0.40	1.12 ± 0.02	8.31 ± 1.10
Trimer without Lys	7a	116.00 ± 0.17	2.58 ± 0.05	1.10 ± 0.04	4.11 ± 0.52	1.09 ± 0.05	6.39 ± 0.91
Protected hexamer	8c	115.28 ± 0.24	3.00 ± 0.00	1.03 ± 0.02	3.96 ± 0.34	1.16 ± 0.06	7.58 ± 0.55
Protected trimer	7c	119.23 ± 0.15	2.66 ± 0.29	1.13 ± 0.01	2.41 ± 0.18	1.05 ± 0.01	10.39 ± 0.68
Protected dimer	6b	122.48 ± 1.39	2.60 ± 0.00	1.05 ± 0.05	3.09 ± 0.50	1.16 ± 0.05	8.57 ± 1.31
Deprotected hexamer	8c*	123.85 ± 0.31	3.35 ± 0.35	0.85 ± 0.02	6.16 ± 0.93	1.47 ± 0.04	5.59 ± 1.41
Deprotected trimer	7c*	133.20 ± 0.14	3.06 ± 0.06	0.92 ± 0.01	5.40 ± 0.38	1.46 ± 0.02	5.71 ± 0.33
Deprotected dimer	6b*	147.65 ± 0.13	3.10 ± 0.00	1.35 ± 0.03	3.68 ± 0.13	1.10 ± 0.02	8.42 ± 0.24

*Deprotected azapeptides **6b'**, **7b'** and **8b'** have obtained from the corresponding protected analogues by catalytic hydrogenolysis (See Experimental Section).





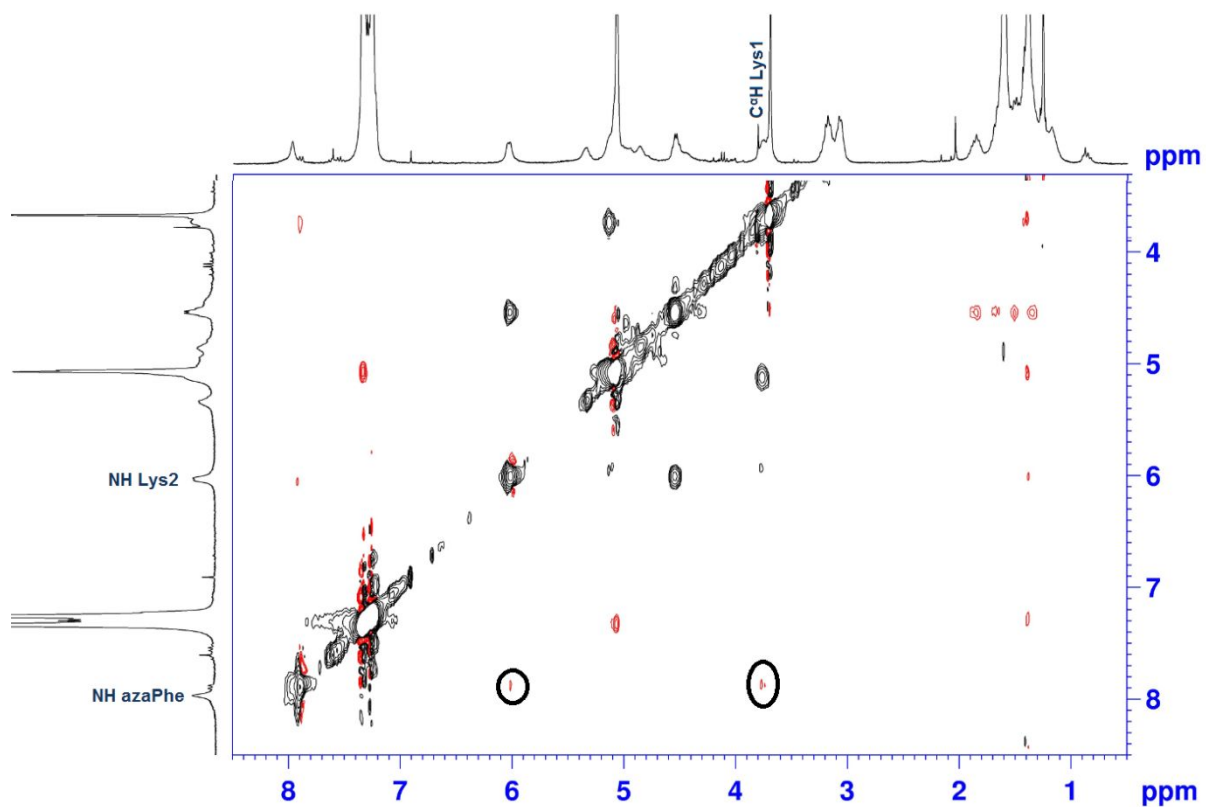


Figure S3. The 2D ROESY spectrum illustrating the correlations of β II-turn conformation in **7c** (300 MHz, 3.0 mmol L⁻¹, CDCl₃, 300 K).

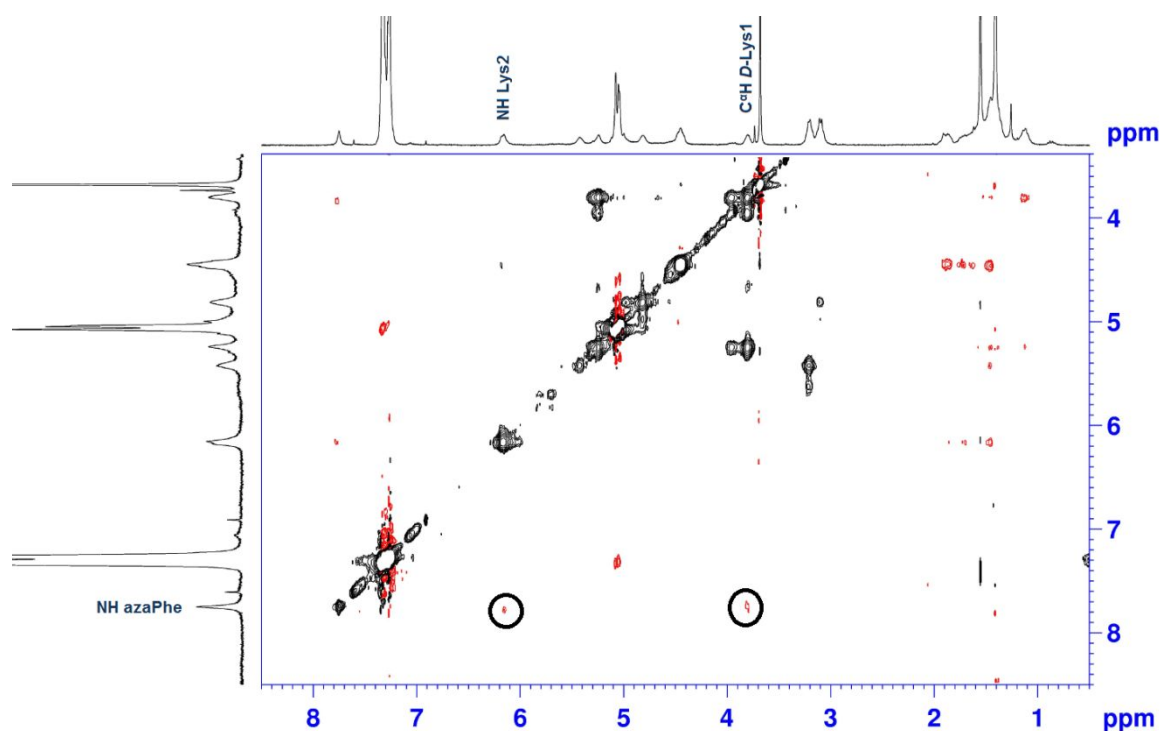


Figure S4. The 2D ROESY spectrum illustrating the correlations of β II'-turn conformation in **7d** (300 MHz, 3.0 mmol L⁻¹, CDCl₃, 300 K).

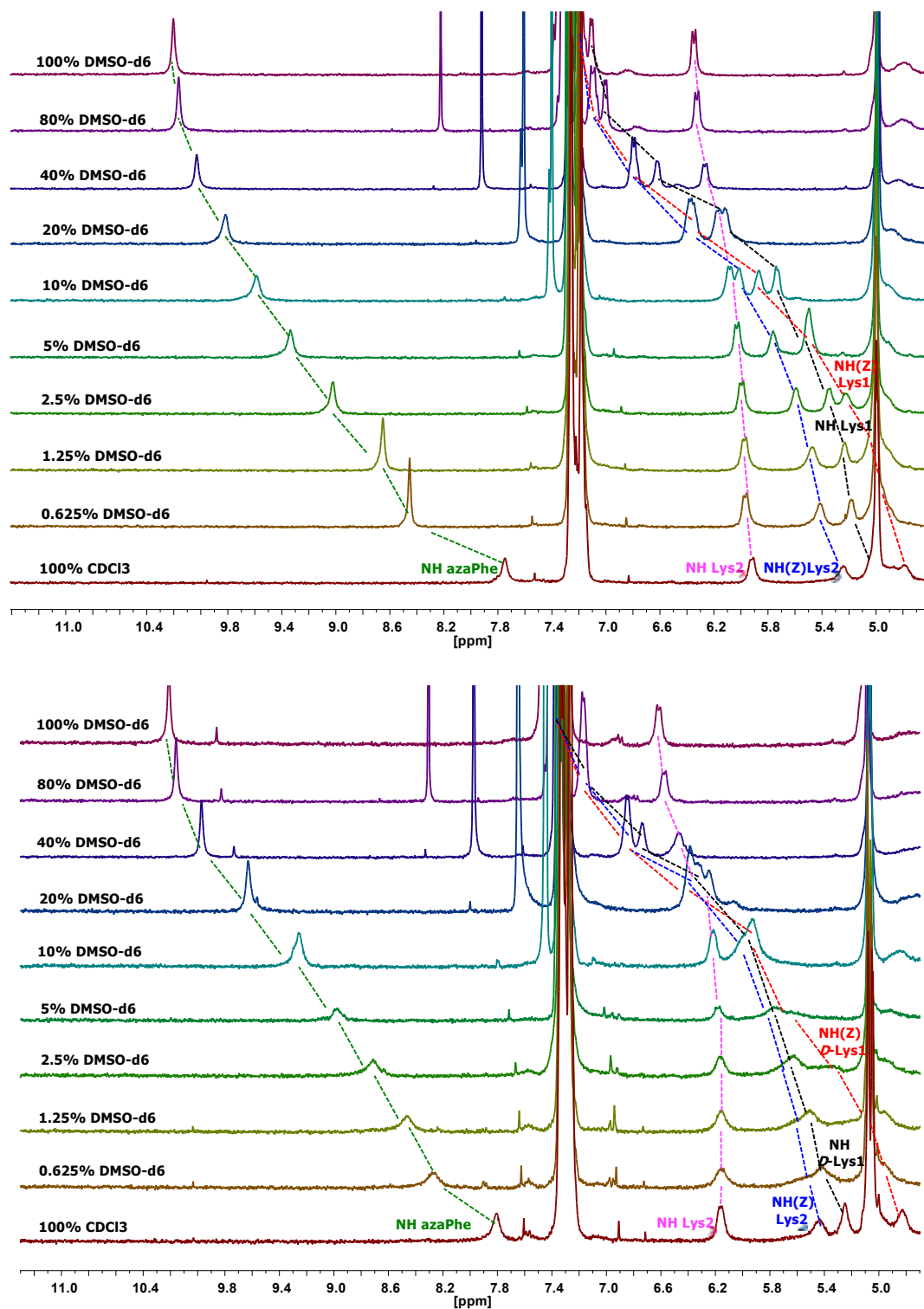


Figure S5. Chemical shift-variations (δ) ppm of NH protons for: **7c** (up); and **7d** (bottom) as a function of % $[\text{CDCl}_3/\text{DMSO-}d_6]$ mixtures; (300 MHz, 3.0 mmol L^{-1}).

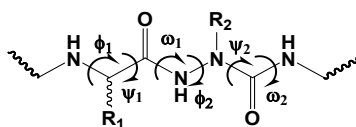


Figure S6. Nomenclature used for the backbone dihedral angles of four oligomers (**7c**, **7d**, **8c** and **8d**).

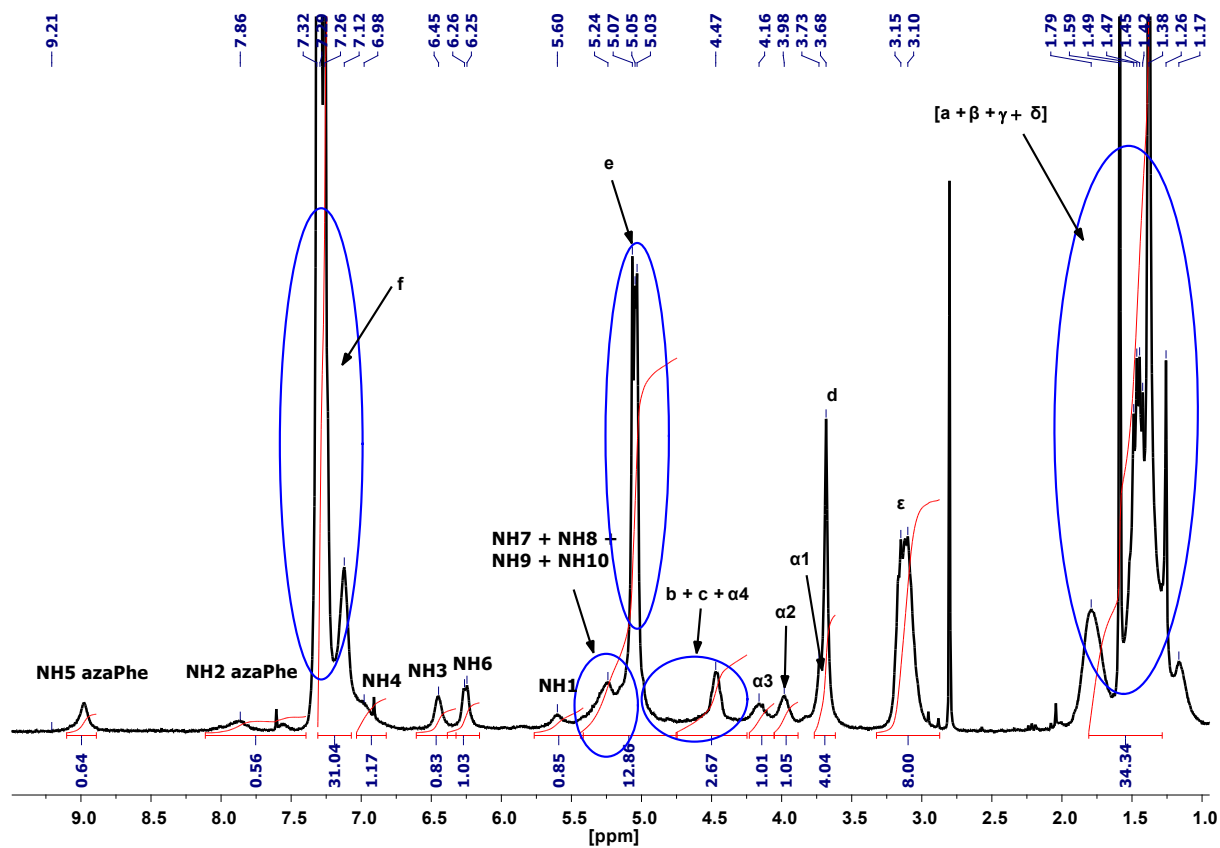
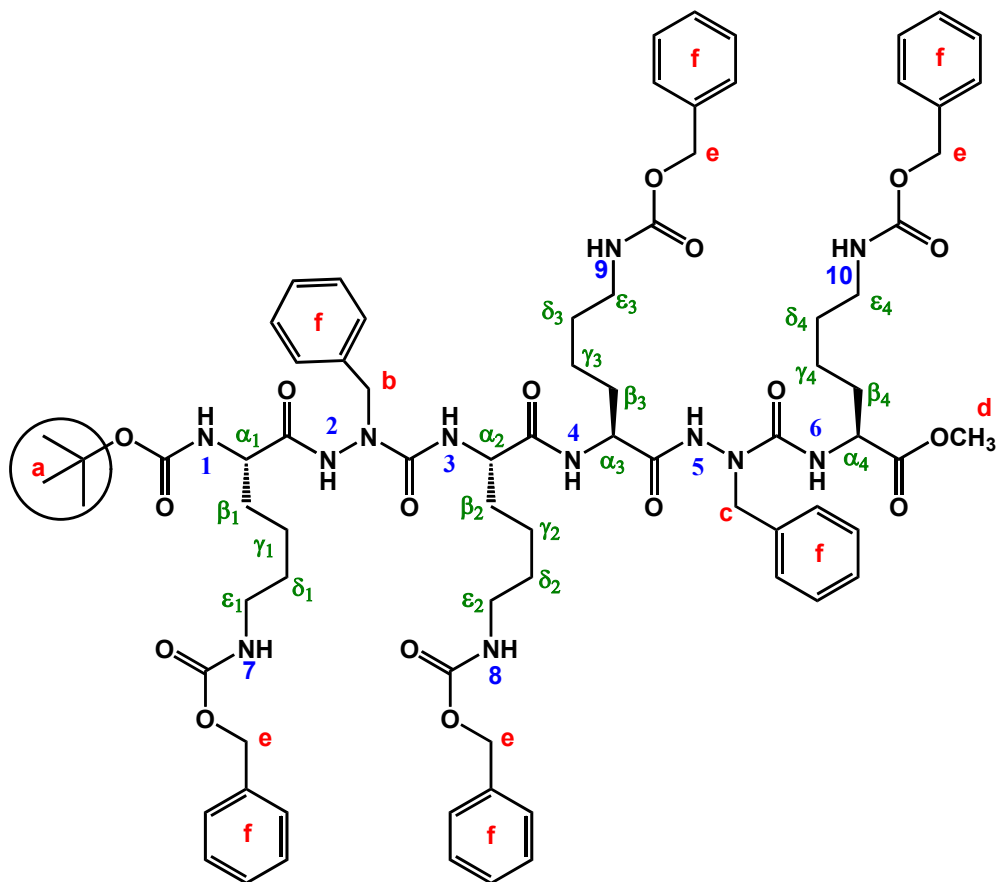


Figure S7. The ^1H spectrum of **8c** (4.0 mmol L^{-1} , CDCl_3 , 300 K).



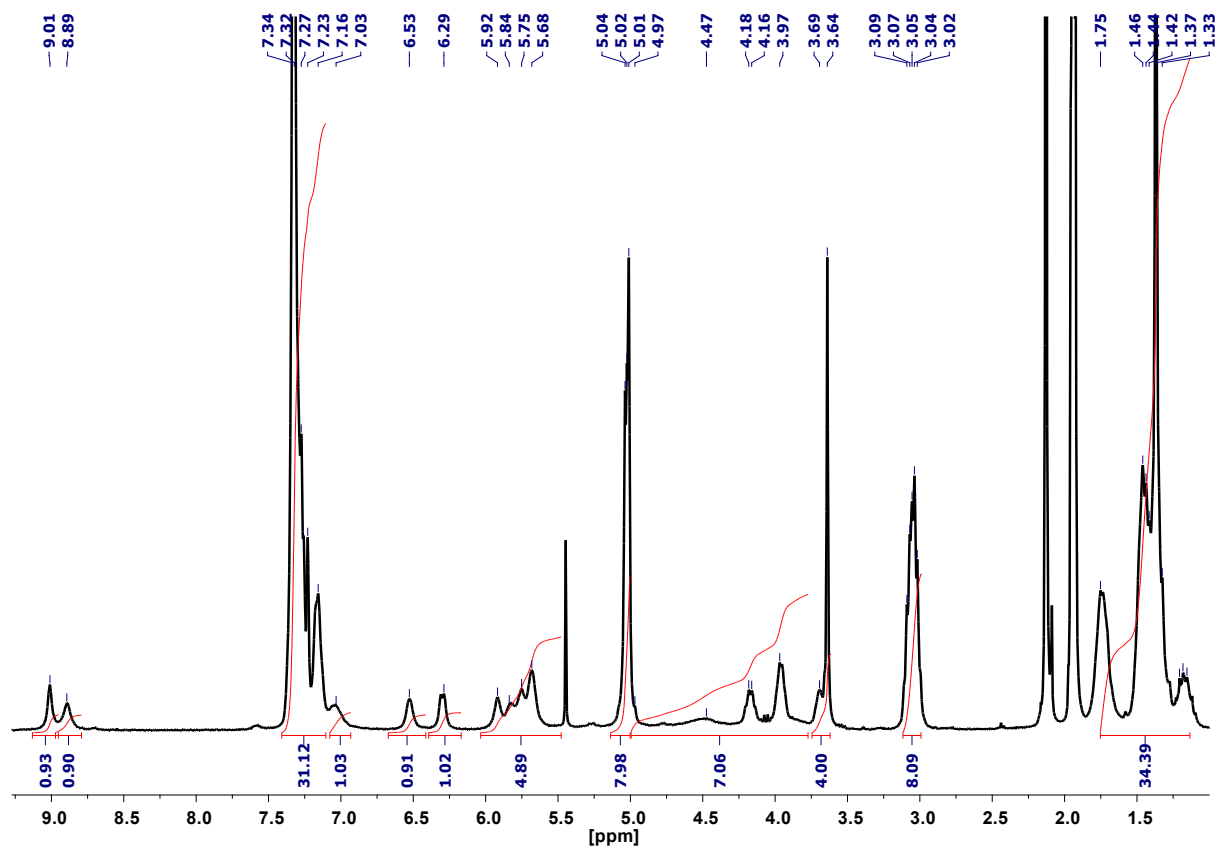


Figure S8a. The ^1H spectrum of **8c** (4.0 mmol L^{-1} , CD_3CN , 300 K).

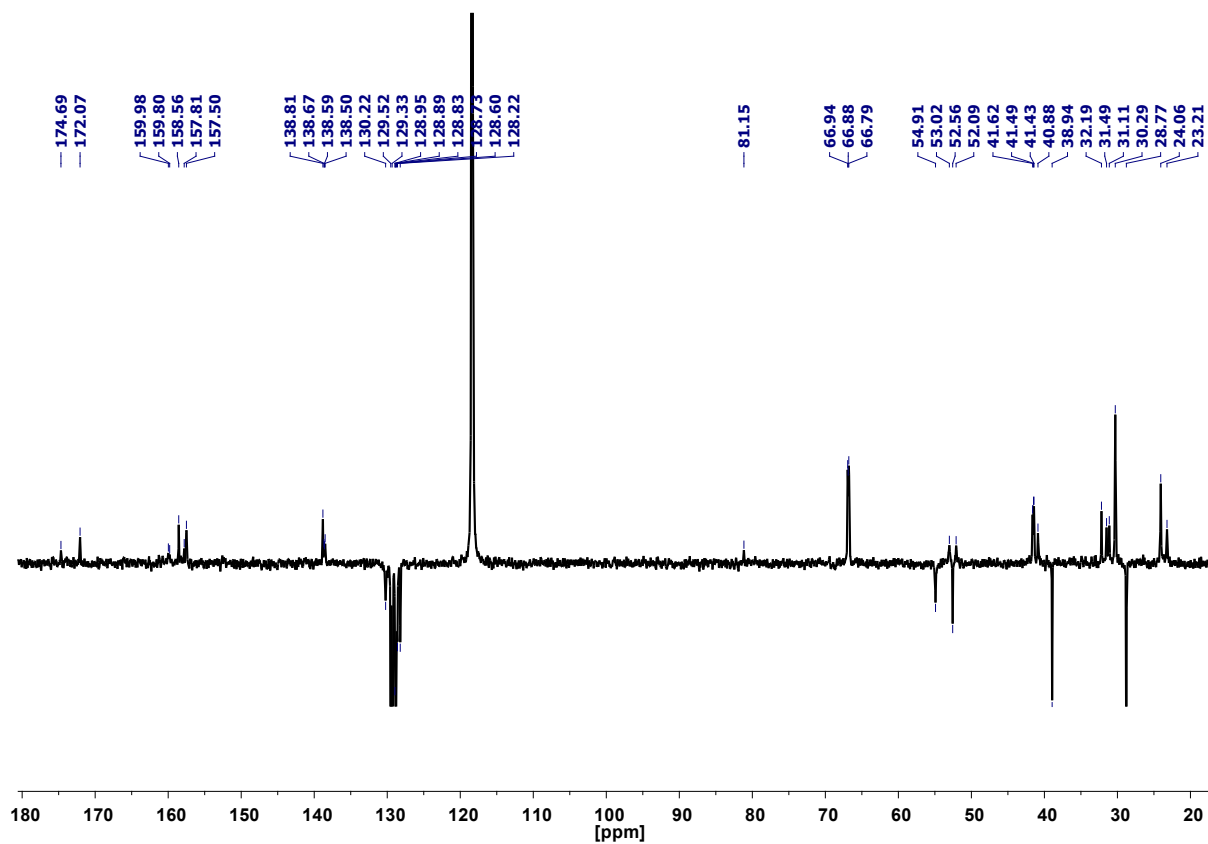


Figure S8b. The ^{13}C spectrum of **8c** (4.0 mmol L^{-1} , CD_3CN , 300 K).

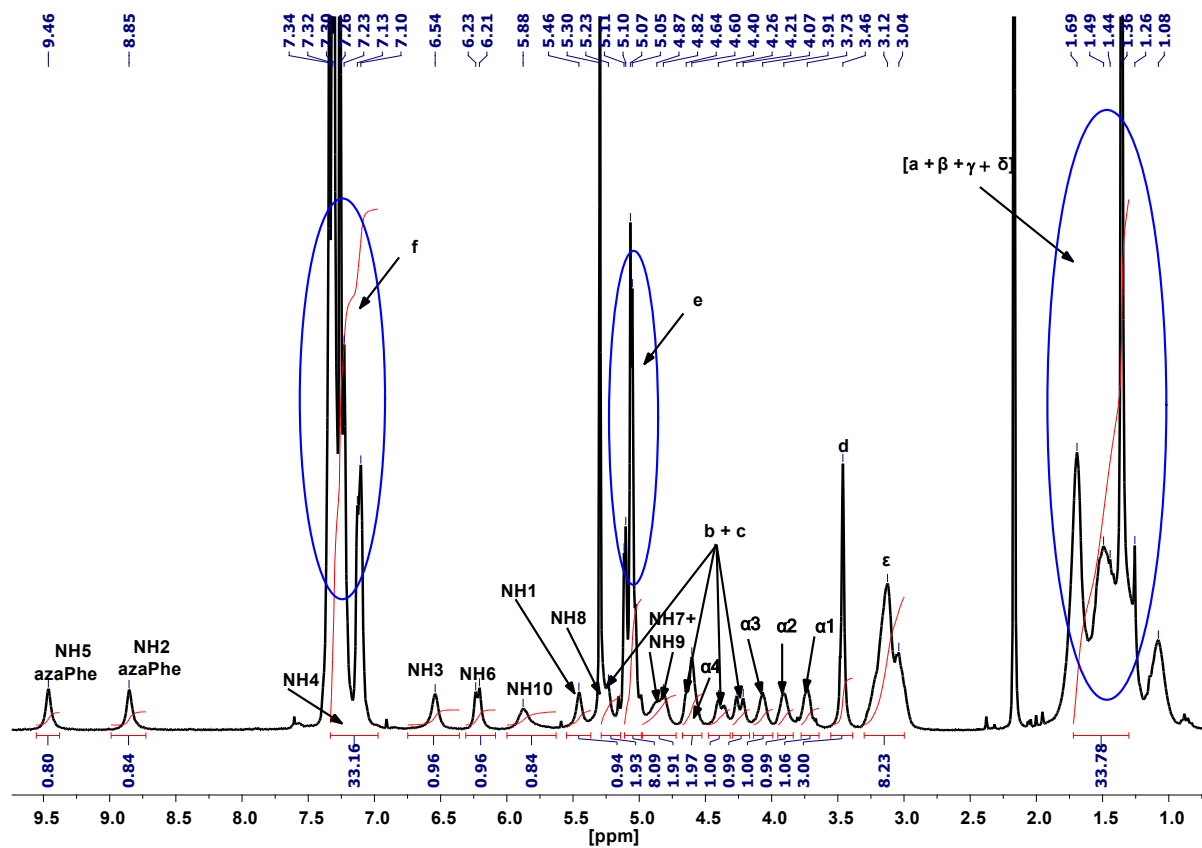
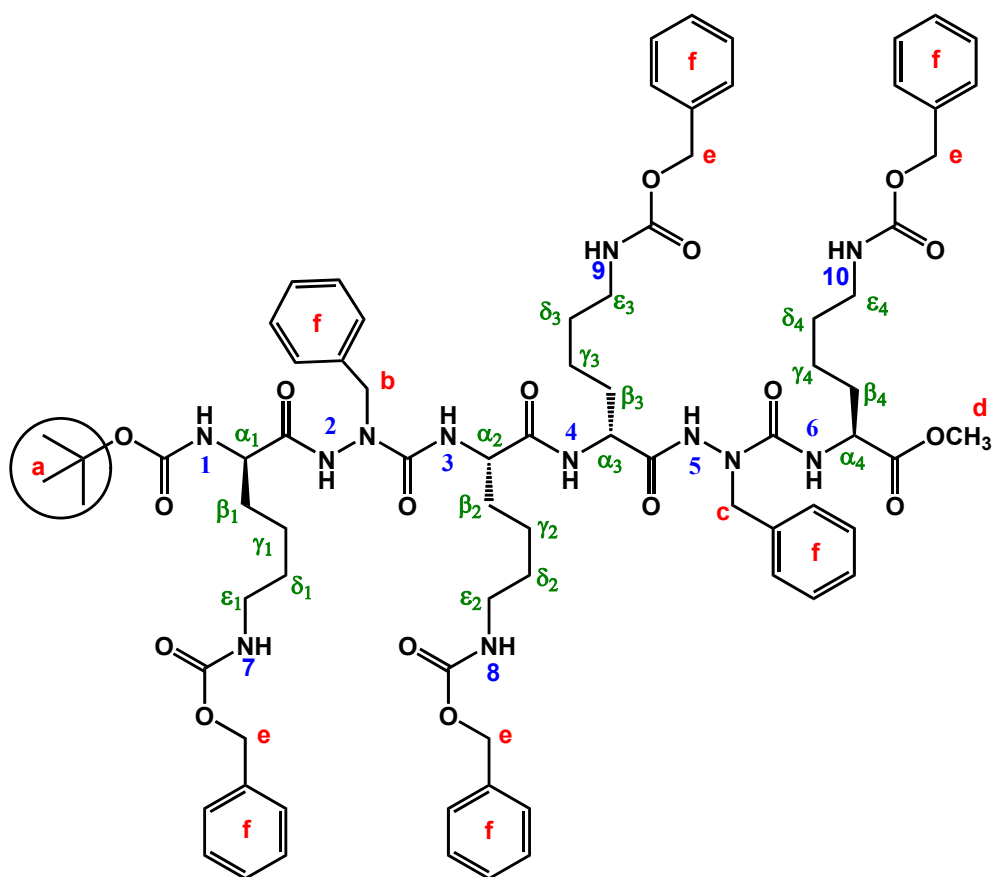


Figure S9a. The ^1H spectrum of **8d** (4.0 mmol L^{-1} , CDCl_3 , 300 K).



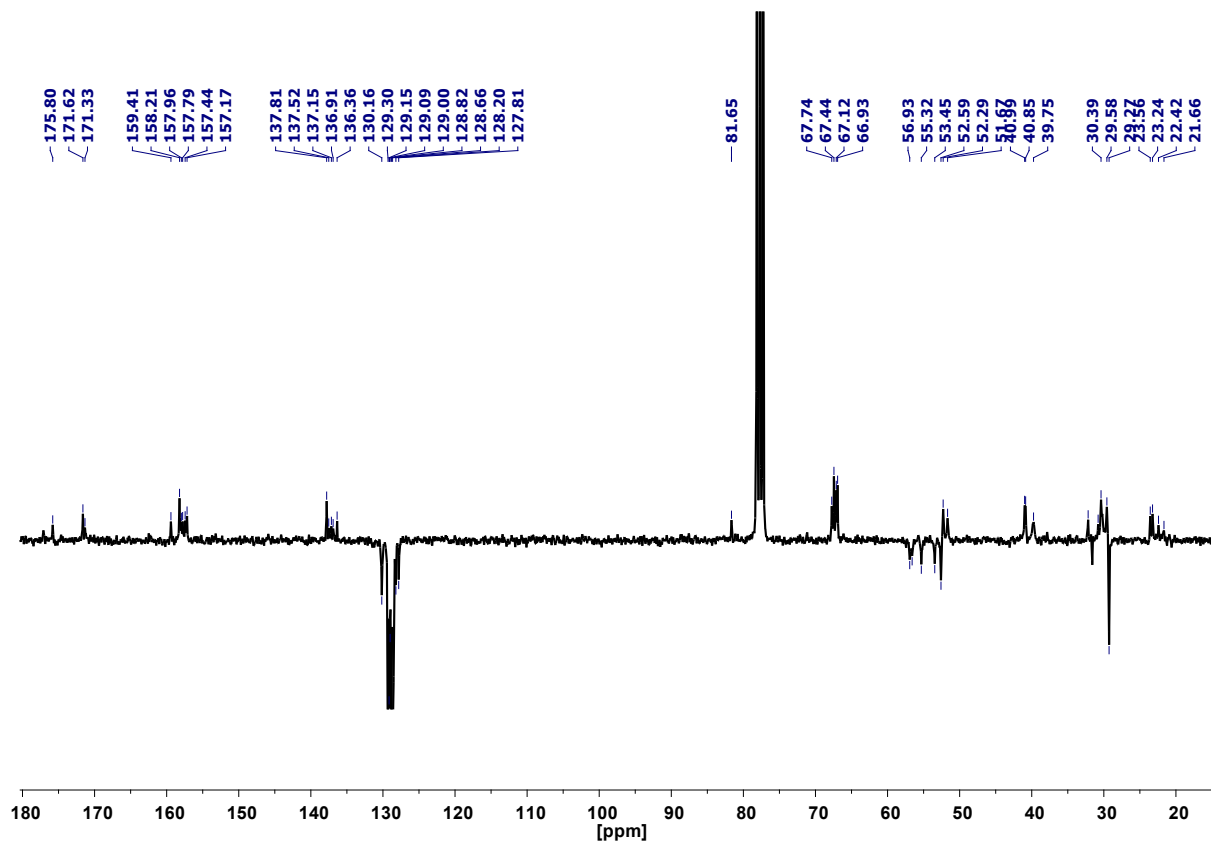


Figure S9b. The ^{13}C spectrum of **8d** (5.0 mmol L^{-1} , CDCl_3 , 300 K).

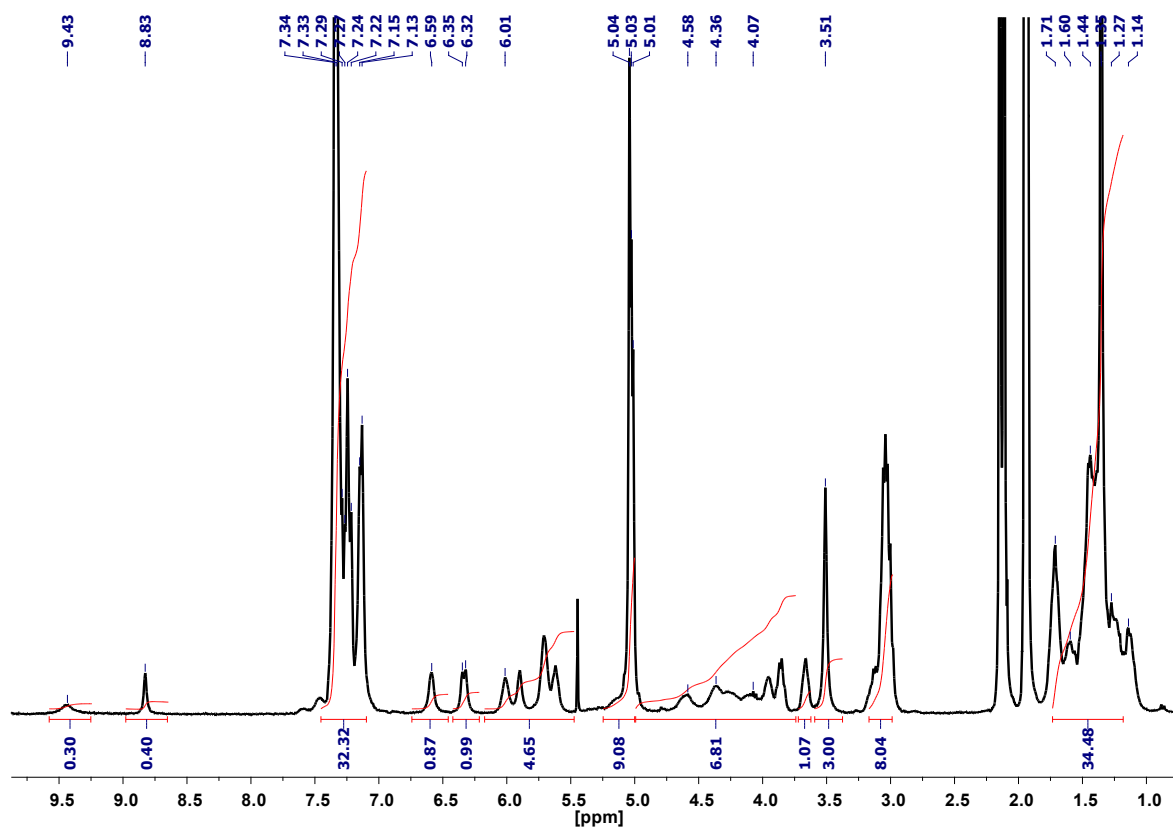


Figure S10. The ^1H spectrum of **8d** (4.0 mmol L^{-1} , CD_3CN , 300 K).

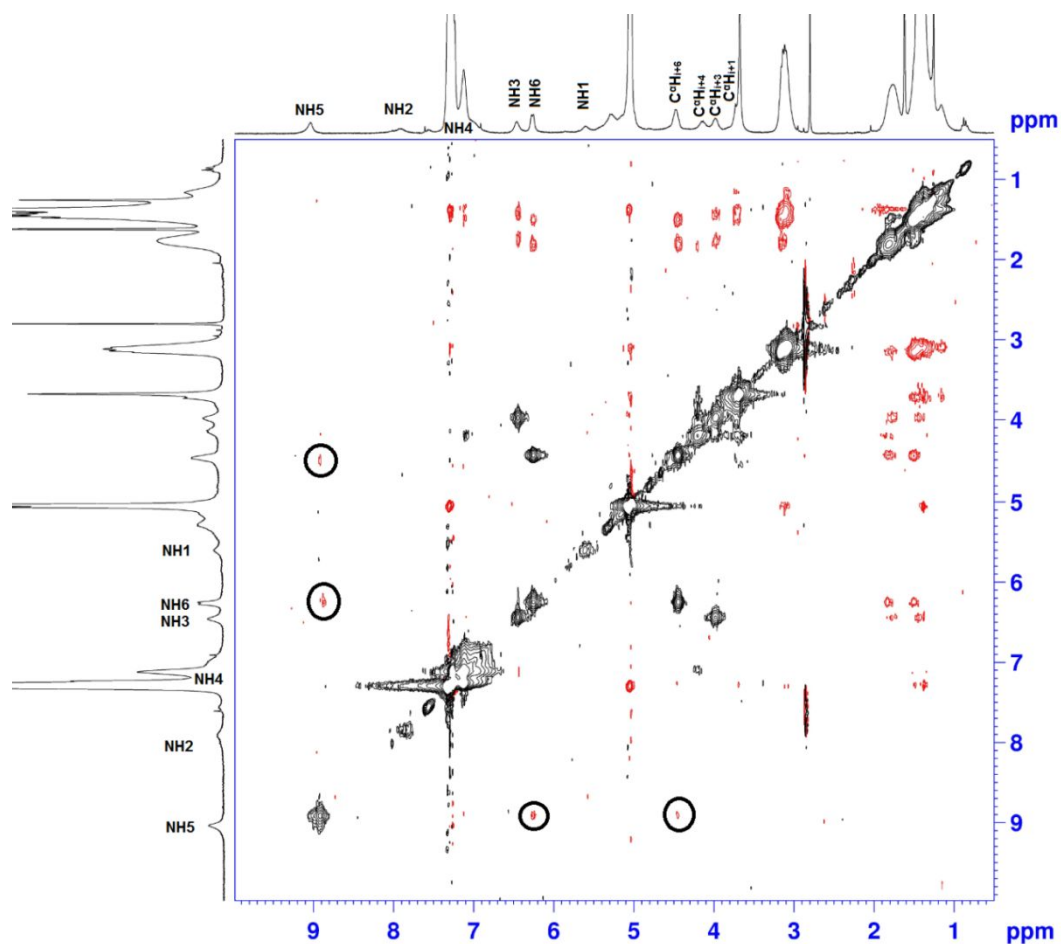


Figure S11. The 2D ROESY spectrum illustrating the β -turn conformation in **8c**; (300 MHz, 4.0 mmol L⁻¹, CDCl₃, 300 K).

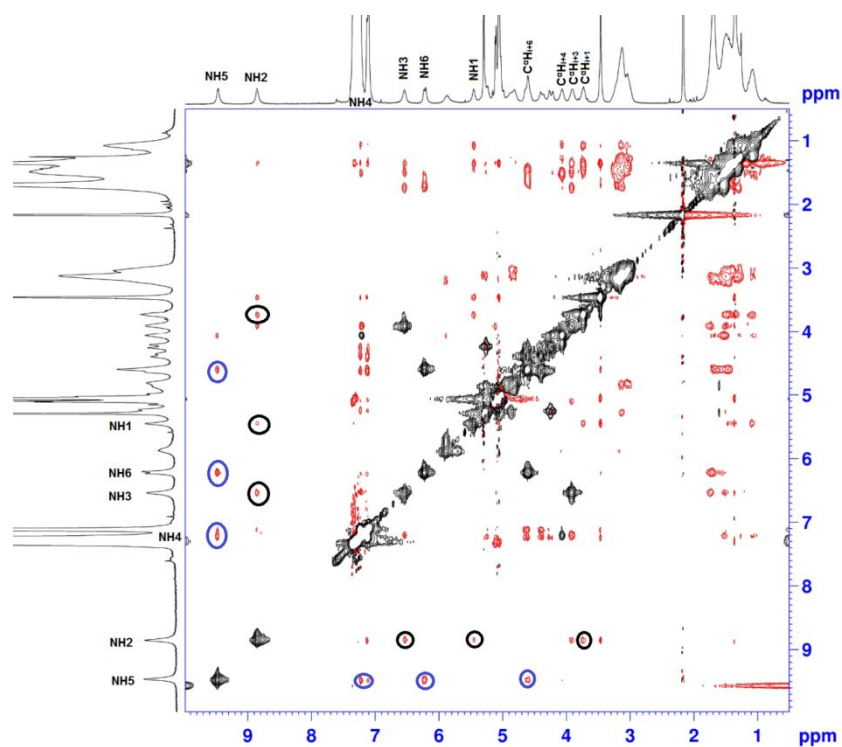


Figure S12. The 2D ROESY spectrum illustrating the correlations of β -turn conformation in **8d**, (300 MHz, 4.0 mmol L⁻¹, CDCl₃, 300 K).

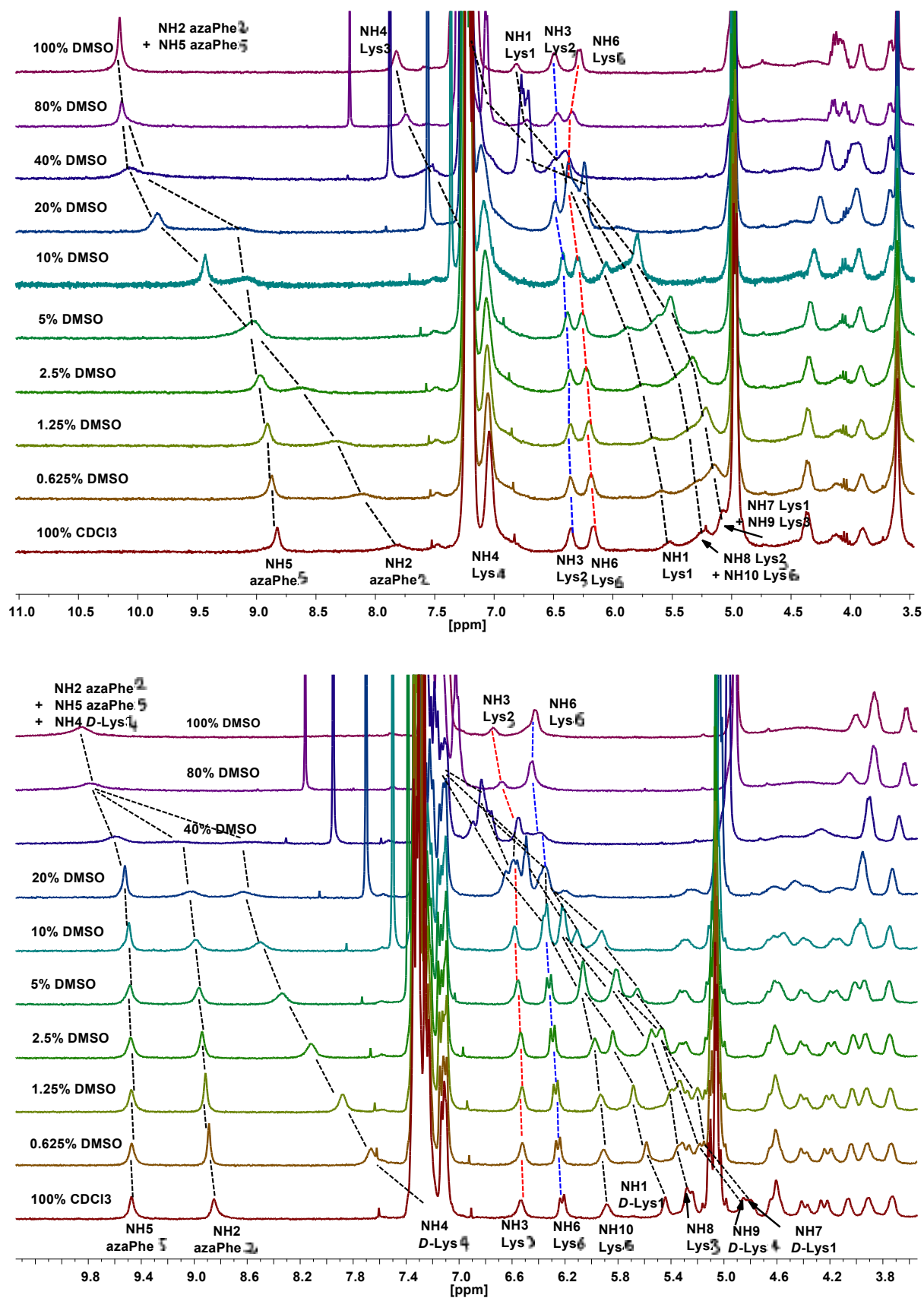


Figure S13. Chemical shift-variations (δ) of NH protons for: **8c** (up); and **8d** (bottom) as a function of % $[\text{CDCl}_3/\text{DMSO-}d_6]$ mixtures.



Figure S14. (a) Evaporation of butanol during membrane casting on a PTFE mold, and (b) example of a prepared membrane containing 4.0 wt% of the deprotected trimer (**7c'**) pseudopeptide as additive in Pebax[®]1074 polymer before gases separation test.